INVESTIGATIONS ON MULTIBAND METAMATERIAL ANTENNA DESIGN FOR WIRELESS APPLICATIONS

Submitted in partial fulfilment of the requirements
for the award of the degree of

Doctor of Philosophy

by

Junuthula Ashish
(Roll No. 718040)

Supervisor

Dr. A. Prakasa Rao
Associate Professor, Dept. of ECE

Department of Electronics & Communication Engineering
NATIONAL INSTITUTE OF TECHNOLOGY WARANGAL – 506004, T.S, INDIA
November-2023

Dedicated to My

Family, Gurus, & Friends

APPROVAL SHEET

This thesis entitled "**Investigations on Multiband Metamaterial Antenna Design for Wireless Applications**" by Mr. **Junuthula Ashish** is approved for the degree of **Doctor of Philosophy**.

Examiners

_____

_____

Supervisor

_____

Dr. A. Prakasa Rao

Associate Professor, Electronics and Communication Engineering Department,

NIT WARANGAL

Chairman

_____

Prof. D. Vakula

Head, Electronics and Communication Engineering Department,

NIT WARANGAL

Date:

Place: Warangal

DECLARATION

This is to certify that the work presented in the thesis entitled "**Investigations on Mutiband Metamaterial Antenna Design for Wireless Applications**" is a bona fide work done by me under the supervision of **Dr. A. Prakasa Rao**, Department of Electronics and Communication Engineering, National Institute of Technology Warangal, and was not submitted elsewhere for the award of any degree.

I declare that this written submission represents my ideas in my own words and where others' ideas or words have been included, I have adequately cited and referenced the original sources. I also declare that I have adhered to all principles of academic honesty and integrity and have not misrepresented or fabricated or falsified any idea/date/fact/source in my submission. I understand that any violation of the above will be cause for disciplinary action by the institute and can also evoke penal action from the sources which have thus not been properly cited or from whom proper permission has not been taken when needed.

Junuthula Ashish

Roll No: 718040

Date:

Place: Warangal

Department of Electronics and Communication Engineering
National Institute of Technology
Warangal – 506 004, Telangana, India

CERTIFICATE

This is to certify that the dissertation work entitled **"Investigations on Multiband Metamaterial Antenna Design for Wireless Applications"**, which is being submitted by Mr. Junuthula Ashish (Roll No.718040), is a bona fide work submitted to National Institute of Technology Warangal in partial fulfilment of the requirement for the award of the degree of *Doctor of Philosophy in Electronics and Communication Engineering.*

To the best of our knowledge, the work incorporated in this thesis has not been submitted elsewhere for the award of any degree.

Dr. A. Prakasa Rao
Supervisor
Department of ECE
National Institute of Technology
Warangal – 506004

ACKNOWLEDGEMENTS

I am grateful to many people who made this work possible and helped me during my Ph.D studies. I am greatly indebted to my research supervisor Dr. A. Prakasa Rao for giving me excellent support during my research activity at NIT Warangal. He encouraged me in choosing my research topic, his vision in my research area led to successful investigations. I am very much thankful to him for giving research freedom and guidance, support in non-academic matters and for the humanity shown to me. With his inimitable qualities as a good teacher, he chiseled my path towards perfection. Ever since I met him, he has been an eternal source of motivation, inspiration, encouragement, and enlightenment. He is responsible for making the period of my research work as an educative and enjoyable learning experience. The thesis would not have seen the light of the day without his insistent support and cooperation.

I am also grateful to Prof. D. Vakula, Head of the Department, Dept. of Electronics and Communication Engineering, for her valuable suggestions and support that she shared during my research tenure.

I take this privilege to thank all my Doctoral Scrutiny Committee members, Prof. L. Anjaneyulu, Department of Electronics and Communication Engineering, Prof. D. Vakula, Department of Electronics and Communication Engineering, Prof. C. Venkaiah, Department of Electrical and Electronics Engineering, Prof. D. M. Vinod Kumar, Department of Electrical and Electronics Engineering and Prof. NVSN Sarma, Department of Electronics and Communication Engineering for their detailed review, constructive suggestions and excellent advice during the progress of this research work. Also, thank Dr. P. Muthu, Department of Mathematics for helping me during the course work.

I am grateful to the former Heads of the ECE department Prof. P. Sreehari Rao, Prof. L. Anjaneyulu, and Prof. N. Bheema Rao for their continuous support and encouragement. I would also appreciate the encouragement from teaching, non-teaching members and fraternity of Dept. of E C E of N I T Warangal. They have always been encouraging and supportive.

I take this opportunity to convey my regards to my closest friends for being always next to me. Thanks to K. Krishna Reddy, S. Karthik Sairam, P. Raveendra, C. Jayram, T. Nageswara

Rao and C. Sudharani from Department of Electronics and Communication Engineering for their motivation and support throughout my work.

I acknowledge my gratitude to all my teachers and colleagues at various places for supporting and cooperating me to complete this work.

I would like to thank my family members (J. Sambashiva Reddy, J. Padma, J. Nandini, J. Aadya and J. Ashwini) for giving me mental support and inspiration. They have motivated and helped me to complete my thesis work successfully.

Finally, I thank God for filling me every day with new hopes, strength, purpose, and faith.

J Ashish

ABSTRACT

This thesis presents a few multiband antennas designed by exploiting the unique properties of metamaterials. The use of metamaterials in the design not only helps us in realizing multiband antennas but also aids in improving certain performance parameters. All the designed antennas are microstrip fed and use via less metamaterial structures. The design of these antennas is aimed at wireless applications below 6 GHz.

The rapid increase in the use of wireless operating devices and their capability of handling multiple technologies has led to an increase in the demand of antennas operating at multiple frequency bands. The monopole antennas have low profile and can be easily manufactured and integrated into the devices. Hence, a proper combination of these antennas with an embedded metamaterial structures in the design is feasible for realising multiband antennas. The slots, composite right left-handed transmission line (CRLH-TL), split ring resonators (SRR), composite split ring resonators (CSRR) and meandered line structures are incorporated in the antenna design to realize the multiband antennas. Moreover, to enhance the certain performance parameters of the antenna, metasurfaces formed by artificial magnetic conductors (AMC) and perfect electric conductors (PEC) have been employed.

In this thesis, the design of antennas targeted towards the WLAN, WiMAX, and sub-6 GHz 5G applications has been presented. Initially, a monopole antenna with slots etched on the radiator has been presented in chapter three. The slots are employed in the design to realise the dual band (2.38 - 2.7 GHz, and 3.28 - 5.8 GHz) nature of the antenna and it is backed by an AMC surface for enhancing the gain of 5dBi in the first band and 2.8 dBi in the second band. In chapter four, a compact antenna of the order $0.3\lambda_0$ x $0.2\lambda_0$ x $0.01\lambda_0$, dual band (3.15 - 4.09 GHz and 5.35 - 5.84 GHz) CRLH-TL metamaterial inspired design and the circuit realization of the antenna are also presented. In chapter five, a meandered line loaded dual band (3.26 – 3.61 GHz, and 5.06 – 6.77 GHz) antenna backed by a meta surface has been designed and presented with circular polarisation in one of the bands. Finally, a split ring resonator (SRR) and complementary split ring resonator (CSRR) based multi band antennas suitable for 2.5/3.5/5.5 GHz WiMAX, and 5.2/5.8 GHz WLAN applications has been presented in chapter six.

CONTENTS

List of Figures

List of Tables

Nomenclature

4G	4th Generation
5G	5th Generation
ABW	Absolute Bandwidth
ADS	Advanced Design System
AMC	Artificial Magnetic Conductor
CP	Circular Polarization
CPW	Coplanar Waveguide
CRLH	Complementary Right Left-Handed
CST	Computer Simulation Technology
CSRR	Complementary Split Ring Resonator
EM	Electro Magnetic
ENG	Epsilon Negative
FCC	Federal Communications Commission
FBW	Fractional Bandwidth
GPS	Global Positioning System
GSM	Global System for Mobile Communication
HFSS	High Frequency Structured Simulator
IEEE	Institute of Electrical and Electronics Engineers
ISM	Industrial Scientific and Medical
LH	Left-Handed
LOS	Line of Sight
MIMO	Multi Input Multi Output
MNG	Mu-Negative
MTM	Metamaterial
NB	Narrowband
NR	New Radio
PEC	Perfect Electric Conductor
PIN	P-type Intrinsic N-type
PMA	Printed Monopole Antenna

RF	Radio Frequency
RH	Right-Handed
SMA	Sub Miniature version A
SRR	Split Ring Resonator
TL	Transmission Line
UWB	Ultra-Wideband
VSWR	Voltage Standing Wave Ratio
WB	Wideband
Wi-Fi	Wireless Fidelity
WiMAX	Worldwide Interoperability for Microwave Access
WLAN	Wireless Local Area Networks

Chapter-1

Introduction

1.1. Introduction

The demand for wireless operating devices, such as smartphones, laptops, tablets, and other wireless devices, has been steadily increasing over the years. With the technology advancement and widely accessible high speed wireless networks, such devices have become a crucial part of our everyday life. However, the miniaturization and incorporation of multifunctions into this wireless equipment is of great interest. An antenna is one of them, modern wireless devices require antennas to support portability, allowed to be integrated into different devices, operating across multiple frequency bands, handling multifunctions, adapting to emerging technologies etc.

Many technical solutions have been introduced as part of the design to satisfy the afore-mentioned requirements. The utilization of electromagnetic metamaterials in antenna design can boost its performance on the basis of miniaturization, increasing gain, enhancing bandwidth, generating multiband frequencies, beam steering etc. Metamaterials are a unique class of artificial materials with distinctive electromagnetic properties which are non-existent in naturally occurring materials.

The classification of metamaterials is based on the sign of permittivity, ε, and permeability, μ of a homogeneous materials and is represented in Fig. 1.1. The materials corresponding to the first, second and fourth quadrant are conventional and naturally existing, but the materials corresponding to the third quadrant where both permittivity and permeability are negative are called double negative materials which are not found in the nature, and they exhibit unusual properties. These materials when properly loaded as part of the antenna design

are helpful in realizing antennas with unique and novel characteristics. The interest in using metamaterials for antenna design to enhance its performance characteristics has been growing and the scope for research in this area is existent.

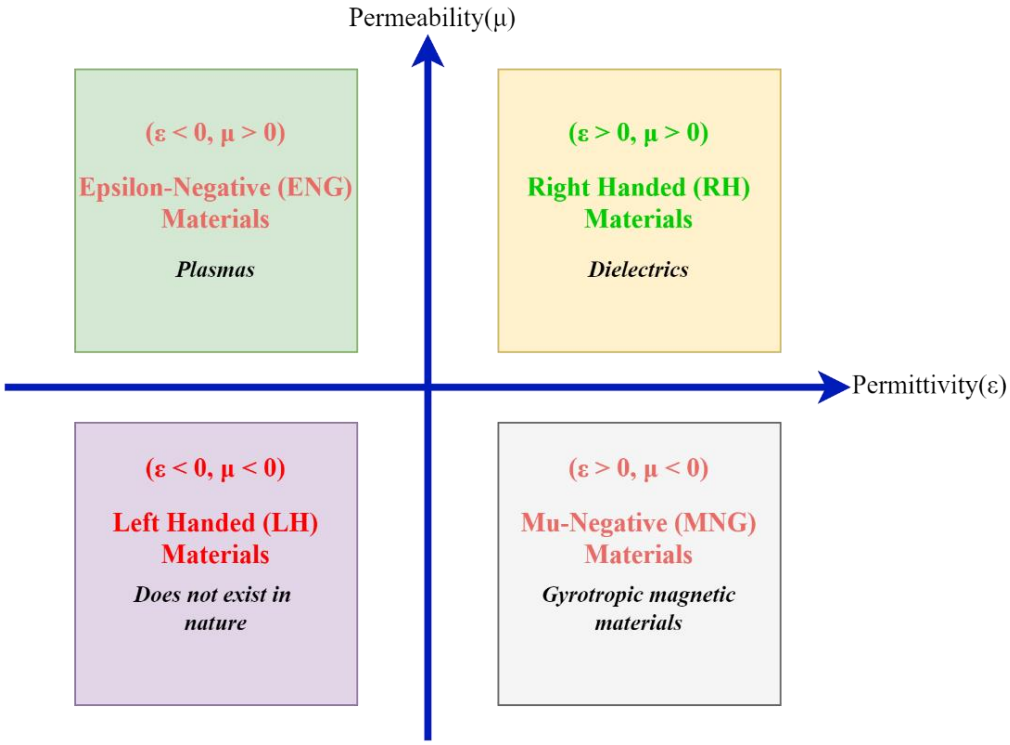

Fig. 1.1. Classification of metamaterials based on ε and μ values[11]

1.2. Basics of an Antenna

An antenna is an inevitable building block in all wireless communication systems and no wireless communication is imagined without having an antenna. It is a normal metallic device (typically rod or a wire) used for either radiating or receiving radio waves according to Webster's dictionary. As per IEEE standard 145-1983, it is defined as "a source that is meant for radiating radio waves or receiving radio waves" [1]. As depicted in Fig. 1.2, the transmission line (guiding device) transports the electromagnetic energy to the antenna from the transmitting source. Finally, electrical signals are converted to electromagnetic waves by the antenna. At the receiving end, the antenna behaves as a sensor to capture the electromagnetic waves.

As illustrated in Fig. 1.3, a sinusoidal voltage source, which has a peak voltage V, has been to an antenna. The internal resistance is R_s and reactance is X_s of the source respectively.

R_l, R_r, and X_a represent loss resistance, radiation resistance, and reactance of the antenna, respectively.

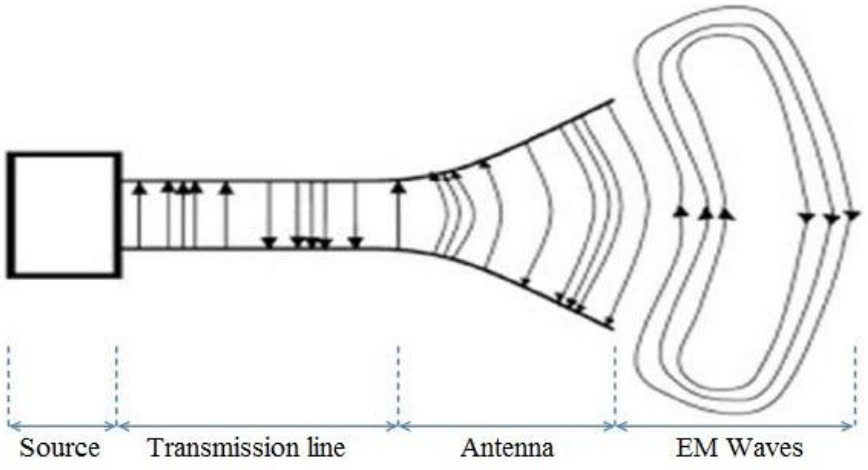

Fig. 1.2. Antenna as a transition device [2]

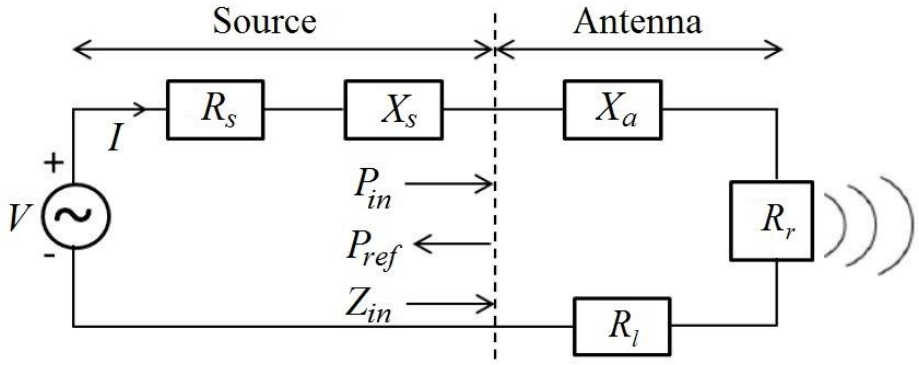

Fig. 1.3. Equivalent circuit of an antenna [2]

Several antenna parameters are defined as follows:

1.2.1. Input Impedance

The input impedance of an antenna is described as the ratio of the voltage to current at the terminals of the input. If V_a is the voltage and I is the current that are fed to the antenna, the mathematical expression of the input impedance is defined as

$$Z_{in} = \frac{V_a}{I} \tag{1.1}$$

If R_a is the antenna's resistance and X_a is the antenna's reactance then the input impedance of antenna is given as

$$Z_{in} = R_a + jX_a \quad (1.2)$$

R_a is expressed as sum of antenna's loss resistance R_l and antenna's radiation resistance R_r.

$$R_a = R_l + R_r \quad (1.3)$$

All conductor losses and dielectric losses are accounted in case of loss resistance R_l. For maximum power to transfer to the antenna, source impedance Z_s and input impedance Z_{in} must match properly. So, impedance must be equal to the conjugate of the impedance of the source for perfect impedance matching according to the maximum power transfer theorem.

$$Z_{in} = Z_s^* \quad (1.4)$$

$$\text{So, } R_a = R_s \text{ and } X_a = -X_s \quad (1.5)$$

Generally, the internal resistance is 50 Ohms for all microstrip antennas. Therefore, the input impedance of the antenna must be equal to 50 Ohms for perfect impedance matching.

1.2.2. Reflection Coefficient

Reflection coefficient Γ is a crucial parameter to find out how much incident power being reflected back to source. It is the amount of mismatch between the antenna and source and is referred to as the ratio of the reflected power P_{ref} to the incident power P_{in}.

$$\Gamma = \frac{P_{ref}}{P_{in}} \quad (1.6)$$

When it is expressed in dB, the mathematical expression for the reflection coefficient is given as

$$\Gamma \text{ (dB)} = 10 \log \left(\frac{P_{ref}}{P_{in}}\right) \quad (1.7)$$

Return loss is also a parameter of antenna similar to reflection coefficient. It can also be expressed in dB and given as

$$\text{Return loss (dB)} = -\Gamma \text{ (dB)} \quad (1.8)$$

A reflection coefficient of -15 dB indicates a return loss of 15 dB. So, return loss is always a positive quantity since reflection coefficient is a negative quantity. Generally, reflection

coefficient < -10 dB is preferred for an antenna. Reflection coefficient of -10dB indicates that one-tenth of the incident power is reflected.

1.2.3. VSWR

Voltage standing wave ratio (VSWR) is an important parameter to find out how much incident power is reflected to source. The acceptable VSWR for an antenna is less than 2. VSWR is used to find out the reflected power in another way and can be found out from the mathematical expression given below.

$$\text{VSWR} = \frac{1 + |\Gamma|}{1 - |\Gamma|} \tag{1.9}$$

1.2.4. Bandwidth

The antenna's bandwidth is normally nothing but the frequency range, where the antenna works properly. The antenna's parameters such as polarization, reflection coefficient, beam width, radiation efficiency, gain, etc., are within their acceptable value in the bandwidth of an antenna. Two types of bandwidths are generally used to express the bandwidth of an antenna. They are absolute bandwidth (ABW) and fractional bandwidth (FBW). The absolute bandwidth is nothing but the separation between the upper and lower cut-off frequencies f_H and f_L respectively. Whereas the FBW is considered as the percentage difference of upper and lower cut-off frequencies over centre frequency f_C. The mathematical expressions of absolute bandwidth and fractional bandwidth are given as

$$\text{FBW (\%)} = \frac{f_H - f_L}{f_C} \times 100 \tag{1.10}$$

where

$$f_C = \frac{f_L + f_H}{2} \tag{1.11}$$

The fractional bandwidth percentage for wideband antennas and UWB antennas should be more than 10% and 20%, respectively, as per FCC. In case of narrowband antennas, it is less than 10%. Impedance bandwidth is mostly considered for any antenna and generally, it is the range of frequency with the return loss of less than 10 dB is termed as the impedance bandwidth.

1.2.5. Polarization

The plane in which the electric field exists determines the orientation of radio wave. This orientation of the radio wave is nothing but the polarization of the antenna. In general, three different types of polarization (linear, circular, and elliptical polarizations) are generally possible for an antenna. The concept of axial ratio is used to find out the polarization. The ratio of the orthogonal electric field components gives the axial ratio. Axial ratio is unity for a circularly polarized antenna since orthogonal components of electric field are equal in magnitude. It is greater than 1 in case of an elliptically polarized antenna, whereas it is infinity in case of a perfect linearly polarized antenna.

1.2.6. Directivity and Gain

The directivity is described as "the ratio of the radiation intensity U from the antenna in a specific direction to the radiation intensity of an isotropic source U_0" as per the *IEEE Standard Definition of Terms for Antennas*. The radiation intensity U_0 is $\frac{P_{rad}}{4\pi}$ for an isotropic source, where P_{rad} is the radiated power of the antenna. The mathematical expression of directivity is shown below.

$$\text{Directivity} = \frac{U}{U_0} = \frac{U}{\frac{P_{rad}}{4\pi}} = \frac{4\pi U}{P_{rad}} \tag{1.12}$$

Gain is also a crucial parameter to describe the antenna's radiation performance. The directivity and radiation efficiency are taken into account in case of antenna gain. Antenna gain in a specific direction is described as the ratio of the radiation intensity in a specific direction $U\ (\theta, \phi)$ that is achieved if the power, which is fed to the antenna, is equally radiated in all directions. If P_{in} is the total input power or power fed to antenna then the radiation intensity of the power radiated equally in all directions is $\frac{P_{in}}{4\pi}$. The antenna gain is given as

$$\text{Gain} = \frac{radiation\ intensity}{\frac{total\ input\ power}{4\pi}} = 4\pi\ \frac{radiation\ intensity}{total\ input\ power} = 4\pi\ \frac{U\ (\theta,\ \phi)}{P_{in}} \tag{1.13}$$

Normally, antenna's reported gain is considered in most of the cases. It is described as the power gain of antenna in a given direction to the power gain of an antenna that is considered as reference in its referenced direction. Both of the antennas must be fed with same input power in this case. Typically, dipole antennas, horn antennas, etc., for which their gains are known,

are taken as reference antennas. The reference antennas in most of the cases are lossless isotropic sources. The mathematical expression for the antenna relative gain is given as

$$\text{Gain} = 4\pi \ \frac{U\ (\theta,\ \phi)}{P_{in}\ (lossless\ isotropic\ source)} \tag{1.14}$$

The expression for gain in terms of directivity and radiation efficiency is given as

$$\text{Gain} = \text{Directivity} \times \text{Radiation Efficiency} \tag{1.15}$$

where radiation efficiency ρ_{rad}, described as the ratio of power radiated to the power fed to the antenna (input power). Its mathematical expression is shown below.

$$\rho_{rad} = \frac{P_{rad}}{P_{in}} = \frac{R_r}{R_r + R_l} \tag{1.16}$$

1.2.7. Radiation Pattern

Radiation pattern is a graphical representation of the radiation of the antenna as a function of space coordinates or a mathematical function according to IEEE std 145-1983. It is found out in the far-field region in most of the cases and is demonstrated as a function of the directional coordinates.

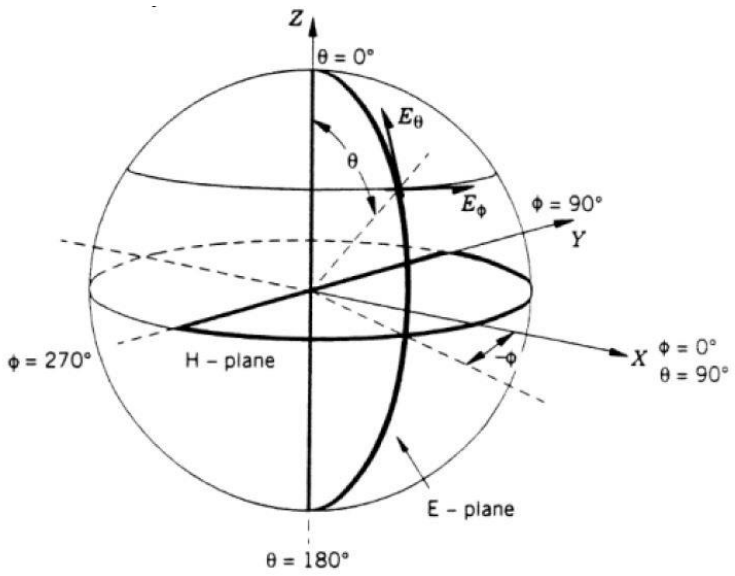

Fig. 1.4. Three-dimensional spatial radiation distribution of an antenna [2]

The radiation properties comprise field strength, power flux density, directivity, radiation intensity, polarization. Typically, the radiation pattern is spatial distribution of the electromagnetic energy radiated. The spatial distribution is either two dimensional or three

dimensional. Fig. 1.4 shows the 3D coordinate system in terms of θ and ϕ in space. A combination of several two-dimensional antenna radiation patterns gives a three-dimensional antenna radiation pattern.

Antenna's radiation performance is demonstrated with reference to two patterns in principal planes (E and H) in case of linearly polarized antennas. The E-plane and the H-plane are defined as "the plane that comprises the electric field vector and the maximum radiation's direction" and "the plane that comprises the magnetic field vector and the maximum radiation's direction", respectively. Radiation patterns are classified into three types as per the radiation behaviour of the antenna. The first type, the second type, and third type are isotropic, directional, and omnidirectional, respectively. An isotropic radiation pattern, which does not exist in practice, is a lossless antenna radiation pattern in which same radiation exists in any direction.

The directive properties of antennas that are under test are described by taking an isotropic antenna as reference. But the isotropic is an ideal antenna that is not physically realizable. In case of antenna that has directional radiation pattern, radiation or reception of electromagnetic energy occurs more in some specific directions than other directions. If the maximum directivity of an antenna is more than that of directivity of a normal dipole antenna then the pattern of that antenna will be directional. If the radiation pattern of an antenna is non-directional in one plane and directional in orthogonal planes then the antenna pattern is said to be omnidirectional.

1.3. Microstrip Antenna

Despite many varieties of antennas, such as linear wire antennas, loop antennas, horn antennas, lens antennas, reflector antennas etc., are being utilized for different applications in wireless systems, microstrip antennas have grabbed more attention due to their advantages, such as light weight, compactness, inexpensive, easy manufacturability with modern printed circuit technology, simple integration with planar structures, and conformable to nonplanar surfaces as well. However, the microstrip antennas have disadvantages like narrow bandwidth, low efficiency, low power, spurious feed radiation, etc. Microstrip antennas are often called as patch antennas.

Even though the microstrip antenna was discovered in 1953, it has grabbed good attention in 1970s. Since then, rigorous research in microstrip antennas has been going on for

different applications. The geometry of the basic patch antenna is shown in Fig. 1.5. As depicted in Fig. 1.5, it comprises of a dielectric substrate having h and has two conducting layers at the front and back portions of the substrate. Typically, copper is used for conducting layers.

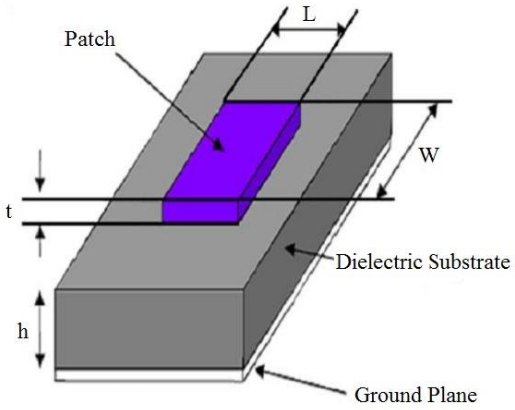

Fig. 1.5. Structure of basic patch antenna [1]

The upper and lower conducting layers are referred as radiating patch and ground plane, respectively. Rectangular and circular radiating patches are normally more preferred in practice. Depending on the requirements, other shapes can also be used. Various complex structures have also been investigated in the literature as they can be simulated easily with the help of some advanced simulators. Some shapes of the radiating patches are displayed in Fig. 1.6.

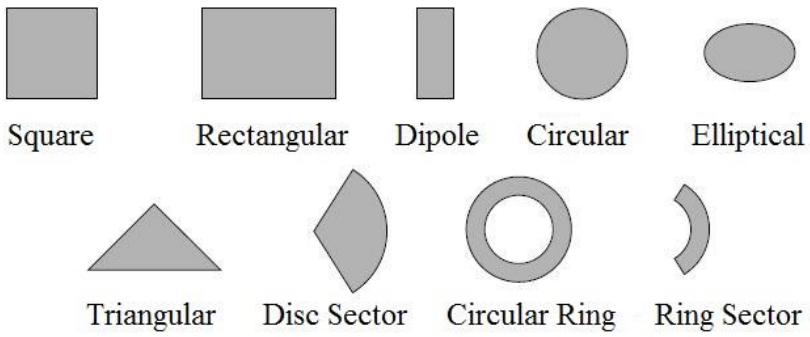

Fig. 1.6. Different shapes of the radiating patches [1]

In order to feed microstrip antenna, many feeding techniques are used. Some of them [3, 4] are the microstrip line feed [5, 6], coaxial probe feed [7], proximity and aperture coupling. Microstrip line feed is the simplest technique among them since its fabrication is easy and impedance matching of the radiating patch and the microstrip feed line can be done easily [8]. The microstrip line feed patch antenna is represented in Fig. 1.7.

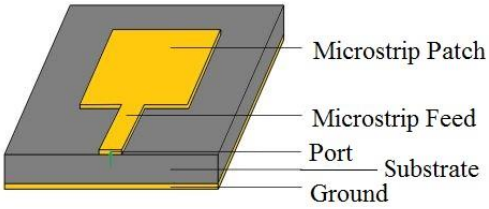

Fig. 1.7. Microstrip line fed patch antenna [9]

The mathematical equations for finding out the dimensions of the radiating patches with different shapes are given in [1]. The conventional radiating patches produce single resonating band with narrow bandwidth. So, to generate multiband, slots are incorporated in the radiating patches as incorporation of slots in patch leads to multiple resonating paths. Also, incorporation of slots in ground plane can also produce multiple resonant frequencies. When some portion of the ground plane is etched, perturbations in the current distributions occur. The perturbations in the ground plane generated by slots and the energy coupling that exists between the slots generate multiple resonant frequencies.

In case of a rectangular patch, the equations involved[1] in the design for an efficient radiation considering the substrate dielectric constant (ε_r), its height (h), and the resonant frequency (f_r) are:

$$\text{Width, } W = \frac{1}{2f_r\sqrt{\mu_0\varepsilon_0}}\sqrt{\frac{2}{\varepsilon_r+1}} = \frac{v_0}{2f_r}\sqrt{\frac{2}{\varepsilon_r+1}} \tag{1.17}$$

$$\text{Length, L} = \frac{1}{2f_r\sqrt{\varepsilon_{reff}}\sqrt{\mu_0\varepsilon_0}} - 2\Delta L \tag{1.18}$$

where ΔL is the extension of the length and ε_{reff} is the effective dielectric constant.

In designing the circular patch and assuming dielectric constant of the substrate(ε_r), resonant frequency (f_r) and height of the substrate as h. The equations for solving the radius(a) of the patch[1] are

$$a = \frac{F}{\left\{1+\frac{2h}{\pi\varepsilon_r F}\left[ln\left(\frac{\pi F}{2h}\right)+1.7726\right]\right\}^{1/2}} \tag{1.19}$$

$$F = \frac{8.791\ X\ 10^9}{f_r\sqrt{\varepsilon_r}} \tag{1.20}$$

1.4. Printed Monopole Antenna

The conventional microstrip antennas, microstrip fed slot antennas, and microstrip antennas with defected ground structures have narrow operating bandwidths. Since the world has been witnessing enormous development in modern wireless communication systems, antennas with wide bandwidth are of great demand. Also, single antenna with wide bandwidth covers many applications. A printed monopole antenna is a type of antenna that is fabricated on a printed circuit board (PCB) or other planar substrate. It is a variant of the monopole antenna, which is a simple and widely used antenna configuration with a single radiating element. The term "printed" indicates that the antenna is created using printed circuit board technology. Nowadays, printed monopole antennas (PMAs) are widely being used as they have wide impedance bandwidth. So, they are considered to be the one of the promising candidates due to their omnidirectional pattern in azimuthal plane and wide bandwidth. The conventional microstrip antenna has directional radiation patterns, whereas it is similar to that of radiation pattern of a dipole antenna in case of printed monopole antenna. Integration with other components can be done easily in case of printed monopole antennas since they have reduced size and no backing of ground plane is required. Moreover, these printed monopole antennas are very easy to fabricate. In general, for mobile wireless technology based low-cost systems, cost effective printed monopole antennas, which are generally manufactured on a cost-effective FR-4 substrate, are mostly preferred.

The main consideration while designing an antenna that has an impedance bandwidth ratio of 3.42:1 for VSWR $\leq$ 2 with a large impedance bandwidth is the antenna must have multiple resonances. This can be realized easily by printed monopole antennas. Unlike conventional dipole antennas, conventional monopole antennas, and conventional microstrip antennas that have single resonance, some modified design considerations have to be followed. So, in case of printed monopole antennas, the edge frequency of lower band and bandwidth are the crucial design parameters to be considered. The maximum height of the printed monopole mainly decides the lower band edge frequency. Whereas the impedance matching needs to be ensured between microstrip line and impedance of various modes decides the total bandwidth.

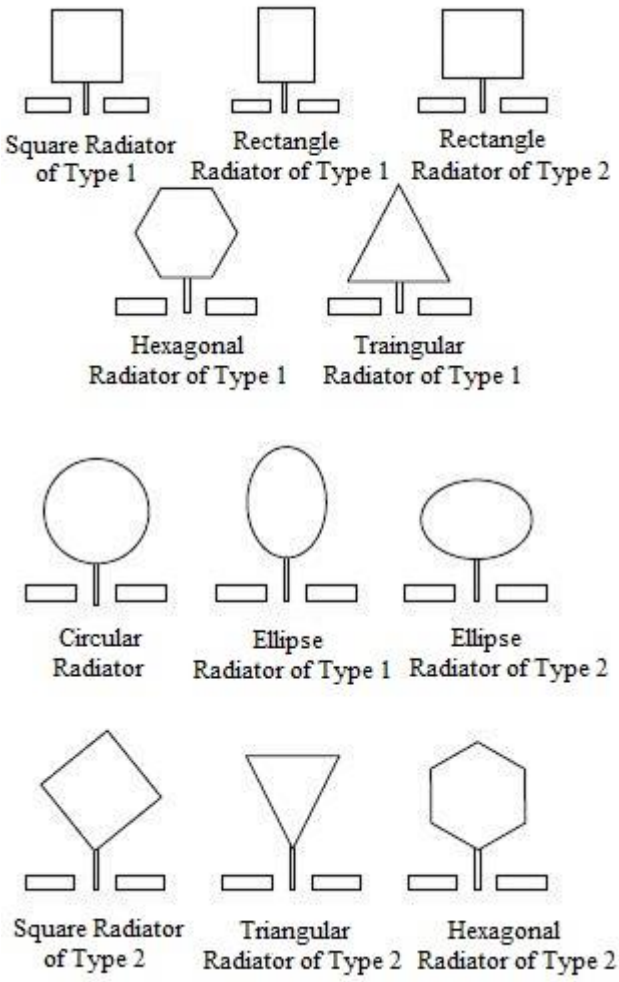

Fig. 1.8. PMAs with various shaped radiators [10]

The printed monopole antenna achieves good azimuthal radiation pattern with very wide impedance bandwidth. The reasons can be demonstrated in two ways. The PMA can be treated as microstrip antenna configuration, whose location of the backing ground plane is at infinity. As it is known that a patch is normally located on a substrate (typically FR4), and it is assumed that the air, which is a thick dielectric substrate and has a relative permittivity of 1, exists above the substrate. This kind of microstrip antenna configuration with a thick dielectric substrate of relative permittivity close to 1 produces large impedance bandwidth.

On the other hand, PMAs can be viewed as vertical monopole antennas. Normally, a monopole antenna comprises a vertical cylindrical wire that is mounted over its ground plane. As its diameter increases, bandwidth also increases. A cylindrical monopole antenna, which has a large effective diameter, can be equated to a PMA. The lower band edge frequencies can be determined using this analogy for all regular shapes of PMAs for various feed configurations.

The PMAs with various shapes are depicted in Fig. 1.8. The shapes of the radiator of PMA include square, rectangle, hexagon, triangle, circle, and ellipse for different feed positions, as illustrated in Fig. 1.8. The mathematical equation relating to lower band edge frequency of PMA with any regular shape is given in [10].

1.5. Metamaterials

Metamaterials are the artificially developed materials that exhibit unique properties like negative permittivity, permeability, and refractive index simultaneously, leading to their unusual behaviour. Meta refers to beyond, and Metamaterials are materials with properties beyond the naturally existing materials. Metamaterials were developed by Victor Veselago, a Russian scientist in 1967[11]. These materials are artificial effectively homogenous structures whose structural average cell size is less than one fourth of the guided wavelength (λ_g). The behaviour of these materials is more because of their metallic structure design. The waves that interact with these metallic structures tends to alter their electromagnetic properties and hence leading to negative values of permeability(μ), permittivity(ε), and the refractive index(n), they are related as

$$n = \pm\sqrt{\varepsilon_r \mu_r} \tag{1.21}$$

As illustrated in the Fig. 1.1, among the possible combinations of (ε, μ), the simultaneous negative μ and ε corresponds to materials that are left-handed and are characterized by negative refractive index (NRI) or antiparallel phase and group velocities. These LH structures are most often termed as Metamaterials. A left-handed triad of electric, magnetic fields and the wave vector is formed in LH materials as compared to a right-handed triad in conventional materials.

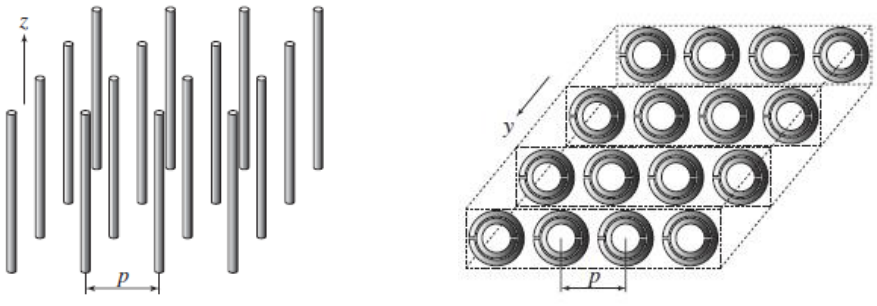

(a) (b)

Fig. 1.9. First Metamaterial structure composed of only metals and dielectrics (a) Thin-wire (b) Split ring resonator structure [11]

The first experimental demonstration of LH material was done 30 years later by Smith[11], which revealed that it is an artificially effective homogenous structure and not natural. Pendry introduced the structures shown in Fig 1.9, which are of plasmonic type with (-ε, +μ) and (+ε, -μ). These structures exhibit an average cell size p less than the guided wavelength (p << λ_g) and hence are homogenous.

Several unique phenomenon that occur for an electromagnetic wave that passes through a LH media as predicted by Veselago, include reversal of Doppler effect, Vavilov-Cerenkov effect, Snell's law, and frequency dispersion etc.

1.5.1. Reversal of Snell's Law

Snell's law describes how light or electromagnetic waves change direction when they pass from one medium into another with a different refractive index. In the context of traditional materials, Snell's law states that the angle of incidence (θ_1) is related to the angle of refraction (θ_2) by the following equation:

$$n_1 sin\theta_1 = n_2 sin\theta_2 \tag{1.22}$$

Where n_1 and n_2 are the refractive index of first and second medium. In metamaterials, which are engineered materials, it is possible to achieve some interesting and unconventional effects, including the reversal of Snell's law. This is often accomplished by manipulating the effective refractive index of the metamaterial. To reverse Snell's law in metamaterials, you would need to design a metamaterial with a negative refractive index. When n_1 and n_2 are both negative, the angles θ_1 and θ_2 can be such that the electromagnetic wave is bent in the opposite direction compared to what is predicted by Snell's law in conventional materials.

Applying metamaterials to antenna design is an important application because antennas with novel characteristics can be designed, that may not be easily attained with the naturally occurring materials. The purpose and structure of the design determines the type of loading of metamaterials. These metamaterials can be applied in the form of a unit cell or a combination of these unit cells forming an array. Initially a unit cell is designed, and its resonance frequency, permittivity and permeability are evaluated and optimized to be operating at a required frequency.

Metamaterials can be used as a part of the antenna design where the structure is embedded within, is helpful in realizing compact antennas and can also be used near the antenna

environment like artificial magnetic conductors and metasurfaces which are likely to improve the gain, bandwidth, directivity, and radiation etc. The metamaterials with left-handed transmission line properties are used to create compact, high-gain antennas and achieve other performance enhancements, such as reducing size of the antenna still maintaining good efficiency.

1.6. Metamaterials in Antenna Design

Metamaterials are incorporated in the antenna design to enhance their performance and capabilitiesand they electromagnetic properties that are unique and not found in naturally occurring materials. They are designed as unit cells, typically using patterns of conductive elements to manipulate electromagnetic waves in for desired performance. Metasurfaces are two-dimensional arrangements of structures designed to control the properties of electromagnetic waves. These surfaces are engineered to manipulate the amplitude, phase, and polarization of incident waves, allowing for control over the radiation from the antenna. Metasurfaces have gained significant interest in the field of antenna design due to their ability to control and manipulate electromagnetic waves with a high degree of precision.

One of the fundamental functionalities of metasurfaces is the ability to control the phase of incoming electromagnetic waves. The AMC has a zero-reflection phase at a desired frequency achieved by adjusting the geometry, size, and arrangement of the structures, metasurfaces formed using these AMC unit cells can introduce the phase shifts to the incident waves and hence reflecting the waves in specific direction leading to an increase in the gain and achieving directional radiation patterns. The PEC based metasurface introduces a phase shift of 180 degrees and is used to control the beam steering of the antenna. The elements on the metasurface are strategically arranged to induce specific phase shifts and amplitude variations for different polarizations and can be used as polarization converters. The use of metamaterials and metasurfaces could impact the performance of antenna based on the type of loading of these metamaterial structures and will enhance the antenna performance in terms of the following aspects:

1.6.1. Miniaturization

Miniaturization is an important aspect of modern mobile communication systems but traditionally the antenna performance is related to its size. However, the zero-order resonance(ZOR) mode of metamaterials is used to realize the miniaturized antennas with a

small electrical size by making the antenna size independent of its operating frequency. The use of CRLH metamaterials helps in achieving this zeroth order resonance and aids in realizing the miniaturized antennas. Metamaterials enable the creation of compact and low-profile antennas which are easily integrated into various devices, including smartphones, IoT sensors, and military equipment.

1.6.2. Dual and Multi-band antennas

The requirement of antennas operating across multiple frequency bands covering multiple technologies has increased tremendously. The dual band and antennas can be realized using the metamaterial which helps in increasing the coverage in terms of operating at different frequency bands. The advantage of using these metamaterials is the generation of additional resonant modes which are symmetric with respect to ZOR and hence resulting in a similar and better radiation patterns at different frequency bands.

1.6.3. Wide Band antennas

Metamaterials can be tailored to cover a wide range of frequencies within a single compact antenna design. This capability is especially important in applications where the antenna needs to operate across multiple frequency bands efficiently. This makes them suitable for systems that require versatile frequency coverage without the need for multiple antennas. Metamaterials can also be engineered to be tunable, and hence are adjusted to achieve the required resonant frequency coverage of the antenna. This feature helps in adapting to the different frequency requirements.

1.6.4. Gain Enhancement and Improved radiation patterns

Metamaterials can also enhance the gain of the antennas, which concentrate the radiation in a specific direction, increasing the signal strength in that direction. This is beneficial for long-distance communication applications. Metamaterial superstrates and substrates placed above or below the antenna can alter the radiation characteristics. Superstrates, placed above the antenna, can collimate the radiation, while substrates, placed below, can enhance the impedance matching. These metasurfaces can be realized using the unit cells designed and can be placed in the antenna environment helpful in achieving the high gain and directional radiation patterns.

1.7. Motivation

The microstrip antennas have several advantages that include low profile, light weight and can be manufactured easily on a PCB. They are manufactured to have different shapes and sizes and are flexible in terms of integration into various devices and components. Several techniques have been applied to microstrip antennas to achieve miniaturization such as using a substrate with high permittivity, some deformations, fractal geometries etc. However, these techniques when employed lead to small bandwidth and low gain. With proper loading of metamaterials to the antenna design its performance could be improved.

Multiband and wideband antennas are very valuable in wireless applications as they will be able to cover multiple frequency bands and wide frequency range. They offer several benefits like cost and space saving, flexibility, and simplified design.

Several attempts were made to design antennas operating at multi bands and to address the requirements of these frequency bands [12-18]. However, the tradeoff between the physical dimensions of the antenna and its performance parameters is of great importance. Some AMC based antennas have been reported [30-32], but with a large sized reflecting surface making the overall antenna size bulky. CRLH metamaterial antennas are suitable for realizing multiband antennas [46-51] but offer less gain due to their small size. Several metasurface backed antennas were reported [79 - 84] where size is a constraint. So, the antennas operating over multiple bands and are designed at a considerably smaller size and offer a decent performance characteristic could serve the purpose.

This has motivated us in presenting microstrip based multiband metamaterial antennas. These antennas enable efficient spectrum utilization and multi standard compatibility through accommodation of different frequency bands in a single antenna structure. The multiband antennas are engineered using metamaterials to be miniaturized and compact and hence can be integrated into small devices facilitating an efficient use of space. As the wireless communication systems are ever evolving, the antennas providing flexibility in adapting to emerging technologies is a key aspect and to be equipped to operate in new frequency bands as they become available is an added advantage. The use of these metamaterials offering unique electromagnetic properties in antenna design improves its performance characteristics such as an enhanced bandwidth, improved gain, better radiation patterns across different frequency bands.

1.8. Research Objectives

The objectives of the proposed work for multiband antennas are:

1. To design and develop a dual band antenna for WLAN, WiMAX, and sub-6 GHz 5G wireless applications and enhance the gain of the antenna considerably (by 4 - 5 dBi) using a metamaterial structure.
2. To design and develop a multiband antenna for wireless applications below 6 GHz, with an increased bandwidth to cover the entire sub-6 GHz 5G bands (from 3.3 - 5 GHz) by incorporating metamaterial structure.
3. To design and develop a multiband antenna for wireless applications below 6 GHz, with compact dimensions of the order $< 0.5\lambda_0$, and a planar structure by making use of transmission line-based metamaterials as a part of the design.

1.9. Thesis Organization

The thesis is organized as seven chapters. A brief overview of each chapter is provided in this section.

Chapter 1: Presents the introduction, reason for choosing the problem and objectives.

Chapter 2: Provides the literature Survey and background information regarding the use of metamaterials and their type of loading.

Chapter 3: Presents the procedure in designing a dual band monopole based radiating antenna for wireless applications. Also, a dual band AMC is proposed for the purpose of increasing gain.

Chapter 4: Describes a composite right left-handed (CRLH) metamaterial inspired compact antenna with dual band operation and the circuit realization of antenna is also presented.

Chapter 5: Illustrates the design of a meandered line incorporated dual band antenna covering some bands of WLAN/WIMAX applications. Additionally, a metasurface is presented for improving the gain and radiation characteristics.

Chapter 6: Comprises of split ring resonator (SRR) and complementary split ring resonator (CSRR) loaded multi band antennas for wireless applications.

Chapter 7: Provides the conclusions and a brief discussion on the future scope of the work.

Chapter-2

Literature Survey

2.1. Introduction

In this chapter, the literature relating to microstrip antenna, monopole antenna, metamaterials and their effect on the performance of the antenna are reported. The literature review has been presented according to the objectives highlighting the current state of art.

2.2. Literature Review

Till now, many works have been presented on metamaterial-based antennas with multiband operation for wireless applications and also antennas backed by metasurface. Some of them are listed as follows:

Ashish *et al*., (2018) proposed a monopole antenna[12] that uses two main radiating elements for generating dual band with resonance at 2.5 and 5.1 GHz. Here, the rectangular strips with different sections L1, L2, L3 and L4 are employed, and the dimensions of these strips are adjusted in order to shift the resonance to a required frequency and achieve good bandwidth.

Karli *et al*., (2015) presented a miniaturized antenna with slots and partial ground plane, operating over a broadband for RFID and WLAN applications[14]. The antenna has a good and consistent omnidirectional radiation patterns and is manufactured on a FR-4 substrate, making it low cost and easily manufacturable using a printed circuit board.

Han Lu *et al*., (2014) proposed a compact antenna with a pair of L-shaped strips operating at 2.45/3/5.5 GHz bands[16]. A size reduction of 20% has been achieved by

controlling the surface currents through the T-shaped patch. The antenna has a stable radiation patterns with good efficiency.

Xiaolei L *et al*., (2013) presented an antenna[18] with radiator of compact size consisting of a stem and two branches working at 2.4 and 3.5 GHz WiMAX applications. Here, the frequency bands are independently set by varying the parameters of the radiating branches. The antenna also has a compact radiator of size 14.5 mm x 8.7 mm.

Malik *et al*., (2015) presented an antenna with a segmented ground plane in order to obtain a monopole like lower band resonance[21]. The microstrip line is loaded with dumbbell shaped defects to better the impedance matching by altering the effective reactance. An equivalent circuit model has also been developed and matching of the scattering parameters were observed.

Chu *et al*., (2015) proposed a CPW-fed rectangular patch etched with two different shaped slots for dual band operation. The slots are responsible in exciting the multi resonant modes and a very wide impedance bandwidth for the upper band[22]. The antenna has a planar design with a size of 30 mm x 25 mm, suitable for several bands of WLAN.

Jaswinder *et al*., (2013) proposed an antenna design that is composed of a pair of L-shaped patches that are inverted and placed symmetrically with a gap and a modified ground plane[25]. Here, the ground plane is modified to achieve an enhanced bandwidth in the upper resonating band. The antenna operates at 3.3 - 3.5 GHz and 4.9 - 6.2 GHz, is designed using an FR-4 substrate making it cost effective.

Bharadwaj *et al*., (2012) presented the study and comparison of different shaped slots like C, E and U over a patch[26]. The c-shaped slotted antenna suffers from narrow bandwidth and high cross polarization. The near field antenna radiation has been analysed to observe the effect of these slots on antennas radiation and is used to explain far-field characteristics.

An *et al*., (2020) proposed an antenna with one main strip and three parasitic strips that are grounded. It has a three-dimensional structure operating over two bands from 0.7 - 0.96 GHz and 1.6 - 5.5 GHz. The antenna covers all the three sub-6 GHz 5G bands[27].

Azim *et al*., (2021) proposed an antenna with multi slots and a low profile for 5G wireless applications[28]. The incorporation of slots introduces capacitive effect and are helpful

in realizing a wideband operation from 3.1 - 5.5 GHz, suitable for sub-6 GHz 5G bands and LTE bands. The antenna offers good patterns with decent gain and efficiency.

An *et al*., (2018) presented an antenna with a wideband for 5G applications. The antenna operates over four resonant modes with different frequencies. All of these are integrated into a single structure in order to increase the bandwidth with an improved gain[29]. Folded walls have been introduced for a better impedance matching.

Zhai *et al*., (2017) presented a dual band and dual-polarized antenna backed by an AMC for WLAN applications. In this article the authors have designed two sets of bowtie dipoles with 45 degrees polarisation and the baluns are used to excite these dipoles[30]. A unidirectional radiation patterns with an increased gain have been achieved with the introduction of an AMC surface.

Coetzee *et al*., (2018) proposed a quad band antenna[31] with complementary microstrip slot pair and secondary slot on a dielectric. An AMC surface is used for the purpose of increasing the gain and directional patterns. The antenna has a good radiation efficiency of greater than 90%.

Liu *et al*., (2020) proposed a miniaturized dual band operating antenna with T-shaped stricture for feeding. The antenna employs a U-shaped slot and a trapezoidal slot on bowtie dipoles to operate at 3.14 - 3.8 GHz and 4.4 - 5.02 GHz bands[32]. The antenna is found useful for applications in sub-6 GHz 5G mobile communications. The antenna offers a gain of 7.1 dBi and 8.23 dBi in two bands.

Zhu *et al*., (2009) presented a metamaterial-inspired antenna for WiFi applications[35]. Initially, a traditional monopole antenna has been designed which induces the only resonance at 5.15 - 5.8 GHz and with the loading of metamaterial an additional resonance for lower WiFi applications has been achieved at 2.4 - 2.48 GHz.

Li *et al*., (2018) proposed a CRLH metamaterial inspired dual band operating antenna with a planar configuration for WLAN and WiMAX applications[40]. The antenna has a folded monopole with a CRLH unit cell loaded. The operating bands are independently regulated as the resonances are due to the two different structures. The antenna offers linear and circular polarization in the first and second bands respectively.

Borhani *et al*., (2015) proposed a frequency reconfigurable printed microstrip antenna with a square slot for WLAN/WiMAX and Bluetooth applications. The antenna has a small size of the order 20 mm x 20 mm with a perturbed ground plane and a backplane with a cross shaped sleeve. The p-i-n diodes have been included as part of the design to achieve frequency reconfigurability[42].

Chien *et al*., (2013) reported a very compact and a uniplanar antenna based on meandered monopole for laptop[44]. The dual band operation is achieved by a tuning stub that is introduced into the meandered design. The stub also ensures impedance matching by providing a proper coupling with the meandered monopole. The antenna has three resonances within the two operating bands.

Sonak *et al*., (2019) presented a CRLH based antenna with zero order resonance and low profile. The antenna has patches of shapes rectangular, square and semi-circle and are optimally arranged and fed using a coplanar waveguide ground plane[45]. The patches form series inductance and the gaps between the patches introduce the series capacitance. The shunt inductance is provided by the meandered line and shunt capacitance by separation of the feed line and ground. The antenna has a very small overall dimensions with respect to the ZOR frequency 1.22 GHz.

Zarrabi *et al*., (2015) reported two forms of antenna composed of CRLH cells with different radiation patterns at two different frequency bands[46]. First antenna has two bands with resonance at 1.8 GHz and 5.5 GHz and the other antenna also has two operating bands supporting WLAN. The CRLH cells are used to tune the radiating patterns of the antenna and radiate omnidirectionally.

Tamrakar *et al*., (2021) presented a CRLH metamaterial antenna for 2.4 GHz and 5 GHz WLAN applications. A pin is used to short the edge of the radiating metal for generating the left-handed nature[47]. The antenna has a radiator and the ground plane separated by a distance of 6 mm apart by an air interface. The authors have also presented the circuit equivalent model of the designed antenna and the antenna has a gain of 2.3 dBi and 8.6 dBi in two bands respectively.

Ameen *et al*., (2021) proposed an antenna with a combination of CRLH transmission line resonator and an AMC, acting as a reflecting metasurface. The antenna has an improved performance parameters like bandwidth, gain and beamwidth with compact dimensions at 3.1

GHz[48]. The metasurface helps in achieving unidirectional radiation patterns in the two operating bands.

Zhou *et al*., (2013) presented an antenna with a CRLH unit cell as part of the radiating element with zero order resonance at lower frequency and positive order resonance at higher frequency bands[53]. An additional square shaped CSRR has been included in the design to achieve circular polarisation. The CRLH unit cell is analysed using the circuit model and the antenna offers linear polarisation in the lower band and circular polarisation in the second band.

Ali *et al*., (2016) proposed a microstrip based slot antenna operating at 2.4 GHz and 5.8 GHz. A metal patch with several slots and a pair of slits are etched in order to achieve the compactness and a total area reduction of 41.2 %, when compared with a patch antenna[72]. The antenna has also provided good and acceptable radiation patterns at the desired operating frequencies.

Garg *et al*., (2019) proposed the design of an antenna inspired by metamaterial for dual band operation in WLAN. Its size is of the order 20 mm x 24 mm, etched over an FR4 substrate and covering 2.4/5 GHz WLAN applications[73]. Here, the authors have made use of a triangular SRR and an open-ended stub to realize the dual operating bands.

Huang *et al*., (2014) investigated a metamaterial loaded multi band antenna covering several applications[75]. The monopole antenna of rectangular shape is designed with a resonance at 5.2 GHz and further a L-shaped inverted slot is incorporated, which introduces a resonance at 4.1 GHz. A reactive metamaterial loading of the antenna has shifted its operating frequency and also the third resonance is generated covering 2.4 GHz band. The antenna has a small size with good radiation and decent gain.

Ji *et al*., (2010) proposed an antenna configuration for the purpose of enhancing the bandwidth by making use of CRLH-TL structure[76]. The dispersion diagram-based analysis of the CRLH-TL is performed and the characteristics of the antenna with wideband operation are realized.

Niu *et al*., (2013) presented an asymmetric coplanar waveguide fed CRLH-TL based antenna with an improved bandwidth for LTE/WLAN/WIMAX applications[77]. The antenna offers an approximate fractional bandwidth of 58%, operating from 2.1 - 3.8 GHz. The ZOR of the antenna aids in size reduction of the antenna.

Sharma *et al*., (2015) proposed a planar antenna design based on composite metamaterial structure which consists of a patch consisting of a series gap, meandered line-based inductor and a radiating stub[78]. The antenna has a very compact size with dual band behaviour resonating at 1.22 GHz and 3.97 GHz. The antenna offers a wide impedance bandwidth of 60% in its second band.

Foroozesh *et al*., (2010) presented an investigation of several artificial magnetic conductors based on their reflection phase[79]. The monopole antenna configuration is used to analyse the performance, L-shaped monopole antenna and vertical monopole antenna are placed above the AMC surface and the effect of this surfaces on the performance parameters such as Gain, bandwidth, beamwidth and size of the antenna are explored. The broadband characteristics are achieved using the smaller size AMC ground planes and hence enabling the compact design.

Yi *et al*., (2013) presented a circularly polarised dual band antenna[80] based on electromagnetic band gap surface which is polarization dependent. The dipole antenna has an operational range of 3 - 3.5 GHz and 6.01 - 6.16 GHz with a bandwidth of 13.4% and 3.2%, is backed by reflector which converts a LP wave to a CP wave and hence leading to circular polarization in both the bands.

Ta *et al.,* (2017) proposed an antenna with an AMC with a low profile and dual band operation[83]. The authors have made use of single feed and two crossed asymmetric dipoles as radiators and is backed by a dual band AMC. Here, fours slits have been incorporated in a single unit cell to reduce the separation between the two bands and adjust them to work at a desired frequency. The antenna operates at 2.2 - 2.6 GHz and 4.9 - 5.5 GHz with 3-dB axial ratio bandwidths of 2.3 - 2.45 GHz and 5.05 - 5.35 GHz respectively.

Xie *et al.,* (2012) presented a CSRR based patch antenna. The CSRRs are etched on the ground plane of the antenna instead of the radiator and hence keeps the radiator as a conventional patch and providing a better gain[85]. The resonances of the antenna are observed at 3.87 GHz and 5.46 GHz respectively.

Ma *et al*., (2010) presented a microstrip antenna with a negative permittivity and permeability generated by CSRR array that is incorporated on ground of the antenna for size reduction. The authors have achieved a size reduction of about 35% with this design due to the

phase compensation between the substrate and the CSRR cells[86]. Further size reduction can also be achieved by tuning the CSRR dimensions properly.

Saurav *et al.,* (2014) proposed two antenna configurations including a tri band linearly polarised antenna and a dual band dually polarised patch antenna[88]. A square slot is etched diagonally on a conventional patch and is further loaded with mushroom unit cell to achieve triple band operating antenna. Later, the lower order modes of the antenna are combined to form a circularly polarised mode and hence realising a dual band dually polarised antenna.

Yousufi *et al.,* (2019) has presented a monopole-based antenna[89] with an inverted L-shape operating at 2.45/5.8 GHz suitable for RFID applications. The monopole is fed by a meandered line the ground plane is perturbed two complimentary split ring resonators. Initial resonance of 2.45 GHz is combined with an additional resonance due to the loading of the CSRRs at 5.8 GHz is realised. The antenna offers a decent bandwidth of 0.4 GHz and 1.6 GHz with an acceptable gain.

Paul *et al.,* (2017) presented a tri band antenna with slots and independent tuning capability. A square shaped slot and two split ring resonators are loaded in order to generate multiband nature[91]. The SRRs are with single and multiple splits to obtain the resonance at 4.3 and 4.7 GHz. The antenna also has an acceptable gain of greater than 3.8 dBi with an omnidirectional patterns in all the bands.

Basaran *et al.,* (2013) proposed a compact and a planar antenna based on complimentary split ring resonators[92]. The CSRRs are used for the purpose of size reduction and has its applications in WiMAX/ WLAN. It exhibits omnidirectional radiation patterns with an overall dimensions of 30 mm x 34 mm with the other dimensions that are optimised to realise the tri band nature.

Cheung *et al.,* (2015) presented a four band antenna[95] with slots wireless applications. The antenna has a rectangular shaped slot with dimensions of 48 mm x 18 mm, E-shaped and T-shaped stubs in order to derive the four bands. The antenna has a reasonable dimensions considering its operation in four frequency bands.

Xu *et al.,* (2017) proposed a tri band operating antenna with wide bands and circular polarisation. The design includes a L-shaped radiator and also the slits for a wide axial ratio bandwidth in the upper band[98]. The antenna offers circular polarisation in all the three

operating bands with an impedance bandwidth measuring up to 44% and 71% making it suitable for WLAN and X-band applications.

Baek *et al*., (2013) proposed a triple band circularly polarised antenna with hexagonal slot and slits[99]. The circular polarisation is achieved by adding these slits to the slot and is excited using a tapered line. A reflector is placed to improve the gain. The antenna operates from 3.2 - 4.5 GHz and 4.7 - 6 GHz having bandwidths of 33.1% and 22.7%.

2.3. Conclusion

It is obvious that the antenna design using the metamaterials for improving the performance and in realizing of multiband antennas is a well-researched topic. However, it is still at stage where most of the antenna designs in the literature survey are compromising on some of the parameters in order to improve certain desired parameters. So, this thesis presents the antenna designs that has an improved performance parameters with a reduced size and simple design configuration.

Chapter-3

Dual Band Antenna Designs with AMC for Wireless Applications

3.1. Introduction

With ever-growing wireless communication systems there is a need for the subsequent increase in the growth of the antenna technology that is being employed in these systems. The requirement for a simple design yet well performing antenna is the need of the hour. 5G wireless communications are being initiated all around the world and the necessity emerges for the design of an antenna covering these 5G bands and the already existing wireless frequency bands. 5G spectrum being divided into three bands low frequency band (below 1GHz), mid frequency band (sub-6 GHz) and high frequency band (mm Wave) with the mid-band offering good data rates with decent coverage.

Multiband antennas are most desirable because they are flexible, and their role becomes even more important in this switching phase as they should be able to operate at both the existing WLAN and WiMAX bands as well as the upcoming technology. The frequency band between 3-5 GHz being promoted for the sub-6 GHz mid-band communications, the N77/N78/N79 bands are being operated in this range and a wider bandwidth covering the entire range is of interest. Microstrip antennas has become a popular choice amongst the different available antennas because they are low profile, inexpensive and easy to integrate within the IC's.

This chapter presents a monopole antenna with dual band operation for WLAN, WiMAX, and sub-6 GHz 5G wireless applications as a first contribution of this thesis. Initially a monopole antenna with U-shaped slot is realized for dual band operation and later in a slight modification to the radiating antenna, an additional rectangular slot is introduced for better

matching and a required band of operation. Moreover, a dual band AMC unit cell exhibiting a reflection phase of zero at 2.5 GHz and 5.5 GHz is designed and used as a reflector by placing it at the ground side of radiator to improve the gain and radiation.

3.2. Dual Band Antenna Design

Initially a patch with circular shape of radius 10.5 mm is designed, and the feeding is provided by the help of a 50-ohm microstrip fed line with the width 3.059 mm on FR4 dielectric substrate offering a relative permittivity ε_r of 4.4 and the substrate thickness of 1.6 mm respectively. The geometrical design of the proposed U-slot antenna is as shown in Fig. 3.1.

A U-shaped slot of length 30 mm in three directions and width 0.6 mm is etched on to the patch. The position and the dimensions of the slot are optimally chosen upon the results obtained from the parametric study. The dimensions of antenna are length, L = 38 mm, width, W = 22 mm, and length of the ground plane, G = 10 mm. The design was simulated with the help of HFSS. The antenna was initially simulated without etching the slot, for which the antenna was operating only at a single band of frequencies and with the etching of U-slot into the antenna design makes it to operate at an extra band of frequencies.

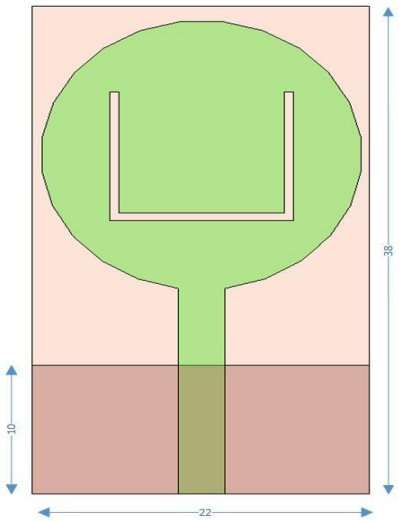

Fig. 3.1. Geometry of the proposed U-slot antenna

3.3. Results and Discussions

The simulation was carried out for the designed antenna and the Return loss characteristics is as shown in Fig. 3.2. It is to be noticed that the antenna is operating at two different frequency bands. The first band of frequencies for which |S11| < -10 dB are ranging from 2.32 - 2.70 with the resonance occurring at 2.45 GHz and the next band of frequencies ranging from 3.4 - 3.76 GHz with a resonance at 3.5 GHz. The percentage impedance bandwidths of the design are

obtained as 15.5 and 10.2 respectively. Fig. 3.2 shows that the antenna is suitable for covering 2.4 GHz WLAN band and 2.5, 3.5 GHz WiMAX bands.

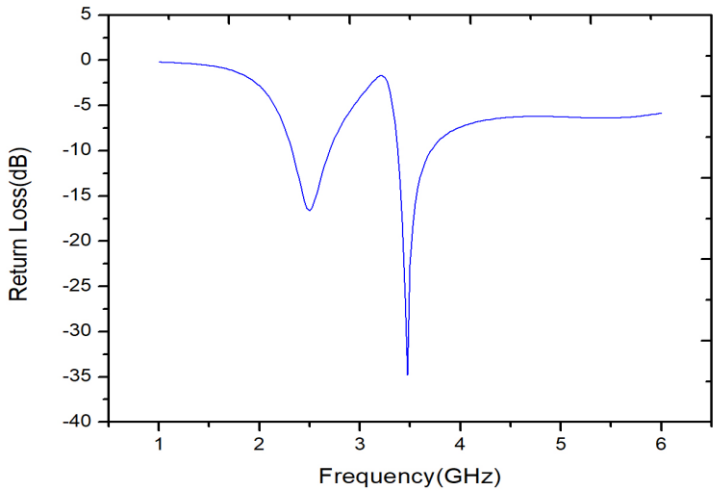

Fig. 3.2. Simulated return loss of proposed U-slot antenna

3.3.1. 3D Radiation Patterns of the Antenna

The 3D Radiation plots from Fig. 3.3 illustrates the radiating nature of the antenna at both the resonant frequencies of 2.45 GHz and 3.5 GHz. It is observed that the radiation is minimal along the X-direction and the maximum in the YZ plane, that is normal to the X direction. The maximum gains of 2.06 dBi and 2.24 dBi were observed along the direction of radiation at their resonant frequencies. The gain was also noticed to be almost stable throughout the range of antenna operation.

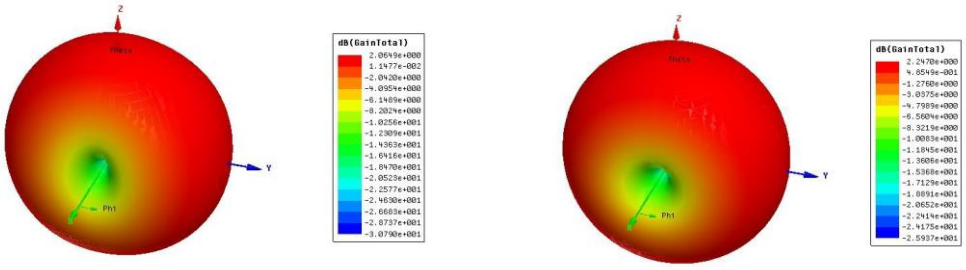

(a) (b)

Fig. 3.3. The 3D radiation pattern at (a) 2.45 GHz, and (b) 3.5 GHz

3.3.2. The E and H plane radiation patterns of the antenna

The Simulated 2D E and H-plane patterns of the U-slot antenna at 2.45 GHz and 3.5 GHz are simulated and presented in Fig. 3.4. At both the resonant frequencies it is noted that the H-plane radiation pattern (phi = 90°) is omnidirectional and in the E-plane (phi = 0°)is observed to be bidirectional, which is comparable to that of the conventional antenna pattern. Hence, the antenna is observed to be providing good radiation characteristics. The antenna besides exhibiting good return loss and radiation characteristics has performed well in terms of radiation efficiency by maintaining it above 90 percent at both the frequency bands.

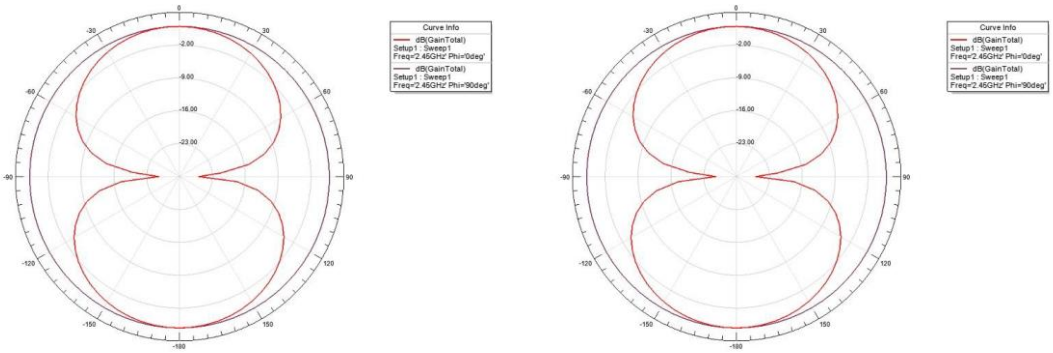

Fig. 3.4. The E and H-plane radiation patterns at (a) 2.45 GHz, and (b) 3.5 GHz

3.4. Dual Band Antenna with AMC

The antenna represented in the Fig. 3.1 has been slightly modified by introducing an extra rectangular shaped slot and an inset feed, which improvises the bandwidth of the antenna. Further, a dual band AMC unit cell has been designed to construct an AMC surface which is placed at a distance from the radiator at the ground side to better the gain and radiation characteristics.

3.4.1. Antenna Design

The radiator is a microstrip circular antenna with a U-shaped slot and a rectangular slot incorporated on it, a symmetrical AMC reflector surface of the size 64 x 64 x 1.6 mm^3 is employed at a distance of H = 14 mm on the ground side of the antenna. A Styrofoam layer with a permittivity value of 1.1, is used to separate the two structures. The overall configuration of the antenna is represented in Fig. 3.5.

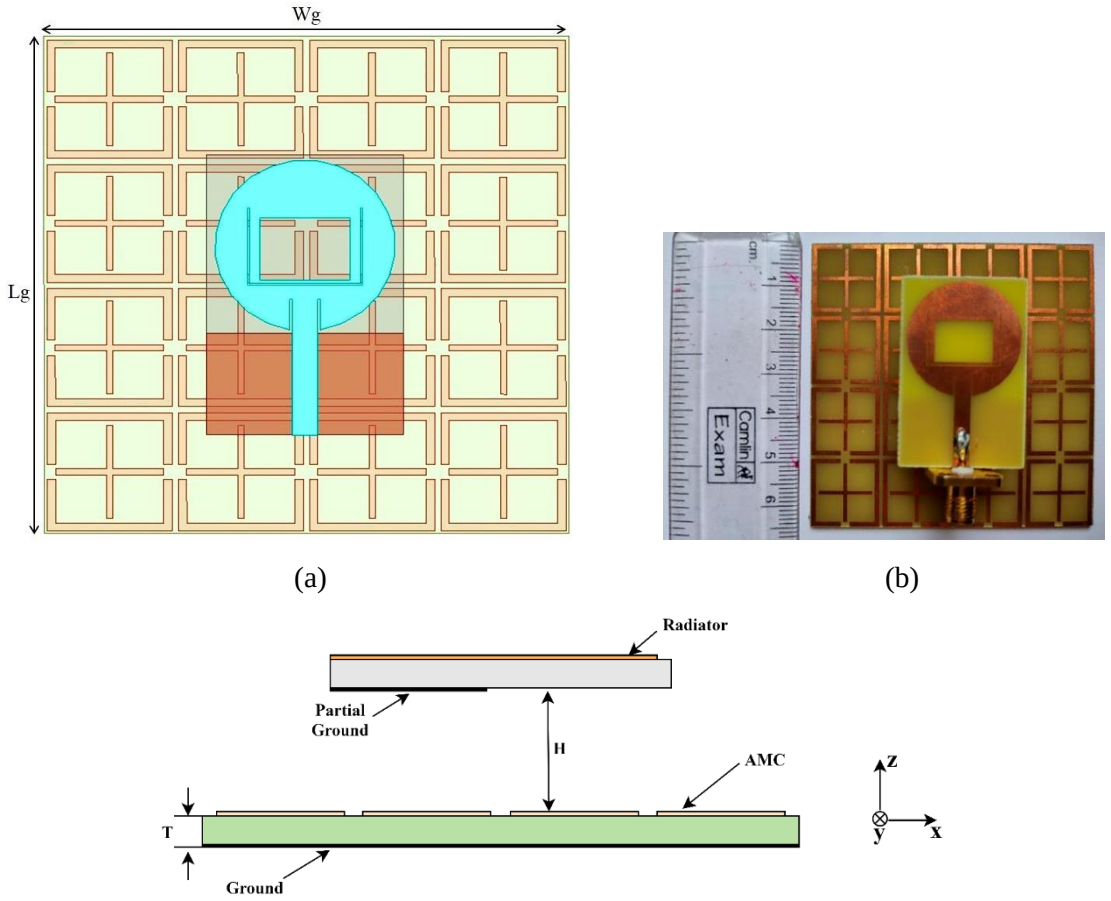

Fig. 3.5. Configuration of dual band AMC backed antenna (a) top view, (b) fabricated prototype, and (c) side view.

The geometry of the main radiator is shown in the Fig. 3.6(a). It is printed on a 1.6 mm thick rectangular FR-4 substrate having a ε_r of 4.4 and a loss tangent value of 0.02. The size of the antenna is of the order of $0.3\lambda_0$ x $0.2\lambda_0$ x $0.01\lambda_0$ (where λ_0 is wavelength pertaining to centre frequency of the first band). It is a microstrip fed antenna with inset feed for better impedance matching. A partial ground plane is being employed on the other side of the substrate in order to achieve a wider bandwidth. A U-shaped slot is introduced at an optimized position on the patch to enhance the bandwidth and lower the cross-polarization levels. Further an additional rectangular slot is also introduced to achieve proper impedance matching levels in the second band. The optimal dimensions antenna are stated in Table 3.1. The simulations were carried out on the Ansys HFSS tool.

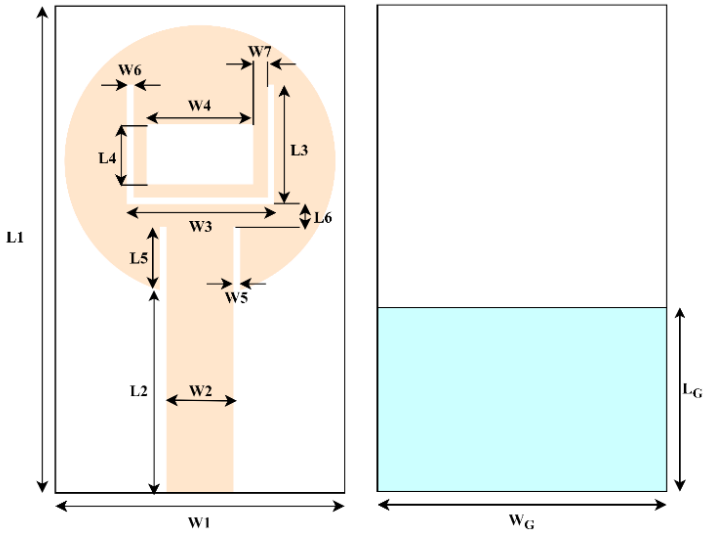

(a)

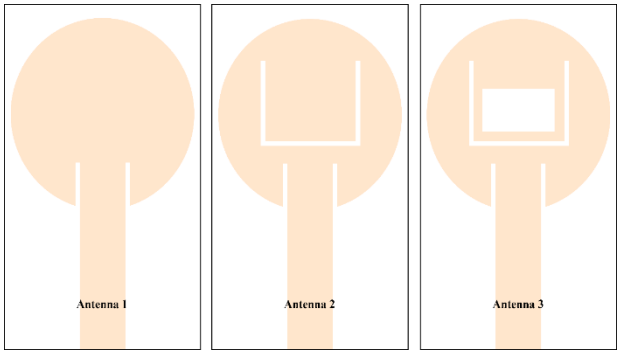

(b)

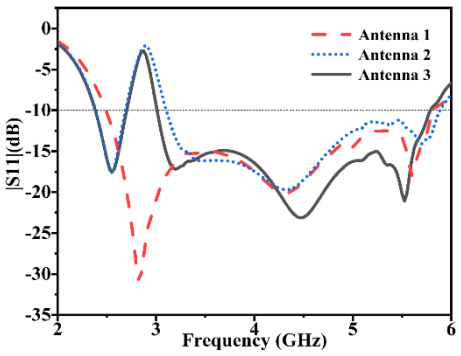

(c)

Fig. 3.6. (a) Design of the radiating antenna, (b) Evolutionary steps in the design of radiator, and (c) Reflection coefficients of the radiating elements.

The evolutionary steps involved in the design of the radiating patch are shown in the Fig. 3.6 (b). The S11 response of them is shown in the Fig. 3.6 (c). A circular patch antenna is initially designed for which a wide band resonance is achieved from 2.9 GHz to 5.9 GHz. Then a U-shaped slot is etched, which introduces a notch at the frequency band between 2.73 - 3.23 GHz. Hence, the antenna now works as a dual band antenna with operating frequencies ranging from 2.49 - 2.73 GHz and 3.23 - 5.73 GHz. Further, with the introduction of an additional rectangular slot, the impedance matching, and the bandwidth of the antenna are enhanced. Finally, the design of the antenna is simple making use of FR-4 substrate which is of low cost, operating in two bands with good impedance bandwidths covering the entire sub-6 GHz 5G frequency bands besides the existing 2.4/5 GHz WLAN, 2.5/3.5/5.5 GHz WiMAX bands.

Table 3.1. Optimized dimensions of the proposed AMC backed slot antenna

Parameter	Dimension(mm)	Parameter	Dimension(mm)
H	14	T	1.6
Lg	64	Wg	64
L1	36	W1	24
L2	13.55	W2	3.059
L3	10	W3	14
L4	8	W4	11
L5	3.9	W5	0.3
L6	1.8	W6	0.2
L_G	13	W7	1.3
La1	16	W_G	24
La2	15.2	Wa1	16
La3	2	Wa2	15.2
La4	0.6	Wa3	0.8
La5	0.8	Wa4	0.8

3.4.2. AMC Design

The design geometry of the artificial magnetic conductor(AMC) unit cell incorporates a square outline with slots at the centre on the opposite sides and an additional cross shaped patch at the centre as shown in the Fig. 3.7 (a). A low-cost FR-4 substrate is employed with relative permittivity of 4.4 and a loss tangent value of 0.02. A metal ground is present at the bottom surface of the unit cell. The unit cell is simulated using the master-slave boundary set up. The reflection phase plot of this dual band AMC is as shown in the Fig. 3.7 (b). Initially a single band AMC with the reflection phase and of zero at 2.5 GHz is designed with no central cross shaped patch and with the introduction of the cross, a dual band AMC is realized with the other zero reflection phase occurring at 5.5 GHz. The reflection magnitude plot is shown in the Fig. 3.7 (c) and the values about 0.78 and 0.71 and is high enough to realize the gain enhancement of the antenna. The AMC unit cell dimensions are evaluated in accordance with the operating frequency range of the antenna which are also listed in the Table 3.1.

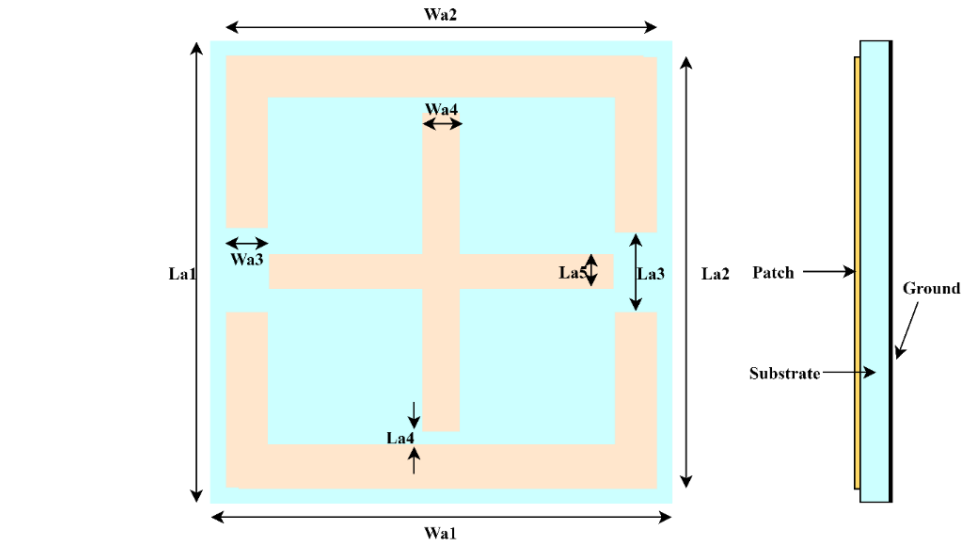

(a)

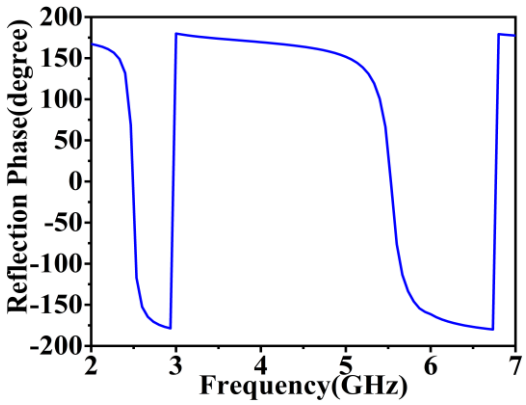

(b)

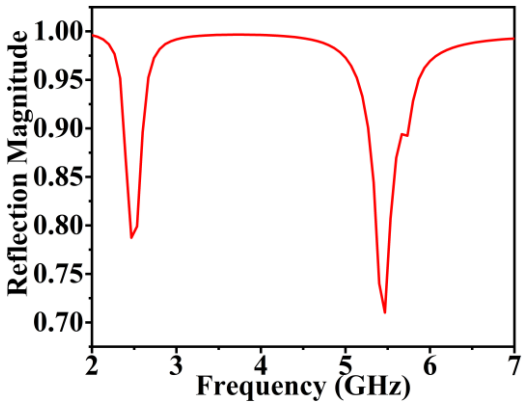

(c)

Fig. 3.7. (a) Geometry of the proposed dual band AMC unit cell, (b) Reflection phase of the AMC unit cell, and (c) Reflection magnitude of the AMC unit cell

3.4.3. Antenna with AMC reflector

The designed dual band AMC unit cell is periodically repeated in x and y directions to form a 4 x 4 array metal surface and is placed at the groundside of the antenna separated by Styrofoam. The effect of the AMC surface on the S11 curve is depicted in the Fig. 3.8 (a). The antenna performance is influenced by the extent of separation between the antenna and the AMC surface. The radiation from the antenna get reflected from the AMC surface with zero phase reversal to aid the radiations unidirectionally and hence increasing the gain of the antenna. A measurable increase in the gain is observed in the first band and a reasonable increase in the second band of operation as shown in the Fig. 3.8 (b).

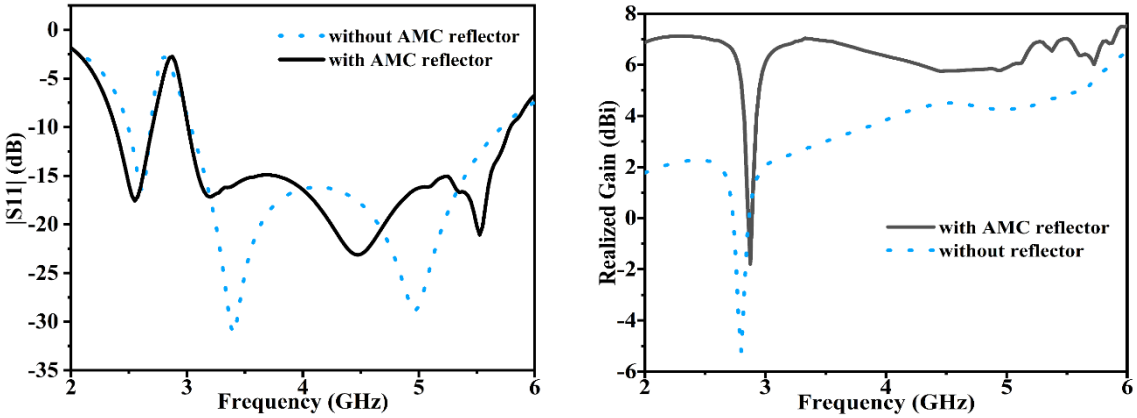

(a) (b)

Fig. 3.8. (a) Simulated S11 of the antenna with and without AMC reflector, and (b) Simulated gain of the antenna with and without AMC reflector.

The performance in terms of the band selection and bandwidth of antenna depends on the dimensions of the slots. A parametric analysis based on the variation of these dimensions is as shown in the Fig. 3.9. The values of these dimensions for which the choice of frequency bands is covered, is considered in the design.

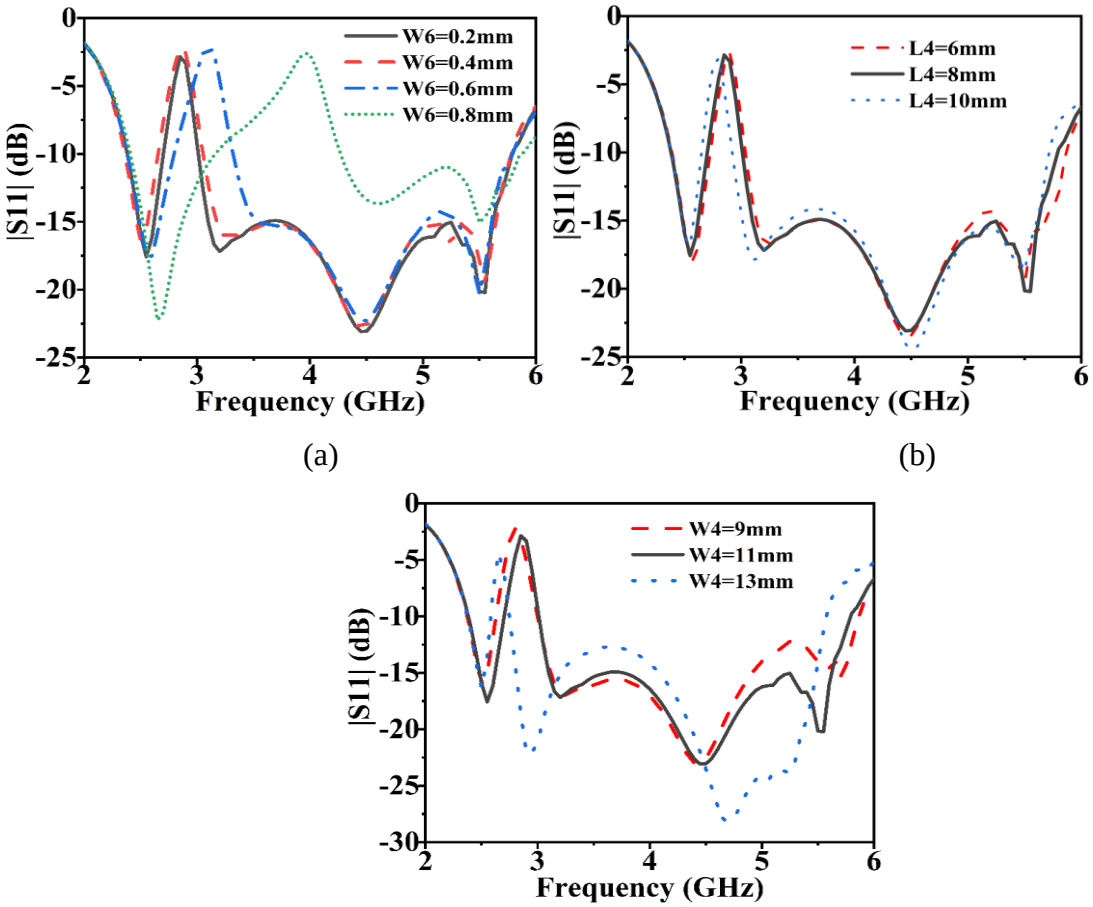

(a) (b)

(c)

Fig. 3.9. Simulated S11 of the antenna for different (a) W6, (b) L4, and (c) W4

3.5. Results and Discussions

The simulated dual band antenna design and the AMC surface are fabricated and is as shown in the Fig. 3.5 (b) and is of the size $0.53\lambda_0$ x $0.53\lambda_0$ x $0.14\lambda_0$. The measurement setup for measuring the reflection coefficient and gain of the antenna is represented in the Fig. 3.10. The reflection coefficient of the antenna is measured using the vector network analyzer . The measured and simulated S11 of the antenna and the AMC surface are shown in the Fig. 3.11 (a). The slight variation in the measured results from the simulated is due to the losses incurred during the fabrication process. A quarter wavelength separation should be maintained between the antenna and the AMC reflector in order to have an effect in the performance of the antenna, but the low-profile nature of the design will get affected. So, a trade-off amongst the performance and size of the antenna needs to be considered. It is observed from the Fig. 3.12, that as the separation decreases, though the gain of the antenna increases, there is deterioration in the S11 performance of the antenna. So, an optimal separation (H=14 mm) is chosen in order to preserve both the S11 and gain performances. The antenna is suited for 2.4/5 GHz WLAN applications, 2.5/3.5/5.5 GHz WiMAX applications and with the second band being wideband is able to cover the entire sub-6 GHz, 5G bands (3.3-3.8 GHz, 3.3-4.2 GHz and 4.4–5 GHz).

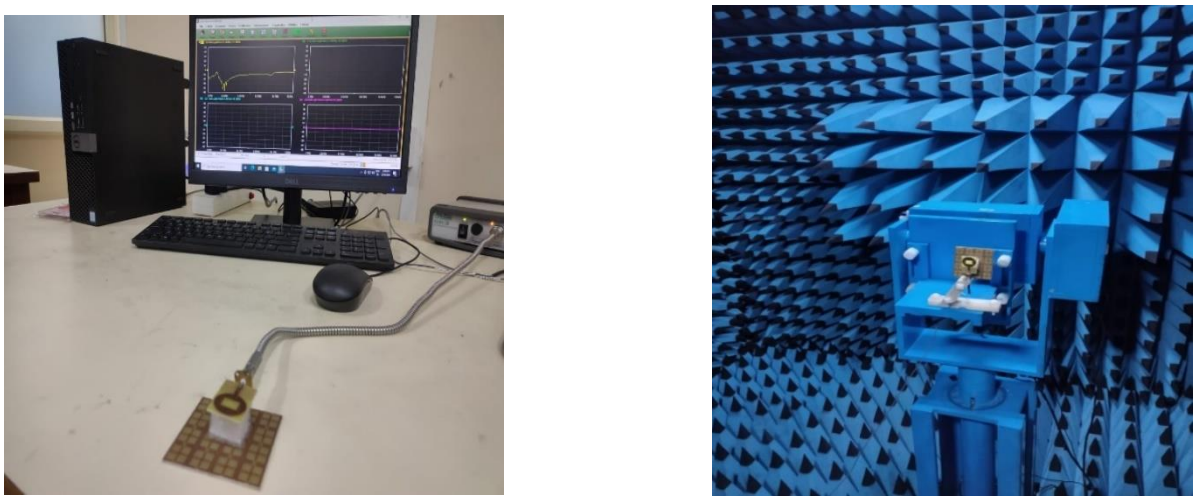

Fig. 3.10. Measurement setup of proposed antenna (a) for S11 using VNA, and (b) in an anechoic chamber.

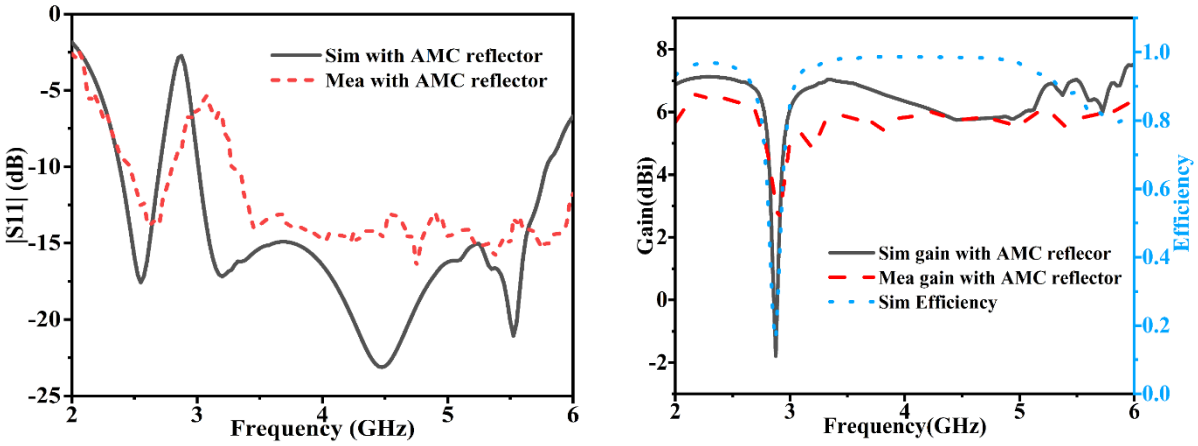

(a) (b)

Fig. 3.11. (a) Simulated and measured Reflection coefficient of the antenna with AMC reflector, and (b) Simulated and measured gain, simulated efficiency of the antenna with AMC

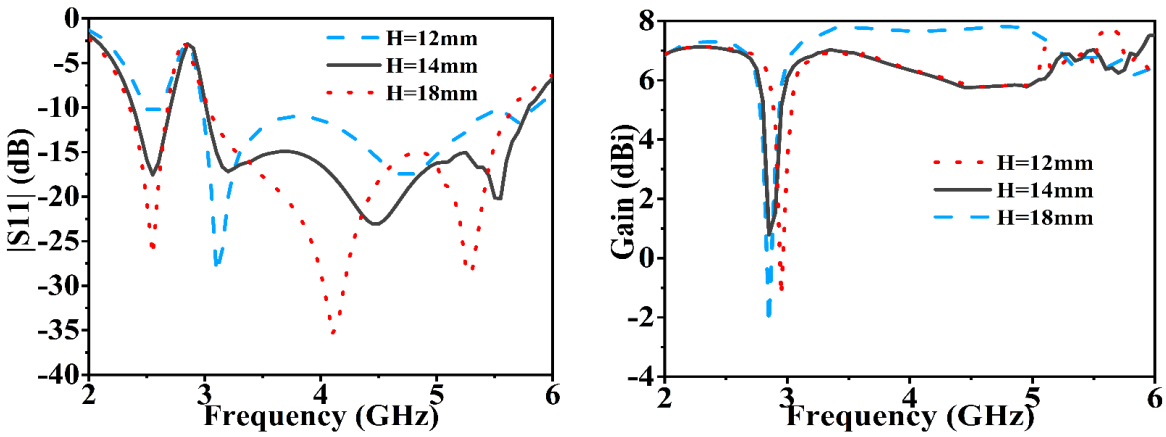

(a) (b)

Fig. 3.12. Simulated (a) S11, and (b) gain, for different H.

The simulated radiation properties of the antenna are validated by radiation pattern measurements. These patterns are measured in an anechoic chamber (controlled environment) using NSI patterns recording system. The antenna was evaluated for its radiation patterns in two cuts(E-plane and H-plane). Antenna gain is also calculated from these radiation patterns by gain comparison/gain transfer method. The standard horn antenna has been used for gain calculations. The patterns of the antenna loaded with the AMC reflector at frequencies 2.55 GHz, 3.6 GHz, 4.7 GHz and 5.5GHz are shown in the Fig. 3.13. The measured and simulated patterns were observed to be agreeing well with each other. The inconsistency in the cross-polarization plots is due to losses that were incurred during the fabrication and measurement process. The antenna exhibits unidirectional patterns because of the reflections from the AMC

surface. The radiation patterns at 5.5 GHz diverge because the antenna is operating in its second mode. The gains of the antenna and the simulated radiation efficiency are shown in the Fig. 3.11(b).

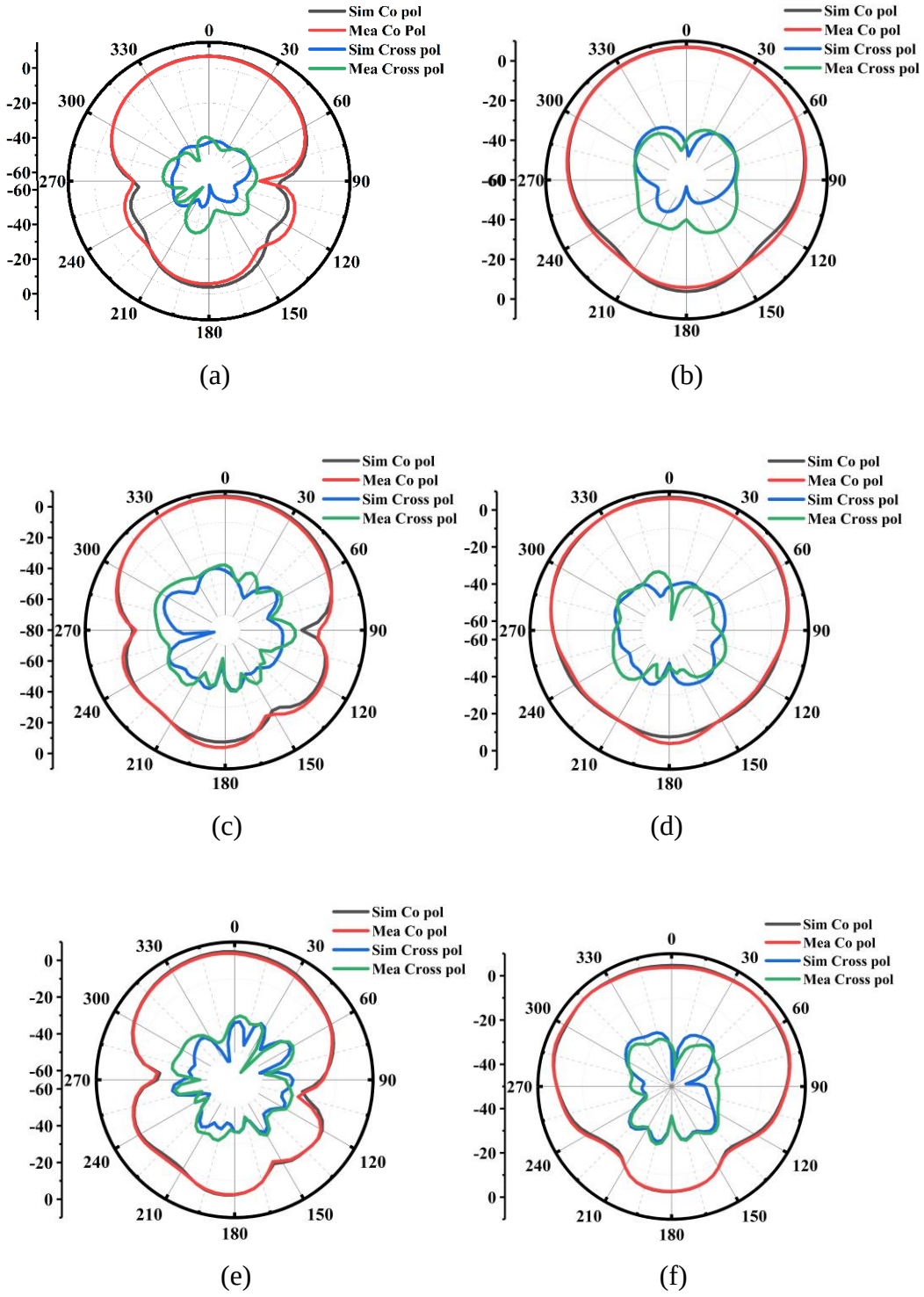

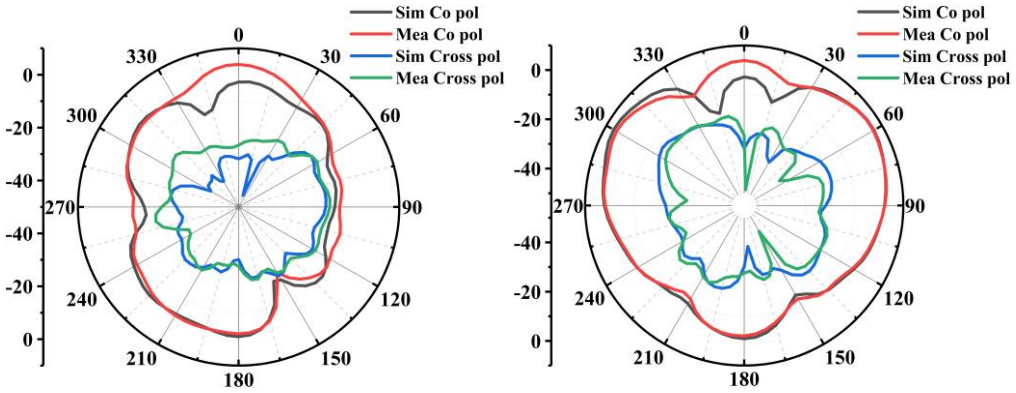

(g) (h)

Fig. 3.13. Simulated and measured patterns of the antenna (a) 2.55 GHz-XZ plane, (b) 2.55 GHz-YZ plane, (c) 3.6 GHz-XZ plane, (d) 3.6 GHz-YZ plane, (e) 4.7 GHz-XZ plane, (f) 4.7 GHz-YZ plane, (g) 5.5 GHz-XZ plane, and (h) 5.5 GHz-YZ plane

Table 3.2. Comparison of the dual band proposed antenna with the existing

Ref.	Size(mm^3)	With AMC Reflector	Operating Range (GHz)	Gain(dBi)	Radiation Efficiency
[27]	135 X 80 X 0.8	No	0.7 - 0.9 1.6 - 5.5	-1.3 - 4.7	(41 - 88) %
[28]	20 X 30 X 1.5	No	3.15 - 5.55	1.8 - 2.7	(68.4 - 79.6)%
[29]	63 X 51.2 X 4.5	No	2.84 - 5.15	4.4 - 6.2	64%
[30]	104 X 104 X 11	Yes	2.36 - 2.76 5.12 - 5.62	7.2 7.3	65%
[32]	63 X 63 X 7	Yes	3.14 - 3.83 4.40 - 5.02	8.2	90%
[33]	105 X 105 X 25	Yes	2.5 - 2.7 3.3 - 3.6	8.4	N/A
proposed	**36 X 24 X 1.6**	**No**	**2.48 - 2.73** **3.15 - 5.8**	**2.1** **4.3**	**>90%** **>80%**
proposed	**64 X 64 X 17.2**	**Yes**	**2.38 - 2.7** **3.28 - 5.8**	**7.1** **7.1**	**>90%** **>80%**

It can be ascertained from the Fig. 3.11(b), that the radiation efficiency is above 90% for the entire first band and the sub-6 GHz 5G operating bands. The measured and simulated gains are about 6.7 dBi and 7.1 dBi in the first band and almost agree with each other for the entire range in the second band.

3.6. Conclusion

In this chapter, a low-profile dual band antenna configuration designed for 2.4/5 GHz WLAN, 2.5/3.5/5.5 GHz WiMAX and sub-6 GHz 5G bands. The antenna is fabricated with both the simulated and measured patterns nearly matched. The size of the antenna without AMC reflector is of the order of $0.3\lambda_0$ x $0.2\lambda_0$ x $0.01\lambda_0$ and with AMC reflector, it is of the order $0.53\lambda_0$ x $0.53\lambda_0$ x $0.14\lambda_0$ (where λ_0 is the free space wavelength of the centre frequency of the first band) with impedance bandwidths of 9.8% (2.48 - 2.73 GHz) and 56% (3.28 - 5.8 GHz). The antenna gain within the bands were observed to be 2.1 and 4.2 dBi respectively. In order to enhance the gain and radiation of the antenna a dual band AMC reflector which was designed at 2.5 GHz and 5.5 GHz was employed. A significant improvement in the gain of 5 dBi in first and 2.8 dBi in the second bands was observed. Therefore, the antenna could be used alone for WLAN, WiMAX and 5G applications or with the AMC reflector for high gain base station applications.

Chapter-4

CRLH Metamaterial-Inspired Dual Band Compact Antenna for Wireless Applications

4.1. Introduction

With an ever-evolving wireless communication technology and miniaturization of the wireless operating gadgets, the need for the antennas capable of operating in multiple bands without losing their low-profile nature [36-38] is of utmost priority. With proper loading of metamaterial cells into the design of the conventional antennas can address some of these requirements [39]. The left-handed nature of the metamaterials helps in exhibiting negative permeability and negative permittivity simultaneously, which are unusual with the existing right-handed materials. MTMs additionally showcase antiparallel phase velocities and group velocities, negative refractive index (NRI) and zero order resonance (ZOR) modes. Composite right left-handed (CRLH) transmission line metamaterial (TL-MTM) provide zeroth-order resonance (ZOR) modes which are useful in designing miniaturized multiband antennas. CRLH TL-MTM possesses both right and left-handed effect with a series and parallel combination of capacitor and inductor providing the ZOR [40]. The ZOR frequency of the antenna is independent of its physical size and hence can be used as an advantage in miniaturization of the antenna. Several techniques have been used to realize multiband antennas like reconfigurability [41], [42] or by loading capacitive elements [43] but increase the design complexity. CRLH MTMs are suitable in realizing the multi band antennas using higher order resonances but may offer less gain due to their small size. However, high gain offering monopole antennas loaded with the CRLH cells could serve the purpose. The traditional monopole antenna with MTM loading, introduces the second resonance in addition to the regular monopole resonance are

proposed [44], [45], operating at 2.4/5/5.2/5.8 GHz WLAN and 5.5 GHz for Wi-Fi applications. Antennas loaded with CRLH unit cell to achieve dual band nature based on the ZOR for wireless applications are realized [46–49]. However, the aforementioned antennas are slightly larger in volume. In [50], a single feed dual band antenna loaded with mushroom like TLMTM structure with circuit analysis is presented. A 2 x 2 array formed by the unit cell elements is loaded to the conventional microstrip patch antenna and a similar mushroom unit cell loaded antenna with dual band nature and dual modes is presented [51], yet the planar nature of the antennas is lost due to the vias that are part of the mushroom unit cells.

In this chapter, a simple and miniaturized dual band monopole antenna incorporated with CRLH MTM inspired unit cell, with circular polarization in one band is proposed. Initially a monopole antenna is designed for single band operation, then with the loading of the MTM inspired unit cell enables it to work as a dual band antenna operating at 3.15–4.09 GHz and 5.35–5.84 GHz. The impedance bandwidths of the antenna in two bands are 26.8% and 8.9% with the maximum peak gain of 4 dBi and 5.1 dBi, respectively. The circular polarization is achieved in the second band with good radiation efficiencies in both the bands. The circuit realization and radiation characteristics of antenna are also discussed. The designed antenna is suitable and can be adapted for 3.5/5.5 GHz WiMAX and mid band 5G wireless applications.

The remaining contents of this chapter are represented as follows: The design procedure of the dual band antenna is presented in Section 4.2. The simulated results and their analysis with comparison to the measured results are mentioned in Section 4.3. The conclusion of this chapter is discussed in Section 4.4.

4.2. Design Procedure of the CRLH MTM Inspired Antenna

The design and configuration of the proposed planar microstrip fed dual band antenna with the MTM unit cell is depicted in Fig. 4.1. The overall size of the antenna along with its dimensions is listed in Table 4.1. The antenna design parameters include a cost effective FR4 as substrate (permittivity of 4.4 and loss tangent value 0.02) of height 1.6 mm and an L-shaped patch with dimensions W1, L2 and L3 which are optimized and fed from a 50-ohm microstrip line that induces resonance at a frequency of 4.3 GHz. A metamaterial unit cell is designed and loaded on either side of the FR4 substrate and is united with the ground on the ground side of the antenna through a thin rectangular strip with dimensions L4 and W5. A partial ground plane is employed to help in improving the bandwidth of antenna. With the loading of the MTM unit cell, the antenna operates works over dual band (S11< –10 dB) with a wider first band and the

resonant frequencies 3.5 GHz and 5.5 GHz. The position of the rectangular strip connected to the ground and the strip part of the unit cell play a significant role in the antenna performance.

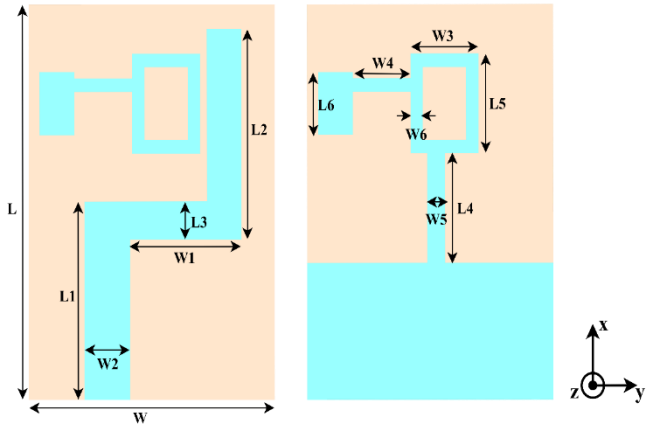

Fig. 4.1. Geometry and configuration of the proposed CRLH MTM inspired antenna.

Table 4.1. Dimensions of the proposed CRLH MTM inspired antenna

Parameter	Dimension(mm)	Parameter	Dimension(mm)
L	24	W	17
L1	13	W1	7
L2	11.5	W2	2.5
L3	2	W3	5
L4	6	W4	4
L5	6	W5	1
L6	4	W6	0.5

4.2.1. Design stages of the proposed antenna

The evolutionary stages of the MTM inspired antenna design are depicted in Fig. 4.2(a) to (d). The respective S11 and axial ratio plots of the aforementioned antenna configurations are shown in Fig. 4.3(a) and (b). Initially an L shaped conventional patch antenna is designed for the purpose of size reduction and fed by strip line, which resonates only in one frequency band ranging from 4 - 4.64 GHz with a mid-frequency of 4.3 GHz (as seen for Antenna 1 in Fig. 4.3(a)). A CRLH MTM-TL inspired unit cell is designed in different steps shown in Fig. 4.2 and is etched only on the ground side of the antenna which induces an additional band. Later unit cell is placed on either side of the substrate, inducing a resonance band near the first band along with the existing band from 5.16 - 5.64 GHz with mid frequency of 5.4 GHz, due to the

additional series and shunt elements. A thin rectangular strip is used to connect the ground with the unit cell ensuring a good impedance matching and a wider first band with a considerably large bandwidth from 3.15 - 4.09 GHz due to the merging of two resonances which are close to each other, and the rectangular strip also ensures that the CP is realized in second band with AR < 3 dB (see Antenna 3 in Fig. 4.3(b)).

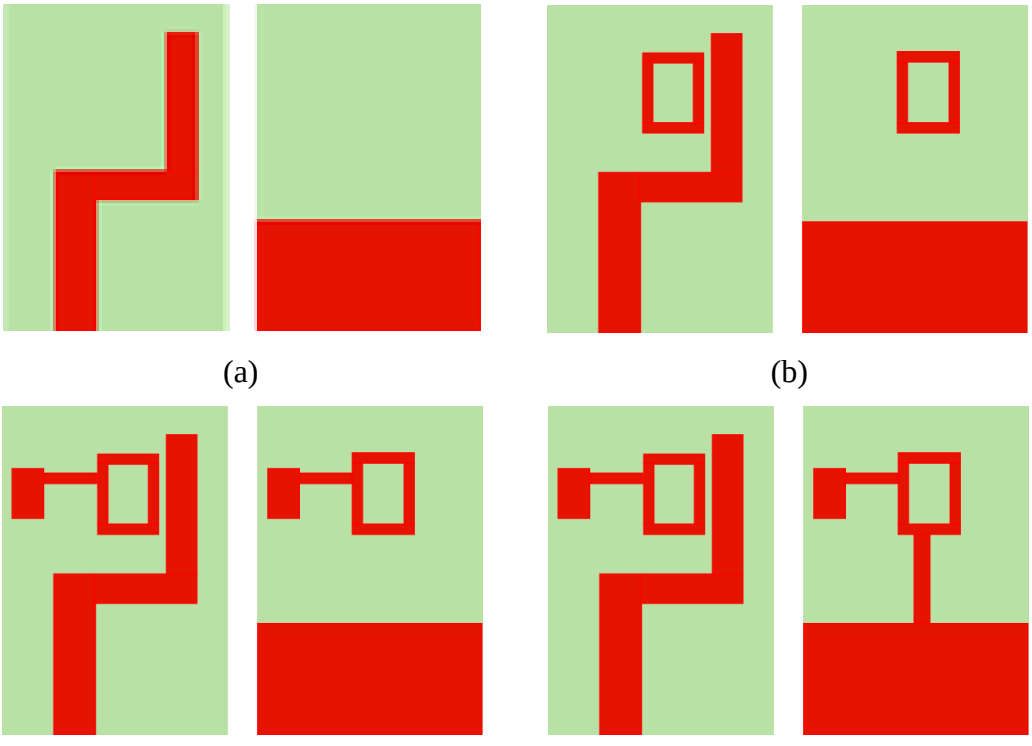

(a) (b)

(c) (d)

Fig. 4.2. Evolutionary stages in the design of the antenna (a) Antenna 1, (b) Antenna 2, (c) Antenna 3, and (d) Antenna 4

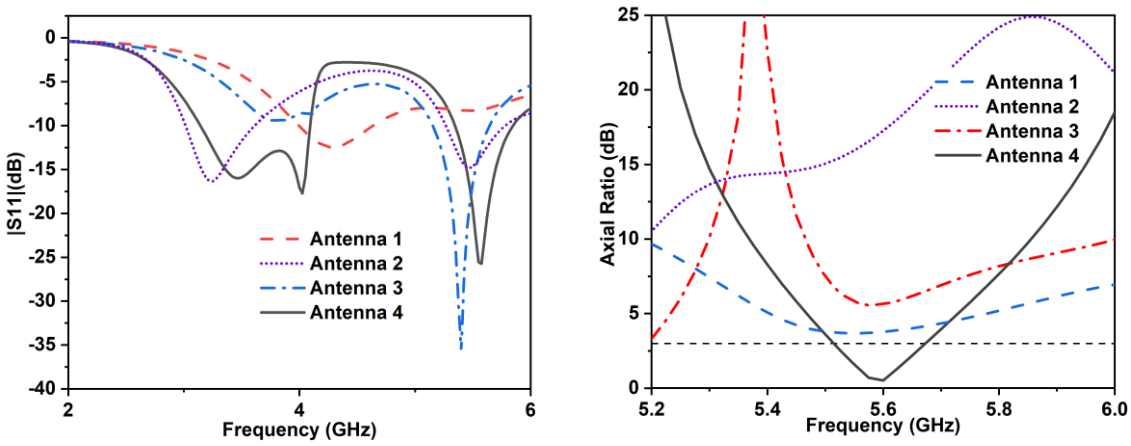

(a) (b)

Fig. 4.3. Simulated design stage responses: (a) Reflection coefficient, and (b) Axial ratio

4.2.2. Circuit realization of the antenna

The antenna geometry indicates that there is a CRLH TL inspired unit cell loaded on either side of the substrate. The unit cell and its effective equivalent circuit are represented in Fig. 4.4(a), and it is evident that there is a series and parallel combination of inductor and capacitor. The series capacitor C_{L} is provided by the gap separating the L shaped radiator and the unit cell, the rectangular ring structure results in the series inductor L_{R}. A thin rectangular strip connected from the rectangular ring structure to the virtual ground indicated in Fig. 4.4(a), forms the shunt inductor L_{L}. The shunt capacitor C_{R} is provided by the solid rectangular patch etched on both the sides of the substrate. The approximate overall equivalent circuit of antenna including the main radiator and the unit cells is as shown in Fig. 4.4(b). In the circuit diagram, the first unit cell etched on top surface of substrate has a series arm with the elements L_{R1}, C_{L1} and shunt arm with the elements L_{L1}, C_{R1}. The cell placed on the ground side of the antenna has a series arm with inductance L_{R2} and shunt arm with inductance L_{L2} and capacitance C_{R2}. The two-unit cells are separated by the FR4 substrate acting as a dielectric and forming a capacitance C_3. The L shaped radiator has an inductance of L_1 and a capacitance C_1 is set up by a line and partial ground plane.

Further, the lumped equivalent circuit represented in Fig. 4.4(b) is simulated with the ADS software and the S11 response is compared to the HFSS simulated result. The obtained lumped element values are L_1 = 1.775 nH, C_1 = 1.15 pF, L_{R1} = 2.675 nH, C_{L1} = 0.92 pF, L_{L1} = 1.525 nH, C_{R1} = 0.5 pF, C_3 = 0.54 pF, L_{R2} = 0.9 nH, L_{L2} = 0.69 nH, and C_{R1} = 1.91 pF. A comparison is drawn between the S11 responses of HFSS simulation and circuit simulation results as displayed in Fig. 4.4(c) and a close match is observed between them. A slight mismatch can be attributed to the parasitic elements such as capacitance, inductance, and resistance can have different values in HFSS and circuit simulations. High-frequency signals may experience transmission line effects, such as reflections and impedance mismatches. HFSS may account for these effects differently than circuit simulators, leading to discrepancies.

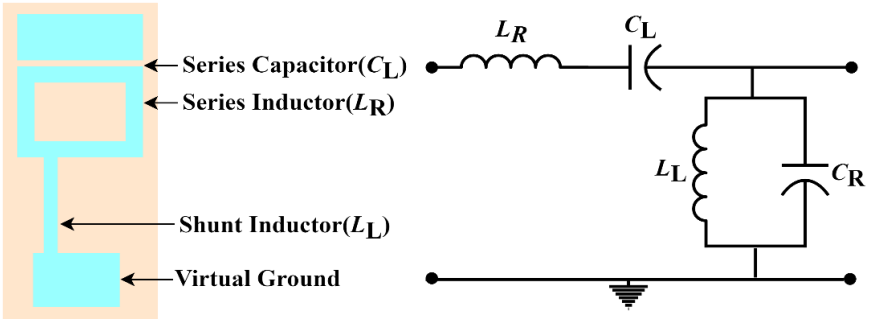

(a)

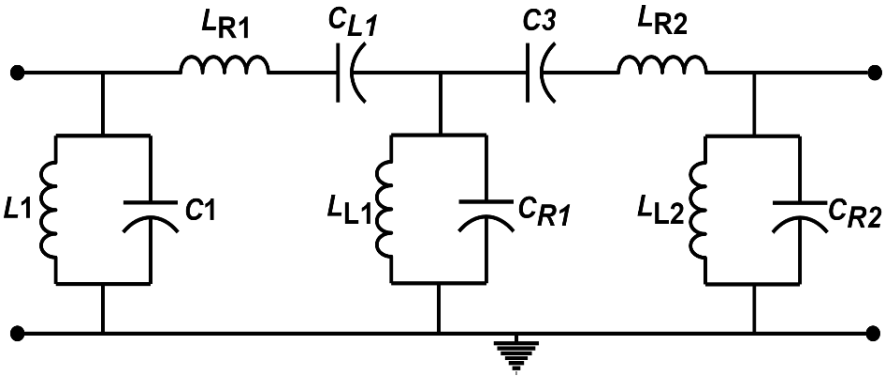

(b)

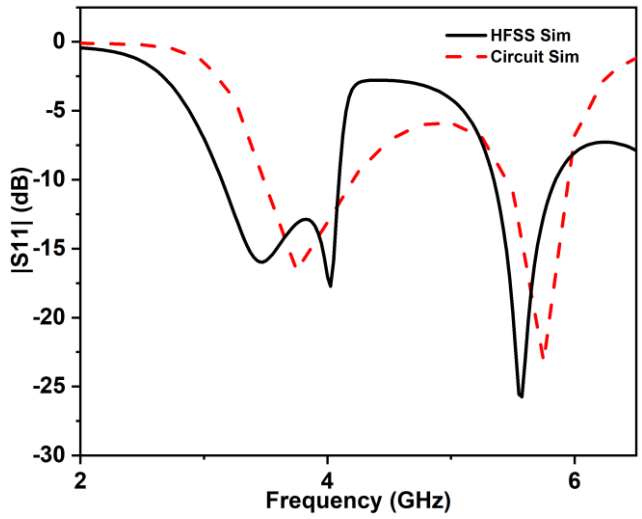

(c)

Fig. 4.4. (a) Circuit realization of the proposed unit cell, (b) Circuit realization of MTM loaded antenna, and (c) Reflection coefficient responses of HFSS and circuit simulation.

4.3. Results and Discussions

4.3.1. Reflection Coefficient

The overall volume of the proposed antenna is 24 mm x 17 mm x 1.6 mm and its size in terms of λ_0 (the wavelength that corresponds to the lowest resonance frequency band's center frequency) is $0.3\lambda_0$ x $0.2\lambda_0$ x $0.01\lambda_0$. Hence, it is of compact size with dimensions smaller than that of the typical monopole antenna operating at the same frequency. The antenna has been fabricated and the prototype of the same is as shown in Fig. 4.5(a). The antenna's S11 characteristics are extracted using a VNA and are illustrated in Fig. 4.5(b). It can be observed from Fig. 4.5(c), that a decent consistency is maintained between the simulated and the measured S11 results. It is observed from the S11 response of antenna that the lower band is wider band ranging from 3.15 - 4.09 GHz with an impedance bandwidth of 26.8%, which is suitable for 3.5 GHz WiMAX, n77 and n78 sub-6 GHz 5G NR bands. The higher band is narrower with frequency range 5.35 - 5.84 GHz and an impedance bandwidth of 8.9% covering the 5.5 GHz WiMAX band. The antenna being dual band, can be well adapted in the devices having multiple applications.

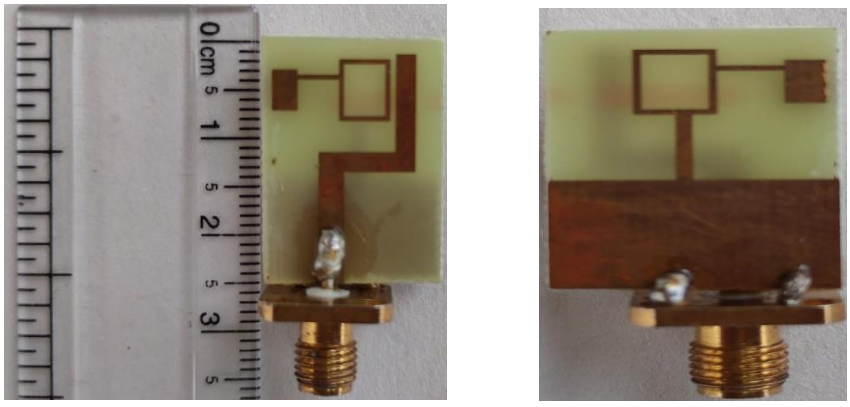

(a)

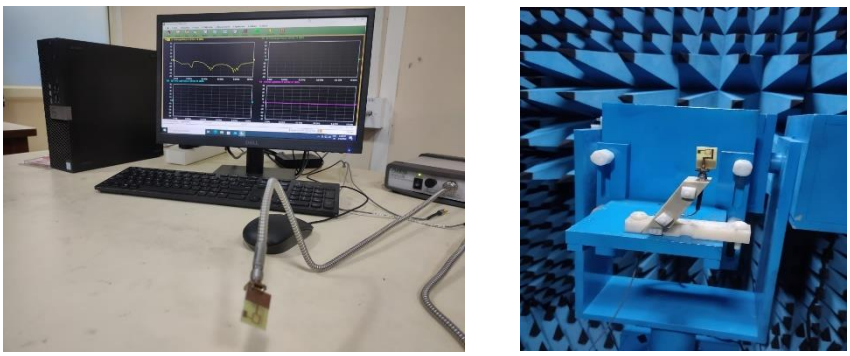

(b)

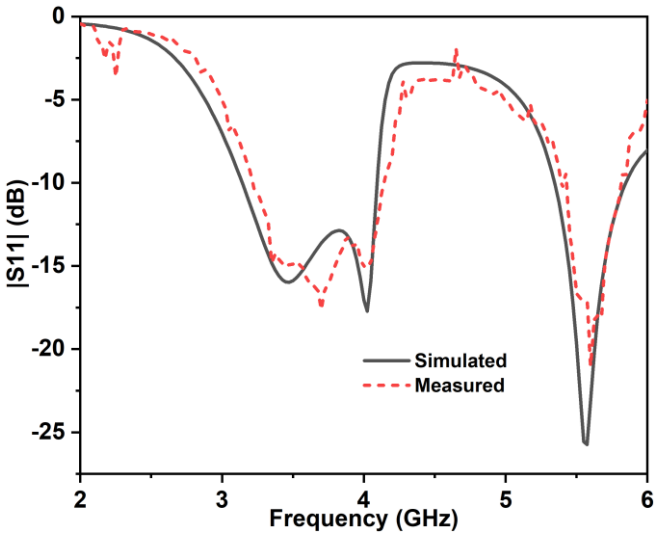

(c)

Fig. 4.5. (a) Front and back view of the fabricated prototype, (b) Measurement setup of the proposed antenna using VNA and in anechoic chamber, and (c) Simulated and measured reflection coefficients

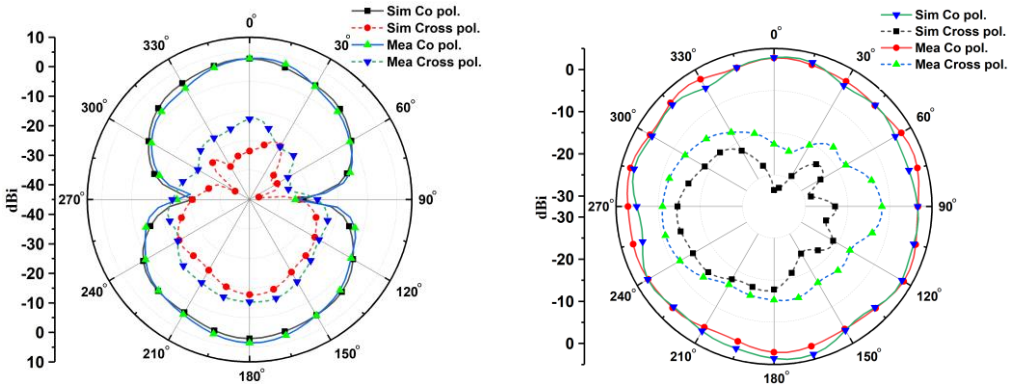

(a) (b)

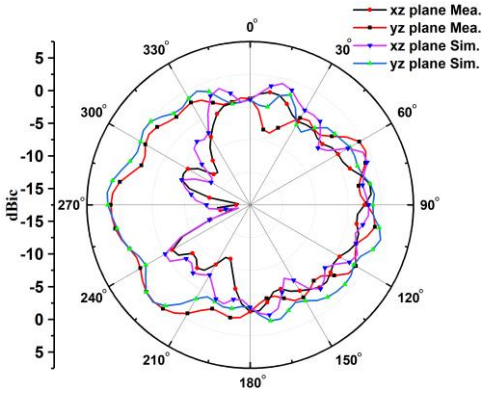

(c)

Fig. 4.6. The radiation patterns of the antenna in the plane:(a) XZ at 3.5 GHz, (b) YZ at 3.5 GHz, and (c) XZ and YZ at 5.6 GHz

4.3.2. Polarization

This section discusses the polarization of the designed antenna in two frequency bands. The axial ratio plot of the antenna indicates that it is below 3 dB from 5.51 to 5.66 GHz as represented in Fig. 4.7(a). The CP of the antenna is achieved from the proper loading of the MTM unit cell at the ground side and adjusting the position of the thin rectangular strip acting as an inductor. Initial L shaped monopole antenna design helps in achieving the CP at a required operating frequency. In the other band linear polarization of the antenna is observed. Hence, the antenna acts as a dual polarized antenna with linear polarization in the first band and circular polarization in the other.

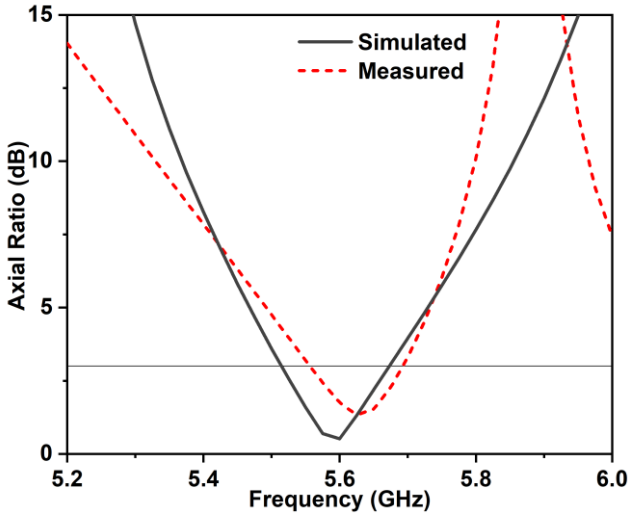

(a)

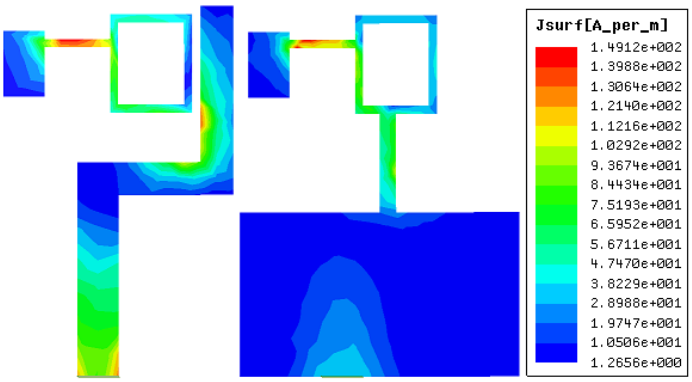

(b)

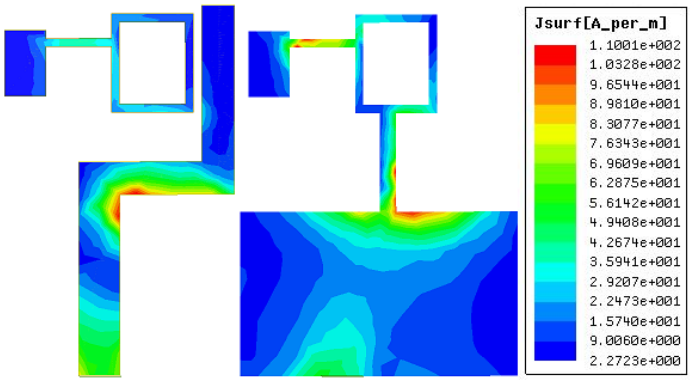

(c)

Fig. 4.7. (a) Simulated and measured axial ratio responses of the antenna, (b) Surface current distributions of the antenna at 3.5 GHz, and (c) Surface current distributions of the antenna at 5.6 GHz

The surface current distributions of the antenna are illustrated in Fig. 4.7(b) and (c). At 3.5 GHz, the strong surface currents are concentrated on the main L shaped radiator and on both the thin rectangular strips that are part of the unit cells. It is also observed that a strong current is passing through the narrow strip connected between the unit cell and the ground plane introducing an inductance. At 5.5 GHz, the strong surface currents are present at the edges of the L shaped radiator and at the strip connecting to the ground plane. The position of the narrow strip part of the unit cell is manoeuvred to attain the CP of antenna in the frequency band 5.51 - 5.66 GHz. The maximum surface current density also exists on this narrow strip representing the current flow through it and hence creating an inductance. It is also observed from Fig. 4.8 that the orthogonal currents with almost an equal magnitude flowing in the opposite directions through the L shaped radiator with a phase shift of 90 degrees are responsible in achieving the circular polarization.

4.3.3. Polarization

The antenna's peak gains both simulated and measured in the two resonant frequency bands with center frequencies, of 3.5 GHz and 5.5 GHz are depicted in Fig. 4.9. The maximum gain that is observed within the first band is 4 dBi and in the second band is 5.2 dBi respectively. It is also noticed from the radiation efficiency plot of Fig. 4.8 that it is >85% in the first band and >90% in the second band. Hence, the antenna offers decent gains and good efficiencies throughout the bands of operation, making it suitable for targeted applications.

4.3.4. Gain and Radiation Efficiency

The simulated radiation properties of the antenna are validated by radiation pattern measurements. These patterns are measured in an anechoic chamber represented in Fig. 4.5(b), using NSI patterns recording system. Antenna gain is also calculated from these radiation patterns by gain comparison/gain transfer method. The standard horn antenna has been used for gain calculations.The antenna's simulated and measured peak gains in the two resonant frequency bands with center frequencies of 3.5 GHz and 5.5 GHz are shown in Fig. 4.9. The maximum gain that is observed within the first band is 4 dBi and in the second band is 5.2 dBi respectively. It is also noticed from the radiation efficiency plot of Fig. 4.9 that it is >85% in its first and >90% in the second band respectively. Hence, the antenna offers decent gains and good efficiencies throughout the bands of operation, making it suitable for targeted applications.

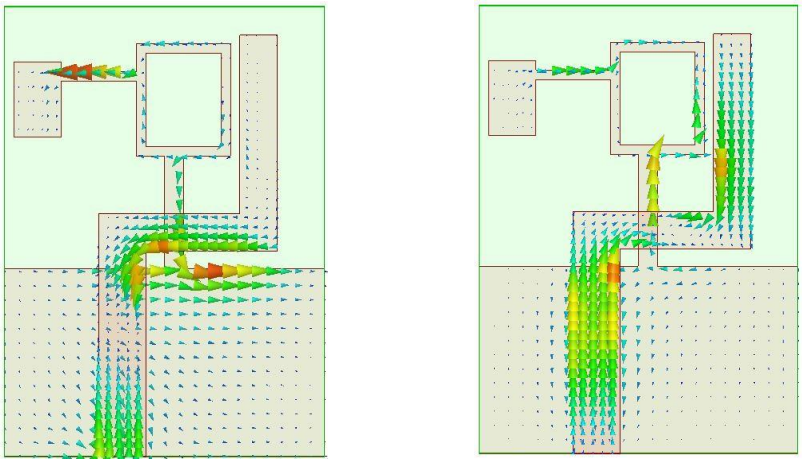

(a) (b)

Fig. 4.8. Vector current distributions of the antenna at 5.5 GHz for phases (a) 0 deg, and (b) 90 deg.

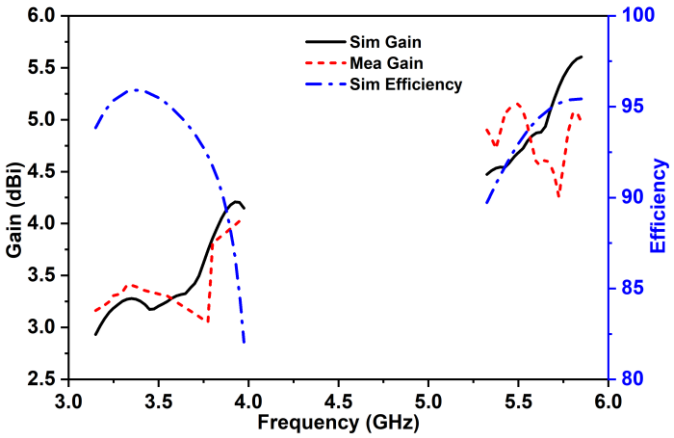

Fig. 4.9. Simulated, measured gains and simulated efficiency of the proposed antenna.

Table 4.2. Comparison of the proposed CRLH MTM inspired work with the existing literature

Ref.	No. of bands	Frequ-ency (GHz)	Physical Size (mm^3)	Electrical Size ($\lambda_0{}^2$)	Impedance Bandwidth (%)	Effici-ency (%)	Gain (dBi)
[35]	2	2.46 5.5	36 x 24 x 1.59	0.26 x 0.19	3.65 52	64 89.2	0.71 1.53
[44]	2	2.5 5.8	44 x 70 x 1.6	0.36 x 0.58	22.8 10.8	94 92.1	> 0.2 > 3.1
[47]	2	1.8 5.2	40 x 30 x 1.6	0.24 x 0.21	2.2 13	>60	-2 4
[48]	2	2.45 5.5	38.2 x 29.1 x 6	0.31 x 0.23	4 12	84.2 90.3	2.3 8.6
[50]	2	2.76 5.23	36 x 36 x 3	0.33 x 0.33	1.44 3.05	79.4 90.8	1.02 6.8
[52]	2	2.6 3.6	31.7 x 27 x 1.6	0.27 x 0.23	2.2 28.53	79.3 95.6	<1.44 <1.98
[39]	3	2.45 3.5 4.7	32 x 25 x 0.064	0.26 x 0.2	3.08 15.17 8.33	-	2.1 2.8 3.5
[57]	3	1.78 4.22 5.8	20 x 20 x 0.508	0.11 x 0.11	3.08 15.17 8.33	70 96 >80	-0.15 2.18 3.58
[58]	3	2.6 3.6 5.8	35 x 32 x 1.6	0.3 x 0.27	7.7 14.1 10.7	-	0 1.6 2.7
proposed	2	3.5 5.5	24 x 17 x 1.6	0.28 x 0.2	26.8 8.9	>82 >89	>2.9 >4.1

4.3.5. Parametric study

The parametric study by varying the positions of rectangular strips is carried out and the results are depicted in Fig. 4.10. The position x1(starting position of the thin rectangular strip part of the unit cell) is varied in the positive *x*-direction and the respective S11 and axial ratio curves are plotted, and it is observed that at an optimum position of x1 = 5.5 mm, the dual band nature with an AR of less than 3 dB is achieved. It is also observed that without a significant

degradation in the S11 performance of the antenna the CP is observed at this position. Since the narrow strip connecting the ground plane with the unit cell placed at the ground side aids the current flow, the starting position of the strip y1 is varied along the positive *y*-direction and the respective S11 and axial ratio plots are indicated in Fig. 4.10(c) and (d). At an optimum position of y1 = 2.5 mm, the restoration of dual band nature with CP in the second band is observed. The parametric analysis is conducted by keeping all the other parameters unchanged except the parameter under consideration.

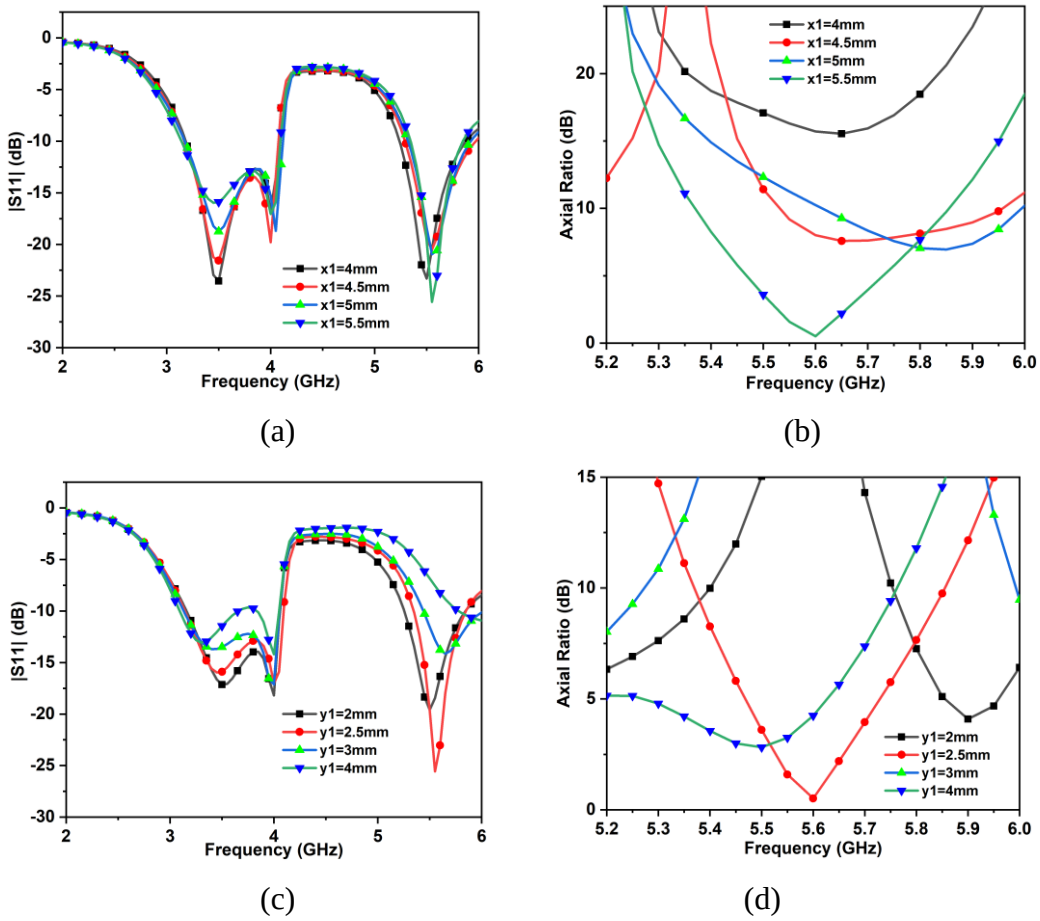

Fig. 4.10. Influence of variation in the position of the (a) x1 on S11, (b) x1 on axial ratio, (c) y1 on S11, and (d) y1 on axial ratio.

The performance of several dual and tri band antennas that are composed of different metamaterial structures and operating in the similar frequency range which are published in the literature, are compared with the proposed antenna in Table 4.2. It can be summarized that the designed antenna offers a larger fractional bandwidth over the first band when compared with other literature mentioned in the table and the antenna also offers circular polarization in the second band with a considerably smaller size. Moreover, the antenna offers a better average

gain across both the bands with good radiation efficiencies throughout the bands. Hence the antenna can become a good candidate for several Wi-Fi applications.

4.4. Conclusion

In this chapter, a new compact CRLH MTM-TL based dual band antenna has been presented. It makes use of a FR4 substrate which is of low cost with a planar structure and hence can be easily fabricated. The CRLH MTM inspired unit cell composed of inductors and capacitors induce the dual band nature with center frequencies of 3.5 GHz and 5.5 GHz. The percentage impedance bandwidths of antenna in two bands are 26.8 and 8.9 with the peak gains ranging in-between 2.9 - 4 dBi and 4.1 - 5.2 dBi. The antenna is linearly polarized in the first band and circularly polarized in the second with good radiation characteristics. A decent size reduction is achieved with a good matching between the simulated and measured results. The antenna has a great potential to be installed in 3.5/5.5 GHz WiMAX bands and the sub-6 GHz 5G bands.

Chapter-5

Dual-Band Meandered Line Based Antenna with Metasurface for Wireless Applications

5.1. Introduction

Metamaterials have been used in antennas because of their distinctive electromagnetic features. Several metamaterial structures have been loaded in the antenna design to achieve dual and multi band nature. Though the traditional microstrip antennas provide some of the required features, the research is going on in realizing the desired compact antennas with optimized performance using metamaterial loading. Traditional monopole antennas with MTM loading are proposed [69], [70], working at 2.4/5 GHz WLAN and 5.5 GHz WiMAX for Wi-Fi applications, introducing an extra resonance in addition to the existing resonance. Multiple techniques were employed in realizing multiband antennas like reconfigurability [71] but with an increase in design complexity. The metamaterials can achieve some of these requirements when properly loaded in the antenna design.

Metamaterials have been used in antennas because of their distinctive electromagnetic features. Several metamaterial structures have been loaded in the antenna design to achieve dual and multi band nature [72-75]. Composite right left-handed transmission line (CRLH-TL) based antennas particularly helps in achieving the miniaturization but with a drawback of narrow bandwidths limiting their applications. Hence, the extension in the bandwidth of such antennas have been the subject of an investigation [76-78]. Several antennas backed by metasurface (MS) have been proposed [79- 84] to improve gain and radiation performance of antenna. The proposed antenna consists of meandered line structures placed as a part of the radiating antenna which leads to an increase in the bandwidth operating from 5.06 - 6.77 GHz with an impedance band width of 33.7% and is realized on a cost-effective FR-4 substrate.

Moreover, the metasurface has been designed and employed as a part of the design to improve the gain.

In this chapter, a dual band meandered line loaded antenna backed by a MS with an improved bandwidth and CP radiation in one of the bands, for wireless application is proposed. The meandered line structure acts as a shorted inductor and aids in realizing the dual band. The antenna has an operating range of 3.26 - 3.61 GHz and 5.06 - 6.77 GHz, working in two bands with a bandwidth of 11.4% and 33.7% respectively. The maximum gain of antenna was noted to be 7.66 dBi and 8.7 dBi within the two bands with decent radiation efficiencies making it suitable for 5.2/5.8 WLAN, 3.5/5.5 WiMAX bands.

The remaining contents of this chapter are detailed as follows: The design comprises of a meandered line-based radiator and the metasurface is described in Section 5.2. The results of the antenna along with the working and discussions pertaining to the performance parameters of antenna are listed in the Section 5.3. The conclusion of this chapter is given in Section 5.4.

5.2. Antenna Design

The proposed meandered line-based antenna configuration is as shown in the Fig. 5.1. The FR4 substrate of height 1.6 mm is used for the main radiator and 3.2 mm is used for the metasurface and is employed at the groundside of the radiating antenna. Firstly, rectangular microstrip fed antenna is designed and a cut is introduced followed by loading a meandered line metamaterial inspired structure. However, to introduce an additional band for dual band operation of the antenna, two more similar meandered line structure are incorporated in the design. In addition, a metasurface layer is also introduced to boost the gain and better the radiation efficiency of the antenna. The antenna's optimized dimensions are listed in the Table 5.1.

Table 5.1. Optimized dimensions of the proposed meandered line-based antenna

Parameter	**Dimension(mm)**	**Parameter**	**Dimension(mm)**
L	27	W_F	3
W	27	L_1	43.8
L_P	12	W_1	43.8
W_P	22	h_1	1.6
L_G	13.5	h_2	3.2
W_G	17	H	18.4
L_F	14		

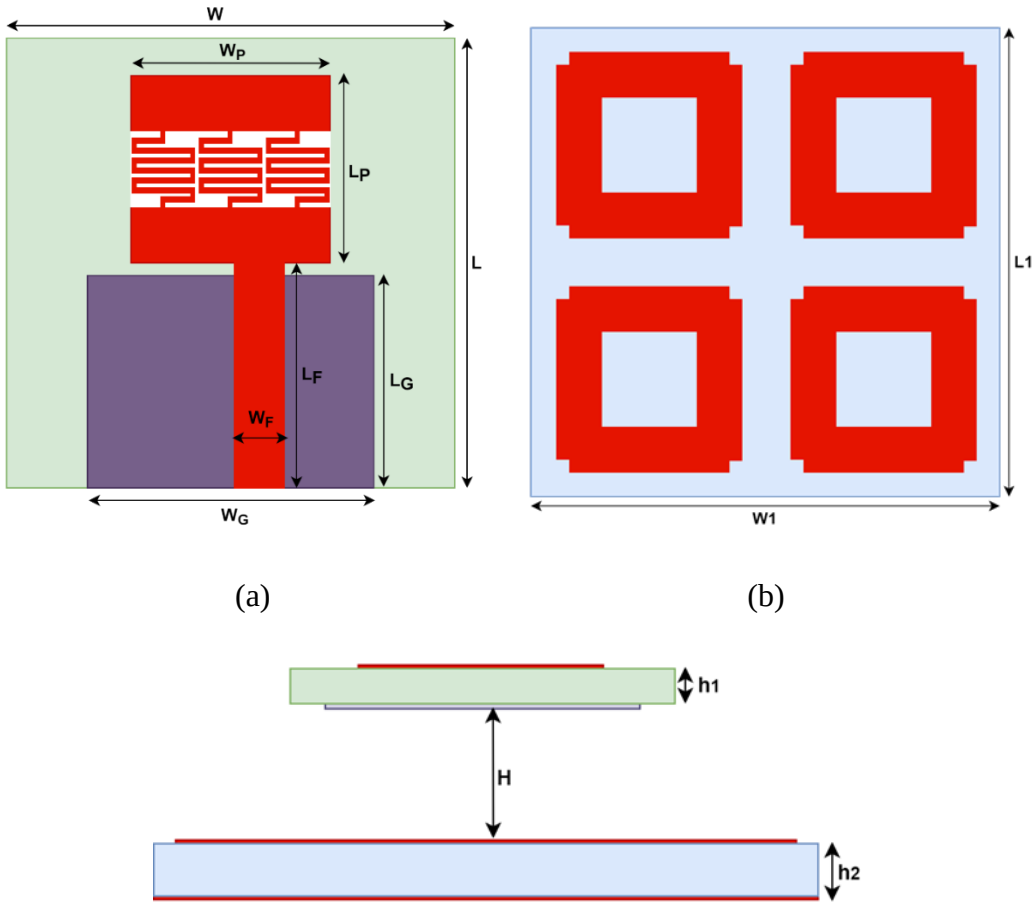

Fig. 5.1. Geometry and configuration of the proposed meandered line loaded antenna (a) Schematic view of the radiator antenna, (b) Metasurface, and (c) Side view of the antenna

5.2.1. Design of the meandered line radiator antenna

The various design stages of the MTM inspired radiating antenna are depicted in the Fig. 5.2. Initially a microstrip fed rectangular patch is designed, that induces a single wide band as represented in the Fig. 5.3(a). Further, a MTM inspired meandered line structure is slotted in, which acts as a shorted inductor and the dimensions of the meandered line structure are adjusted to achieve a single operational wideband from 5.04 - 5.99 GHz having a mid-frequency of 5.63 GHz. The antenna also offers wide band circular polarization almost covering the entire band from 5.08 - 5.81 GHz as depicted in Fig. 5.3(b). With the introduction of two other similar meandered line structures, adds to the inductance and induces an additional band, it also aids in increasing the bandwidth compared to the unloaded antenna. A partial ground is employed to

improve the bandwidth and improve the input reflection coefficient. Antenna 3 as shown in the Fig. 5.2(c), operates at 3.13 - 3.56 GHz and 5.17 - 6.88 GHz with CP in the second band from 5.14 - 5.46 GHz. The S11 and axial ratio performance of the three antennas is shown in the Fig. 5.3.

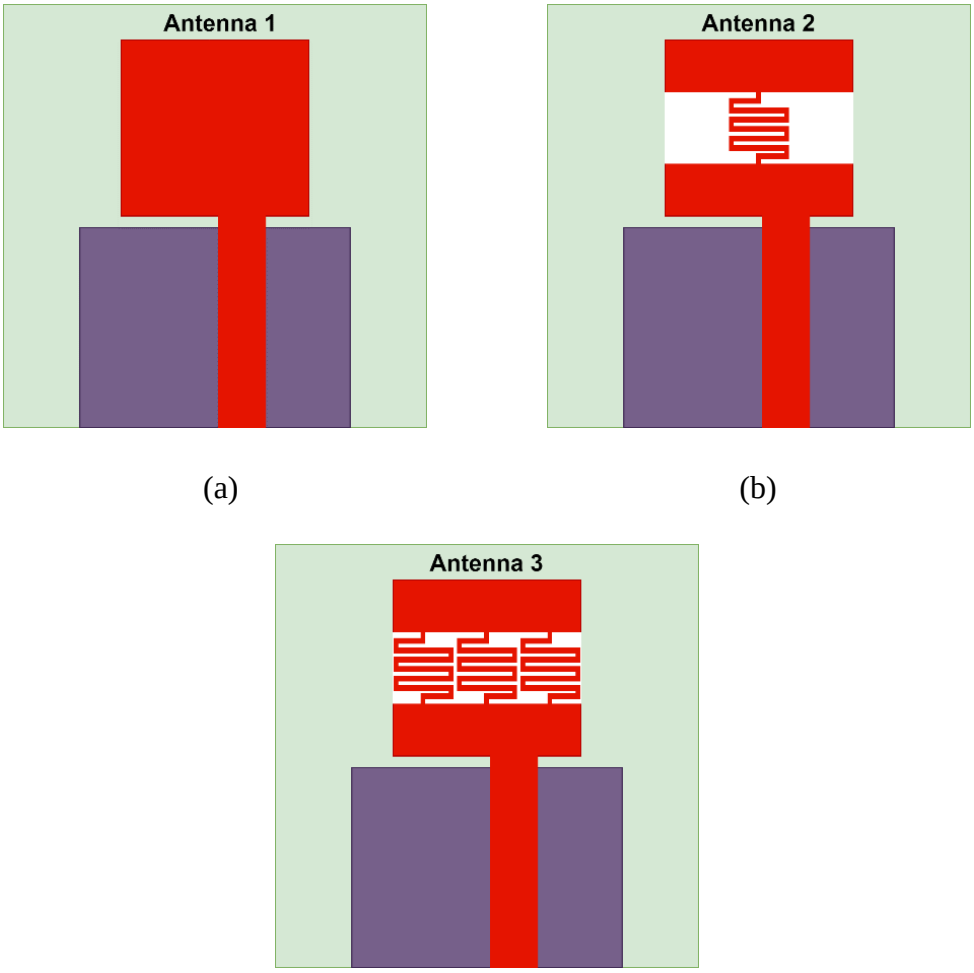

Fig. 5.2. Evolutionary stages involved in design of the proposed antenna (a) Antenna 1, (b) Antenna 2, and (c) Antenna 3.

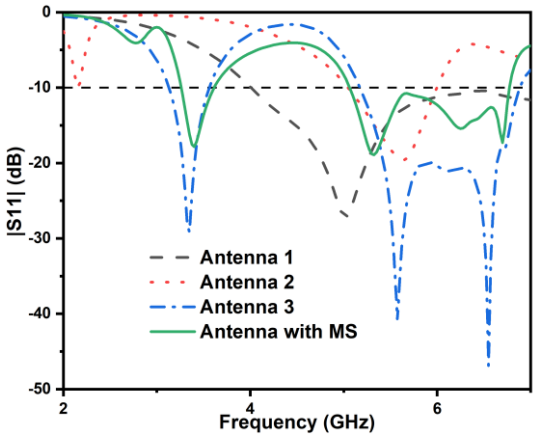

(a)

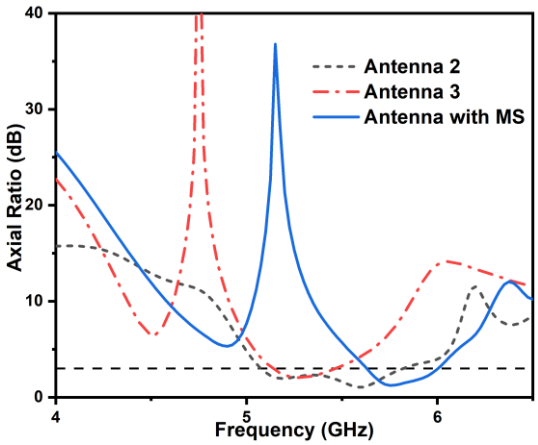

(b)

Fig. 5.3. Antenna Response (a) Reflection Coefficient, and (b) Axial Ratio

5.2.2. Design of the Metasurface

The design configuration of the meandered line antenna backed by MS is displayed in the Fig. 5.1(b). The detailed view of a single unit cell and its dimensions are presented in the Fig. 5.4(a). The optimized dimensions (in mm) are listed as A1 = 21.9, A2 = 18.3, A3 = 10.7, A4 = 1.8. An Artificial magnetic conductor (AMC) unit cell is designed, and its simulated reflection phase plot is presented in Fig. 5.4(b). It has a zero phase at 3.5 GHz which coincides with the first band of the antenna and hence affects an increase in the gain. The AMC unit cell acts as perfect electric conductor (PEC) with 180-degree phase in the second band of antenna operation. The unit cell is repeated to form an array of 2 x 2 AMC-MS and is separated by a distance of H from the radiating antenna. The MS antenna has a reduced size compared to the existing MS backed antennas.

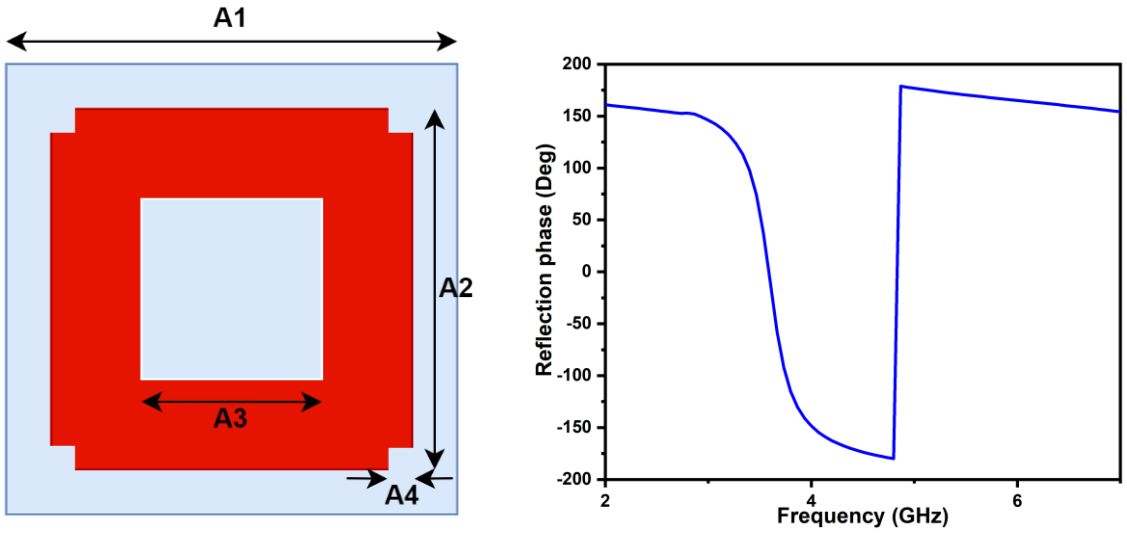

(a) (b)

Fig. 5.4. Proposed Metasurface design (a) Unit cell, and (b) Reflection phase of the unit cell

5.3. Results and Discussions

The photo representing prototype of this proposed meandered line antenna is illustrated in the Fig. 5.5(a) and (b). The measurements were carried out for the antenna using the VNA and the setup is represented in the Fig. 5.5(c) for the frequency range 2 to 7 GHz and its performance is compared with their simulated plots. The measured reflection coefficient of the antenna without and with the metasurface (MS) are depicted in the Fig. 5.6(a) and Fig. 5.6(b). It is seen from the Fig. 5.6(a), that the antenna has dual bands from 3.13 - 3.56 GHz and 5.17 - 6.88 GHz. The antenna has a wider second band with dual resonance, which is due to the loading of the multiple meandered line structures. These meandered line structures introduce resonances which are closer, and they merge to form a wide band. The antenna almost has similar response when backed by a MS, with the S11 ranging from 3.26 - 3.61 GHZ and 5.06 - 6.77 GHz.

The simulated radiation properties of the antenna are validated by radiation pattern measurements. These patterns are measured in an anechoic chamber(controlled environment) represented in the Fig. 5.5(d), using NSI patterns recording system. Antenna gain is also calculated from these radiation patterns by gain comparison/gain transfer method. The standard horn antenna has been used for gain calculations. The peak gains of the antenna with and without the metasurface, in the two operating bands is shown in the Fig. 5.6(c). The maximum gain of the antenna without the MS is observed to be 3.7 dBi and 7.4 dBi and with the

introduction of the MS, due to reflections there is an increase in the radiation in one direction. Hence there is an increase in the antenna gain, measuring 7.66 dBi in the first band with a betterment of 3.96 dBi and 8.7 dBi in the second band with an improvement of 1.3 dBi. A considerable increase in the gain in the first band is due to the zero-reflection phase of the AMC unit cell when compared with the second band where the AMC unit cell acts as PEC.

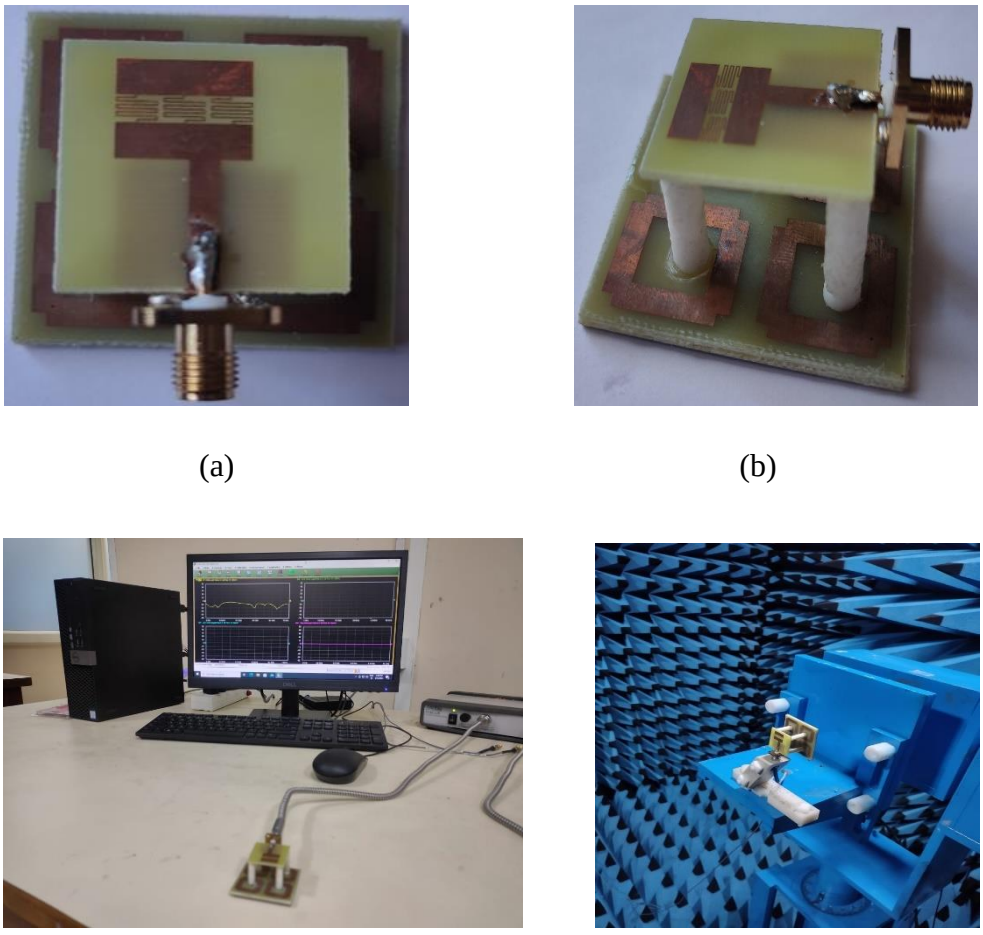

(a) (b)

(c) (d)

Fig. 5.5. Fabricated prototype of the proposed antenna (a) Top view, (b) Side view, (c) Measurement setup for S11 of antenna using VNA, (d) Measurement setup of antenna in anechoic chamber.

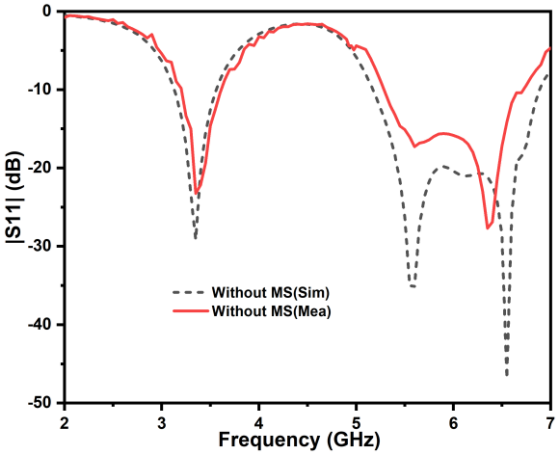

(a)

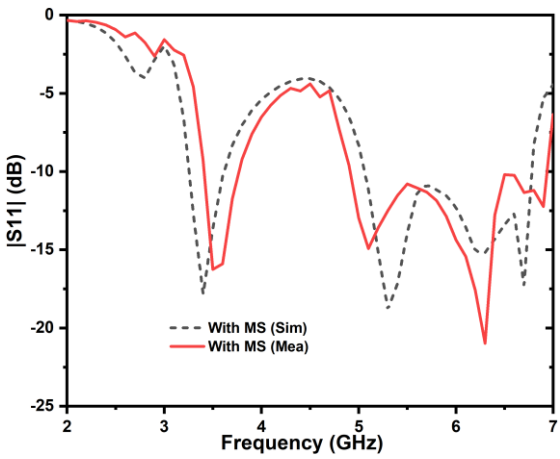

(b)

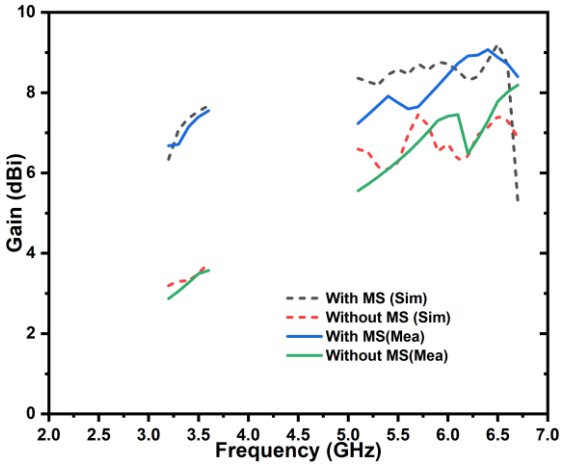

(c)

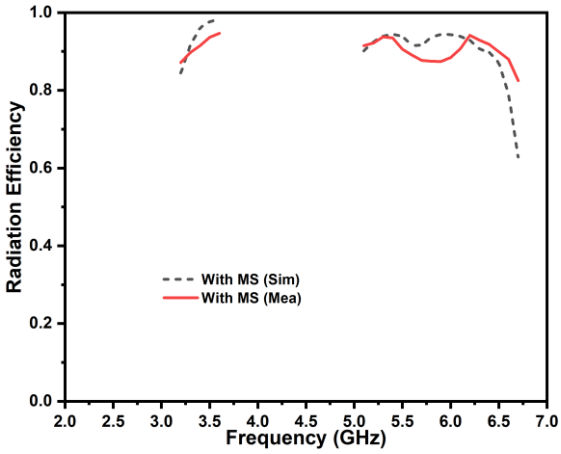

(d)

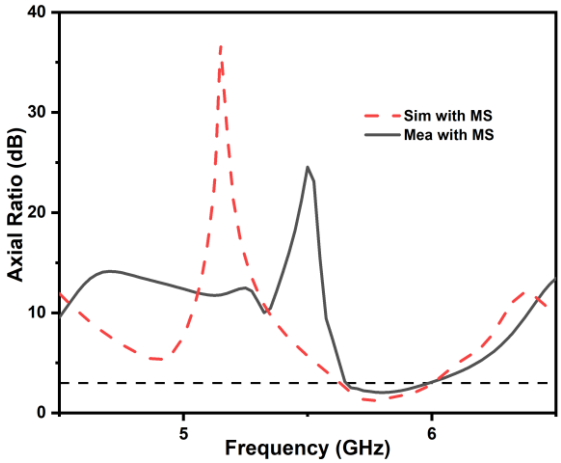

(e)

Fig. 5.6. Simulated and measured results (a) S11 without MS, (b) S11 with MS, (c) Gain, (d) Radiation Efficiency, and (e) Axial Ratio with MS

The radiation efficiency plot is presented in the Fig. 5.6(d), a decent value of >89% in the first and >60% in the second bands (>85% upto 6.4 GHz) is measured. The comparison of the presented work with similar existing MS backed antennas is listed in the Table 5.2. As depicted in the Fig. 5.6(e), the antenna provides the circular polarization in its second band from 5.62 – 5.99 GHz.

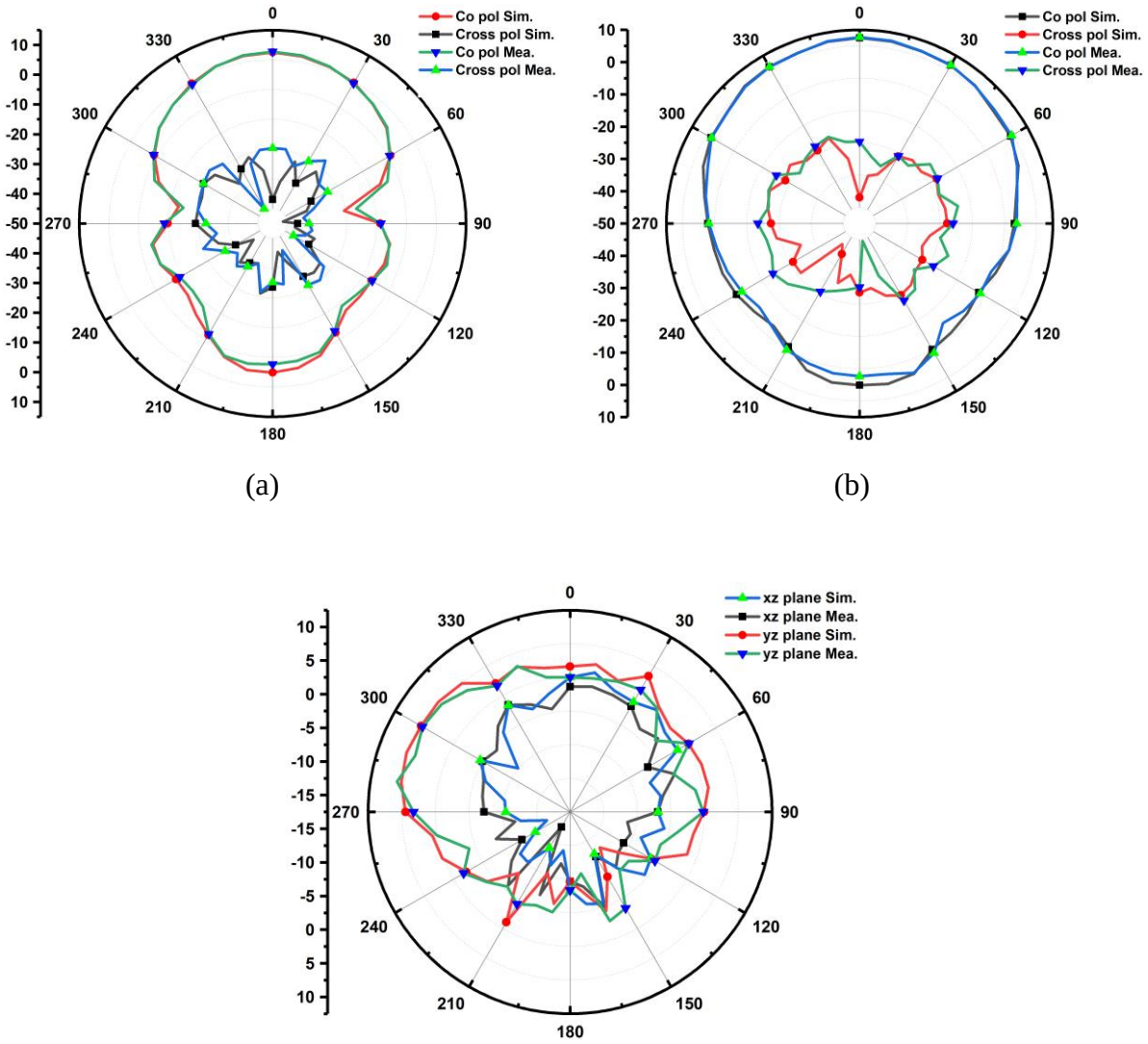

(a) (b)

(c)

Fig. 5.7. The simulated and measured radiating patterns a of the proposed MS backed antenna in (a) XZ plane at 3.45 GHz, (b) YZ plane at 3.45 GHz, and (c) XZ and YZ planes at 5.8 GHz.

Table 5.2. Comparison of the designed MS backed antenna with similar antennas.

Ref. No	Operating Frequency	Overall size of antenna (mm)	Impedance Bandwidth (%)	Gain (dBi)	Radiation Efficiency (%)
[80]	3.25 6.08	80 x 80 x 13.5	15.4 2.5	- -	- -
[81]	2.15 5.45	120 x 120 x 40	60.45 16.51	5.5 5.7	- -
[82]	2.56 5.37	104 x 104 x 11	15.6 9.3	7.2 7.3	>65 >65
[83]	2.42 5.15	72 x 72 x 11	16.7 11.5	>5 >5	>78 >80
[84]	5.6 10	80 x 80 x 14.8	4.1 2.7	10.1 15.2	>80
Proposed Antenna	**3.4 5.5**	**43.8 x 43.8 x 23.2**	**11.4 33.7**	**7.66 8.7**	**>89 >89(upto 6.4 GHz)**

5.4. Conclusion

A meandered line loaded antenna backed by a MS for wireless applications is presented. The antenna makes use of a cost effective FR4 substrate for both radiator and MS layers. The single meandered line loaded antenna operates over a single band from 5.04 - 5.99 GHz with a wide AR bandwidth of 730 MHz. With the loading of two other similar meandered line structures and backed by MS layer, the antenna operates over a dual band from 3.26 - 3.61 GHz and 5.07 - 6.77 GHz with a bandwidth of 11.4% and 33.7% respectively. The antenna has peak gain of 7.66 dBi and 8.7 dBi in the two bands with good radiation characteristics and CP radiation in the second band. A proper match of the simulated results and their respective measured ones were identified making the antenna suitable for 5.2/5.8 GHz WLAN, 3.5/5.5 GHz WiMAX bands.

Chapter-6

SRR and CSRR based Multiband Antennas for Wireless Applications

6.1. Introduction

The SRR and CSRR are a type of metamaterial structures that consists of a split ring with a small gap. They are typically etched or printed on a substrate or circuit board as a part of the design. The size of the ring and the gap can be adjusted in order to vary the resonant behaviour at certain frequencies. The use of these structures allows us in achieving specific properties or to improve the antenna performance. These structures are often employed to manipulate electromagnetic waves in a way that is not possible with conventional materials, leading to a novel antenna design. The focus is to develop and design multiband antennas with simplest of structures and compact in size. The use of split ring and complementary split ring resonators (SRR and CSRR) have attracted a lot of researchers in realizing multiband and miniaturized antennas. A dual band operating antenna is proposed by etching two CSRR on the ground plane [85], but with both narrow bands. An antenna loaded with four CSRR cells has been constructed to achieve size reduction [86]. A modified CSRR being implemented with EBG loading to achieve miniaturization in the design of antenna [87]. A multiband antenna is realized using a mushroom unit cell loaded CSRR to a patch antenna [88]. Several such dual and multi band antennas are proposed for wireless applications [89-92]. However, these antennas have a very low impedance bandwidth or larger in size.

In this chapter, the SRR and CSRR structures have been effectively used to realize multi band antennas with an improved performance characteristics. The antennas incorporated with SRR and CSRR structures provide additional resonance modes and hence allowing the antenna to work across multiple bands. A CSRR loaded antenna with dimensions of 30 mm x 24 mm

1.6 mm is presented with dual band operation of 2.45 - 2.54 GHz and 3.27 - 5.97 GHz. The impedance bandwidths of the antenna are 3.6% and 72%. The antenna is suited for 2.5/3.5/5.5 GHz WiMAX, 5.2/5.8 GHz WLAN, and sub-6 GHz 5G. The efficiency of the antenna was observed to be greater than 62% in the first and more than 80% in the second band.

This chapter also presents a triband antenna with two split ring resonators of different dimensions has been proposed. The inclusion of the split ring resonators induces the additional operating bands, and a slot is etched at the ground side and its dimensions are chosen to offer a good impedance bandwidth and CP in one band. The antenna dimensions are 40 mm × 40 mm × 1.6 mm with operating bands of 2.5 - 2.78 GHz, 3.05 - 3.75 GHz and 4 - 5.9 GHz and peak gains 3.4, 4.81, and 8.15 dBi in the three bands respectively. The antenna has its applications in 2.5/3.5/5.5 GHz WiMAX, 5.2/5.8 GHz WLAN frequency bands.

The remaining contents of this chapter are structured as follows: The design of a CSRR based antenna for WLAN/WiMAX/sub-6 GHz 5G applications is demonstrated in Section 6.2. The design of a SRR loaded multiband antenna for wireless applications is presented in Section 6.3. The conclusion of this chapter is given in Section 6.4.

6.2. A CSRR Based Dual Band Antenna for Wireless Applications

A rectangular patch is employed as a radiator that is etched on a cost effective FR4 substrate of relative permittivity 4.4 and having a thickness of 1.6 mm. The dimensions of designed antenna are 30 x 24 x 1.6 mm^3 and is fed by a simple microstrip line, as represented in the Fig. 6.1. The antenna simulations were done, and its operating range is observed to be 3.27 - 5.97 GHz as shown in the Fig. 6.2.

6.2.1. CSRR loaded Antenna

The antenna loaded with CSRR as shown in the Fig. 6.1. An extra narrow band operating from 2.45 - 2.54 GHz is introduced because of this loading. The dimensions of the CSRR are optimized to obtain a band at the required frequency. The antenna's dimensions are optimally chosen and the same are listed in the Table 6.1. Since its design is simple, makes use of a cost effective FR4 substrate and can be easily integrated in RF devices, it can be considered as a viable option for wireless based devices and applications.

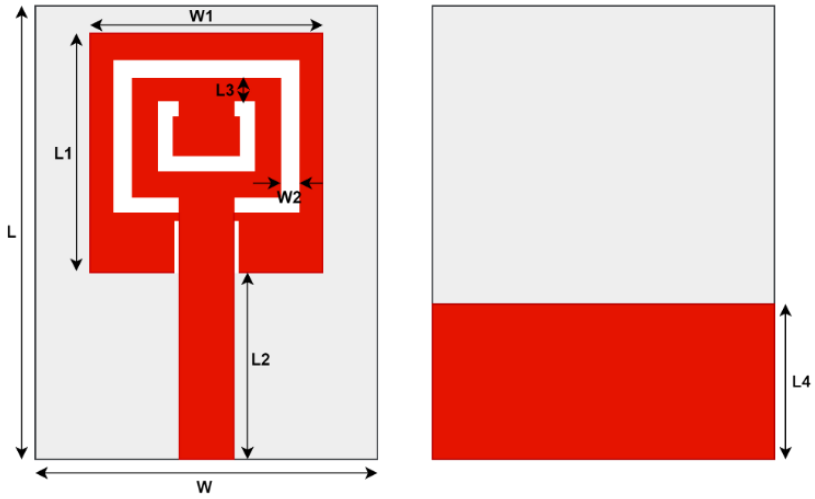

Fig. 6.1. Geometry of the proposed CSRR based antenna

Table 6.1. Dimensions of the proposed CSRR based antenna

Parameter	Value(mm)
L	30
W	24
L1	16
W1	14
L2	11.5
W2	1
L3	2.1
L4	9.5

6.2.2. Results and Discussions

The antenna operates over two bands (|S11| < -10dB) with the first band being a narrow band 2.45 - 2.54 GHz is due to the loading of the CSRR and second being an ultrawide band 3.27 - 5.97 GHz is due to radiating patch, as depicted in S11 curve shown in the Fig. 6.2. The realized bandwidth of antenna in first and the second band is 3.6% and 72% respectively.

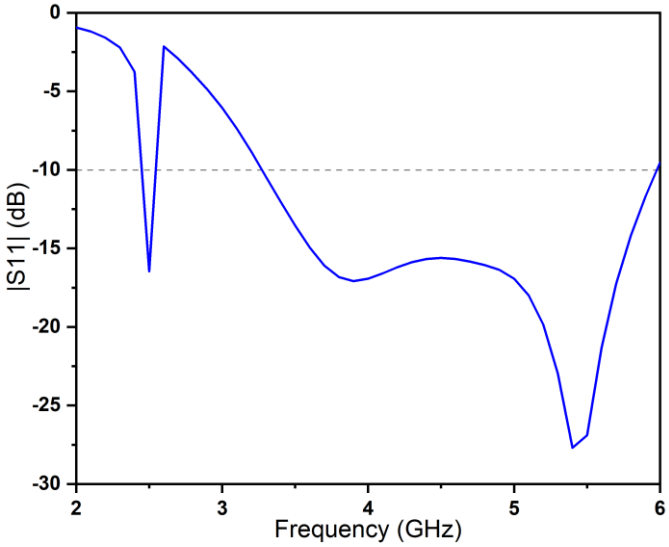

Fig. 6.2. S11 of the CSRR loaded antenna

The radiation characteristic pattern of the antenna at frequency 2.5, 3.7, 4.8 and 5.5 GHz are shown in the Fig. 6.3. It can be noticed that the antenna offers a similar and omnidirectional radiation patterns, but with a slight distortion at higher frequency is due to operation of the antenna in higher ordered modes. From Fig. 6.4, the peak gains are observed to be -1.61, 2.92, 4.33, and 4.49 dBi at 2.5, 3.7, 4.8 and 5.5 GHz respectively. It is also realized that the antenna offers a good radiation efficiency over the two bands.

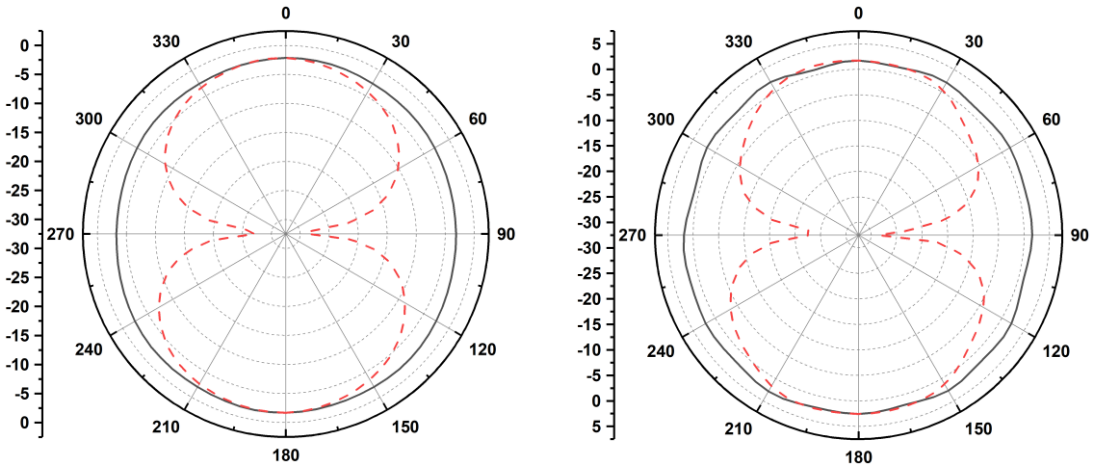

(a) (b)

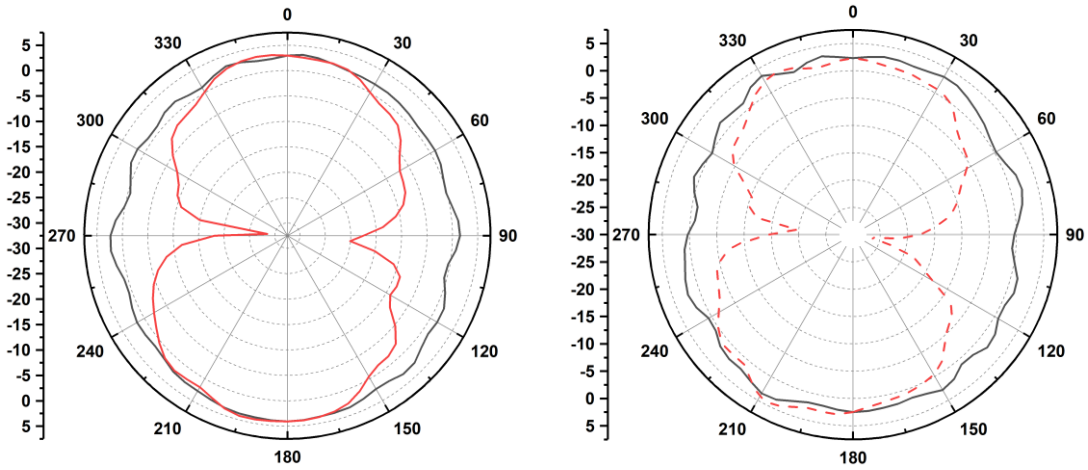

(c) (d)

Fig. 6.3. Antenna's simulated radiation patterns at frequency (a) 2.5 GHz, (b) 3.7 GHz, (c) 4.8 GHz, and (d) 5.5 GHz

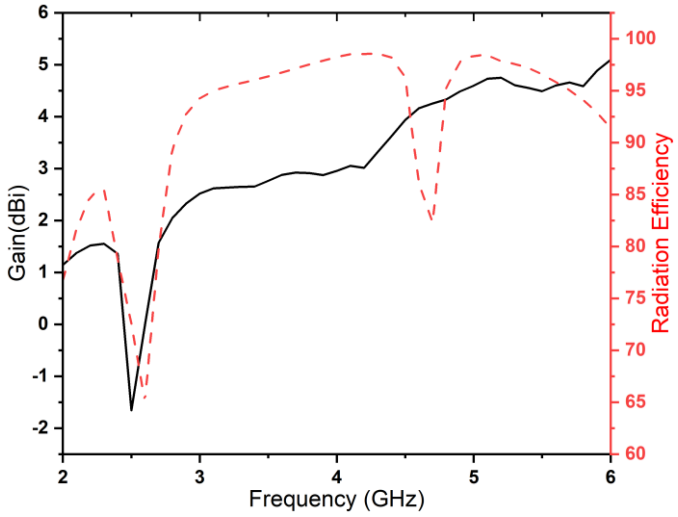

Fig. 6.4. Radiation efficiency and Gain of the proposed antenna

6.3. A Triband Dual SRR Loaded Antenna for Wireless Applications

The antenna is designed on a square shaped FR4 substrate having a relative permittivity 4.4 and with a thickness 1.6 mm. The dimensions are listed in the Table 6.2 with an overall size of 40 x 40 x 1.6 mm^3 and is excited by a simple microstrip feedline, as depicted in the Fig. 6.5. The design of the antenna and its simulations were done using the HFSS software, and the antenna is observed to be operating over three bands as shown in the Fig. 6.6. The slot with the feedline

alone induces a single band and with the introduction of two split ring resonators, two more bands are introduced and hence making it a triband antenna.

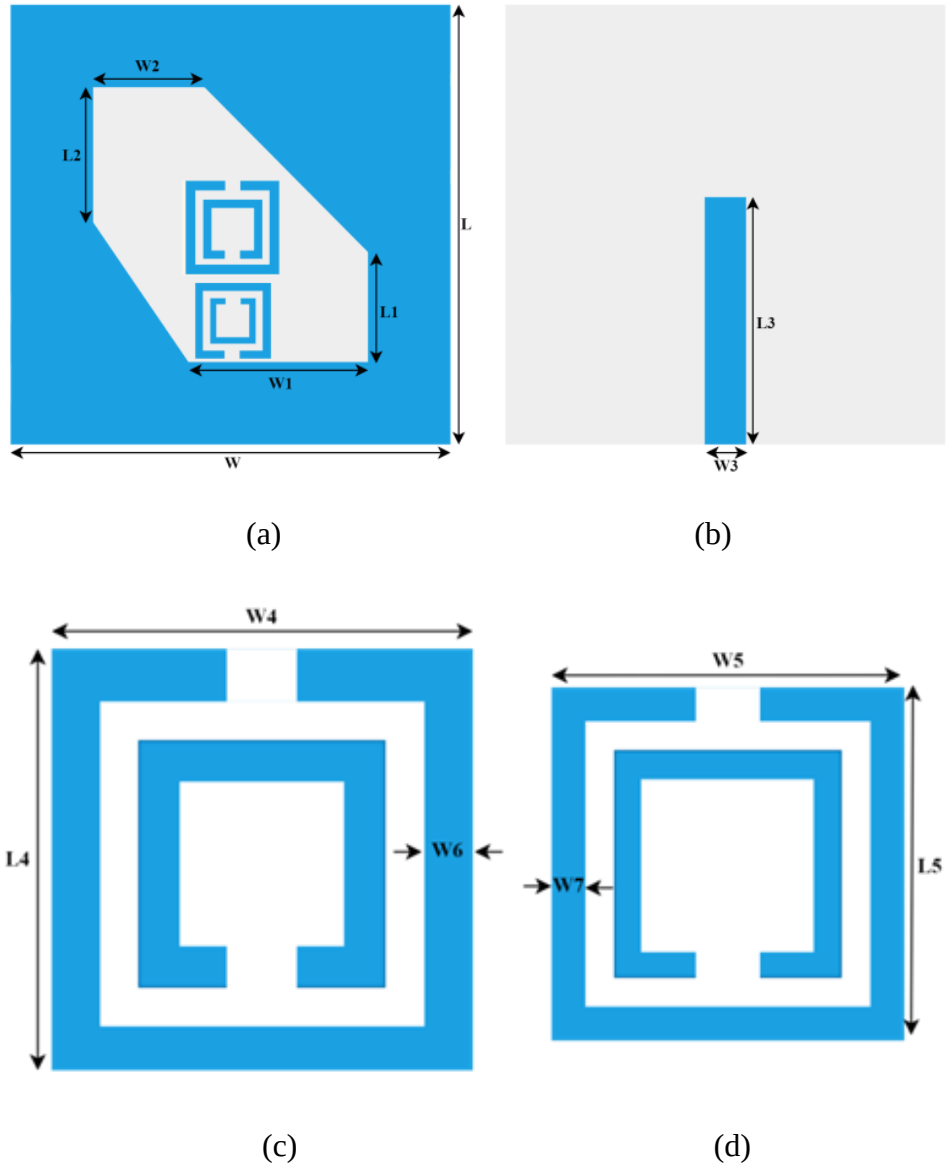

Fig. 6.5. Design Configuration of the SRR loaded antenna (a) Top view, (b) Bottom view, (c) Top SRR, and (d) Bottom SRR

6.3.1. SRR loaded Antenna

The unloaded antenna with only the slot and feedline induces a single band with resonance at 3.3 GHz. The antenna is loaded with the top SRR which induces an additional band and hence making antenna work as a dual band antenna with resonances at 2.7 GHz and 4.5 GHz. Furthermore, a SRR with slightly smaller dimensions as shown in the Fig. 6.5(d) is introduced

at the bottom side of the first SRR and it results in an additional resonance at 5.75 GHz. Hence, the antenna operates over three bands with a wider third band. Moreover, the dimensions of the slot are adjusted in order to achieve circular polarization from 4.87 - 5.2 GHz.

Table 6.2. Dimensions of the proposed SRR based antenna

Parameter	Value(mm)	Parameter	Value(mm)
L	40	W3	2.2
W	40	L4	9
L1	10.5	W4	9
W1	14	L5	6
L2	12	W5	6
W2	10.5	W6	0.9
L3	22	W7	0.6

6.3.2. Results and Discussions

The proposed antenna has a triband operation(|S11| < -10dB) from 2.5 - 2.78 GHz, 3.05 - 3.75 GHz and 4 - 5.9 GHz with resonance at 2.7, 3.55 and 5.75 GHz respectively as displayed in the Fig. 6.6(a). The unloaded antenna with a modified square slot has a single band operation with resonance at 3.3 GHz. The different bands of operation are achieved by the loading of SRRs where the loading of the top SRR induces the first band and the bottom SRR induces the third band. Moreover, the asymmetry in the slot dimensions is due to the parametric optimization carried out to attain the circular polarization in third band from 4.87 - 5.2 GHz as illustrated in the Fig. 6.6(b)

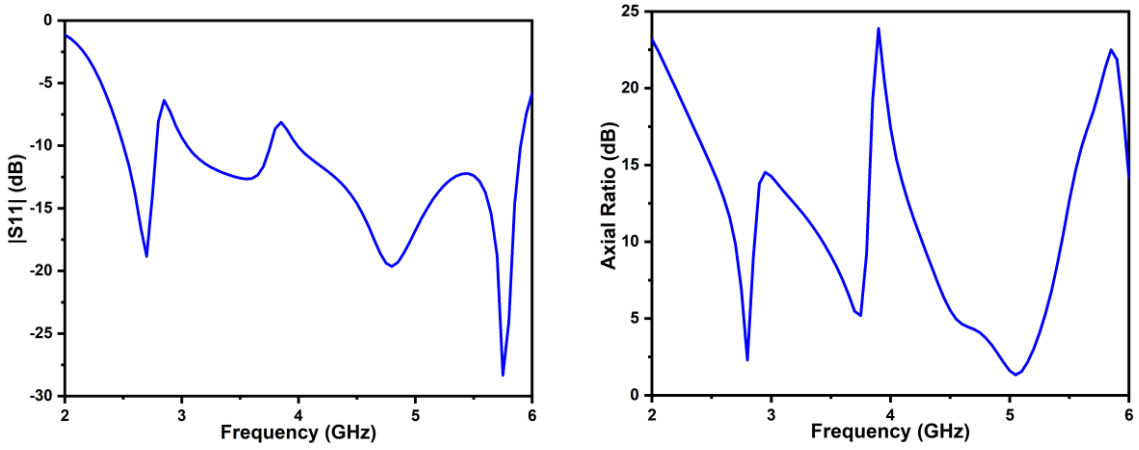

(a) (b)

Fig. 6.6. Simulated Antenna parameters (a) S11, and (b) Axial Ratio

The radiation patterns at frequencies 2.6, 3.55, 5.2 and 5.75 GHz are shown in the Fig. 6.7. The antenna offers a near omnidirectional radiation patterns, but with a slight distortion at higher frequencies due to operation of antenna in higher order modes. From Fig. 6.8, the peak gains of the antenna within three operating bands is observed to be 3.4, 4.81, and 8.15 dBi respectively. It is also realized that the antenna offers good radiation patterns with respectable gains in all the three bands making the antenna a suitable candidate for 2.5/3.5/5.5 GHz WiMAX and 5.2/5.8 GHz WLAN applications.

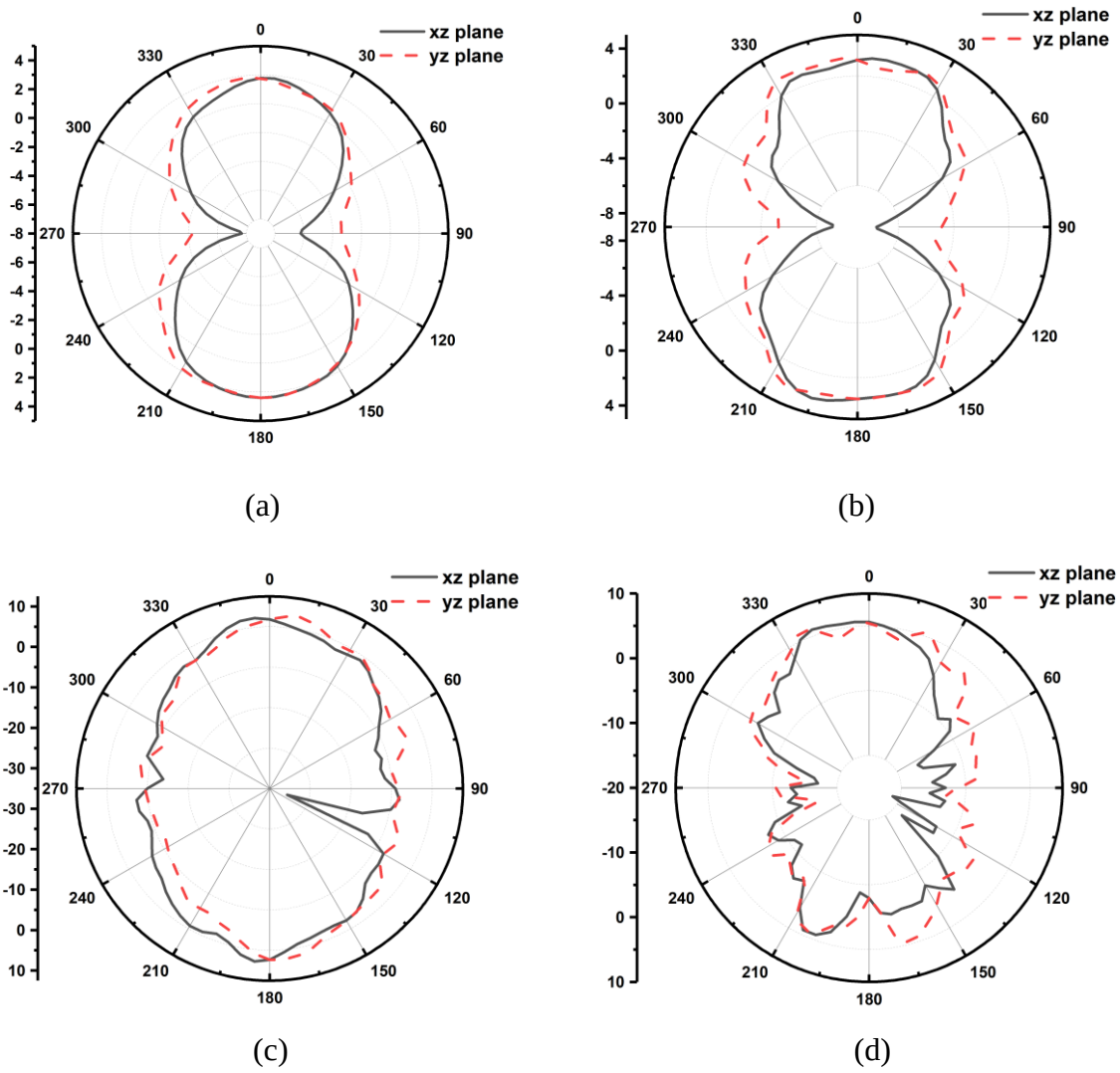

Fig. 6.7. Antenna's simulated radiation patterns at frequency (a) 2.6 GHz, (b) 3.55 GHz, (c) 5.2 GHz, and (d) 5.75 GHz

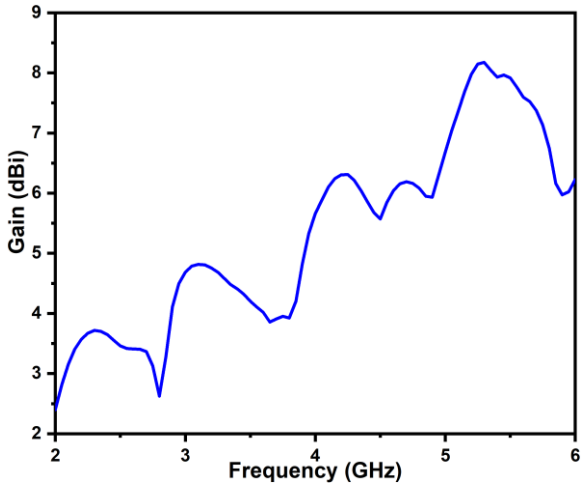

Fig. 6.8. Simulated Gain of the Antenna

6.4. Conclusion

A monopole antenna with a CSRR for wireless applications with dual band operation has been presented in this chapter. The wideband operating antenna is etched with CSRR, which induces a narrow band operating from 2.45 - 2.54 GHz and hence leading to a dual band operation. The antenna offers a wide second band with an impedance bandwidth of 72% and an omnidirectional radiation patterns. This antenna is suited for 2.5/3.5/5.5 GHz WiMAX, 5.2/5.8 GHz WLAN, and sub-6 GHz 5G. Also, a SRR loaded antenna has been presented with a triband operation. The inclusion of the split ring resonators induces the additional operating bands, and a slot is etched at the ground side to achieve good impedance bandwidth and CP in one band. The dimensions are 40 mm × 40 mm × 1.6 mm with operating bands of 2.5 - 2.78 GHz, 3.05 - 3.75 GHz and 4 - 5.9 GHz and peak gains 3.4, 4.81, and 8.15 dBi in the three bands respectively. The antenna has its applications in 2.5/3.5/5.5 GHz WiMAX, 5.2/5.8 GHz WLAN frequency bands. Moreover, the proposed CSRR and SRR based antennas are simple, of low cost and have an advantage of getting easily integrated into the wireless operating devices.

Chapter-7

Conclusions and Future Scope

7.1. Conclusions

In this thesis, the research has been presented on the design of metamaterial-based antennas which include an AMC backed antenna, a CRLH metamaterial inspired compact antenna, a meandered line antenna backed by a metasurface, and CSRR, SRR based antennas for wireless applications. It is composed seven chapters, with this as the last chapter.

In **Chapter 1**, introduction, background, and motivation factor for carrying out this work has been described.

In **Chapter 2**, the literature background of basics of an antenna, different parameters of an antenna, microstrip antenna, printed monopole antenna, metamaterials, and the effect of metamaterial utilization in antenna design have been provided.

In **Chapter 3**, by utilizing the slots that are etched on a monopole antenna, a dual band antenna operating at 2.4 GHz and 3.5 GHz has been designed. Moreover, the radiating antenna has been modified to achieve an increased bandwidth and it is backed by an AMC surface which is designed using a dual band AMC unit cell. The introduction of an AMC surface leads to enhanced gain and directional radiation patterns. The designed antenna has been compared with the other similar antennas which were presented in the previous literatures in terms of size, bands of operation, gain and efficiency. It covers 2.4/5 GHz WLAN applications, 2.5/3.5/5.5 GHz WiMAX applications.

In **Chapter 4**, a CRLH metamaterial inspired dual band antenna operating at 3.15 - 4.09 GHz and 5.35 - 5.84 GHz for wireless applications has been presented. A unit cell based on CRLH metamaterial is designed and has been included as part of the radiating antenna which

helped in realizing a dual band antenna with a wide first band and circular polarisation in the second band. Moreover, the circuit realisation of this unit cell and the overall radiating antenna are also presented. The results of the antenna are represented, and they indicate the antenna has a decent performance and is suitable for 3.5/5.5 GHz WiMAX and mid band 5G wireless applications.

In **Chapter 5**, a meandered line based dual band antenna backed by a MS with an improved bandwidth and CP radiation in one of the bands, for wireless application has been presented. The meandered line structure acts as a shorted inductor and aids in realizing the dual band. A metasurface is also designed using a unit cell which has an AMC behaviour in the lower band and PEC behaviour in the higher band which helps in increasing the gain of antenna. The results of the antenna along with the comparison of them with the existing antennas in the literature is also presented. The antenna is suitable for 5.2/5.8 GHz WLAN, 3.5/5.5 GHz WiMAX bands.

In **Chapter 6**, the SRR and CSRR structures have been effectively used to realize multi band antennas with an improved performance characteristics. A CSRR based antenna with dual operating bands for wireless applications has been presented. The antenna offers a wide second band with an impedance bandwidth of 72% with a near omnidirectional radiation patterns. The antenna is suited for 2.5/3.5/5.5 GHz WiMAX, 5.2/5.8 GHz WLAN, and sub-6 GHz 5G. Also, a dual split ring resonator loaded triband antenna for wireless applications has been presented. The inclusion of the split ring resonators induces additional operating bands, and a slot has been etched at the ground side and its dimensions were optimized to achieve good impedance bandwidth and CP in one band. The antenna has dimensions of 40 mm × 40 mm × 1.6 mm with operating bands of 2.5 - 2.78 GHz, 3.05 - 3.75 GHz and 4 - 5.9 GHz and peak gains 3.4, 4.81, and 8.15 dBi in the three bands respectively. The antenna has its applications in 2.5/3.5/5.5 GHz WiMAX, 5.2/5.8 GHz WLAN frequency bands. Both the designed antennas are multiband operating that are based on the SRR and are covering some of the widely used wireless frequency bands. Moreover, the proposed antennas are very compact, simple, and inexpensive.

All the antennas designed as a part of the thesis were targeted to cover certain frequency bands of WLAN, WiMAX, and sub-6 GHz 5G communications. A total of six antennas were designed and the list of the bands for which the antenna is suitable has been listed in Table 7.1. The antenna designed above can have applications in all the wireless operating devices working at the above-mentioned frequency bands. The size of the antenna is a constraint especially with

the inclusion of a metasurface and these antennas have a comparatively larger dimensions and hence can be used as base station antenna and panel antenna where a higher gain is required.

Table 7.1. List of Antennas designed, and frequency bands covered

Antenna	Frequency bands covered
Antenna 1	2.45 GHz WLAN, 3.5 GHz WiMAX
Antenna 2 (with MS)	2.4/5 GHz WLAN, 2.5/3.5/5.5 WiMAX and sub-6 GHz 5G bands
Antenna 3	3.5/5.5 GHz WiMAX and sub-6 GHz 5G bands
Antenna 4 (with MS)	5.2/5.8 GHz WLAN, and 3.5/5.5 WiMAX
Antenna 5	5.2/5.8 GHz WLAN, 2.5/3.5/5.5 WiMAX and sub-6 GHz 5G bands
Antenna 6	5.2/5.8 GHz WLAN, and 2.5/3.5/5.5 WiMAX

7.2. Future Scope

In this thesis, design of an AMC based antenna, design of CRLH metamaterial inspired antenna, design of a metasurface backed meandered line-based antenna and a CSRR, SRR loaded multi band antennas have been investigated. Based on the work presented in this thesis, many research works may be performed in the future. Some of them are listed below:

- Higher element antenna arrays based on these metamaterial unit cells can be designed for an improved gain and radiation performance, which are better suited for the advanced wireless communication technology.
- Several improvements in the performance parameters can be achieved like circular polarization in each of the operating bands along with polarization diversity could also be realised.
- Also, novel metasurfaces can be designed and used as a part of the antenna design which are helpful in improving its overall performance.

Bibliography

[1] C. A. Balanis, “Antenna Theory Analysis and Design”, 3rd edition, John Wiley & Sons, INC, 2005.

[2] Available online: http://images.elektroda.net/65_1330619143.gif.

[3] M. Bugaj, R. Przesmycki, L. Nowosielski, and K. Piwowarczk, “Analysis Different Methods of Microstrip Antennas Feeding for their Electrical Parameters”, PIERS Proceedings, Kuala Lumpur, Malaysia, pp. 27-30, March 27, 2012.

[4] K. P. Kumar, K. S. Rao, T. Sumanth, N. M. Rao, R. A. Kumar, and Y. Harish, “Effect of Feeding Techniques on the radiation Characteristics of Patch antenna: Design and Analysis”, International Journal of Advanced Research in computer and communication Engineering, vol. 2, no. 2, pp. 1276-1281, 2013.

[5] M. M. Gadag, D. S. Kamshetty, and S. L. Yogi, “Design of Different Feeding techniques of rectangular Microstrip Antenna for 2.4 GHz RFID Applications Using IE3D”, in Proceedings of the International conference on Advances in Computer, Electronics and Electrical Engineering, pp. 522-525, Tamil Nadu, March 2012.

[6] D. M. Elsheakh, and E. A. Abdallah, “Different Feeding Techniques of Microstrip Patch Antennas with Spiral Defected Ground Structure for Size reduction and Ultra-Wide band Operation”, Journal of Electromagnetic Analysis and Applications, vol. 4, no. 10, pp. 410-418, 2012.

[7] A. Majumder, “Rectangular Microstrip patch Antenna Using Coaxial Probe Feeding Technique to operate in S-Band”, International Journal of Engineering Trends and Technology (IJETT), vol. 4, no. 4, April 2013.

[8] V. M. Kumar, and N. Sujith, “Enhancement of Bandwidth and Gain of a Rectangular Microstrip Patch Antenna”, A Thesis Submitted to Electronics and Communication Engineering, National Institute of Technology, Rourkela, 2010.

[9] K.-L. Wong, “Compact and broadband microstrip antennas”. John Wiley & Sons, 2004.

[10] K. P. Ray, “Design aspects of printed monopole antennas for ultra-wide band applications”, International Journal of Antennas and Propagation, vol. 2008, pp. 1-8, 2008.

[11] T. Itoh, and C. Caloz, “Electromagnetic metamaterials: transmission line theory and microwave applications”. John Wiley & Sons. 2005.

[12] A. Pandey, and R. Mishra, “Compact Dual Band Monopole Antenna for RFID and WLAN Applications”, Materials Today: Proceedings 5, no. 1, pp. 403-407, 2018.

[13] S. N. Islam, A. Ghosh, M. Kumar, G. Sen, and S. Das, “A Compact Dual-band Antenna Using Triangular Split Ring Resonator for Bluetooth/WiMax/LTE Applications”. In 2018 IEEE Indian Conference on Antennas and Propagation (InCAP), pp. 1-3, 2018.

[14] K. Radouane, and H. Ammor, “Rectangular patch antenna for dual-band RFID and WLAN applications”, Wireless Personal Communications, vol. 83, no. 2, pp. 995-1007, 2015.

[15] J. Zhu, M. A. Antoniades, and G. V. Eleftheriades, “A compact tri-band monopole antenna with single-cell metamaterial loading”, IEEE Transactions on Antennas and Propagation, vol. 58, no. 4, pp. 1031-1038, 2010.

[16] J. H. Lu, B. R. Zeng, and Y. H. Li, “Planar multi-band monopole antenna for WLAN/WiMAX applications”, in IEEE International Symposium on Antennas and Propagation Conference Proceedings, pp. 475-476, 2014.

[17] I. Ali, and R. Y. Chang, “Design of dual band microstrip patch antenna with defected ground plane for modern wireless applications”, in 2015 IEEE 82nd Vehicular Technology Conference (VTC2015-Fall), pp. 1-5. 2015.

[18] X. L. Sun, S. W. Cheung, and T. I. Yuk, “Dual-Band Monopole Antenna with Compact Radiator for 2.4/3.5 GHz WiMAX Applications”, Microwave and Optical Technology Letters, vol. 55, no. 8, 1765-1770, 2013.

[19] A. Dadhich, P. Samdani, J. K. Deegwal, and M. M. Sharma, “Design and Investigations of Multiband Microstrip Patch Antenna for Wireless Applications”, in Ambient Communications and Computer Systems, Springer, Singapore, pp. 37-45, 2019.

[20] M. J. Sathikbasha, and V. Nagarajan, “DGS based Multiband Frequency Reconfigurable Antenna for Wireless Applications”, in IEEE International Conference on Communication and Signal Processing (ICCSP), pp. 0908-0912, 2019.

[21] J. Malik, A. Patnaik, and M. V. Kartikeyan, “A compact dual-band antenna with omnidirectional radiation pattern”, IEEE Antennas and Wireless Propagation Letters, vol. 14, pp. 503-506, 2014.

[22] Q. X. Chu, and L. H. Ye, “Design of compact dual-wideband antenna with assembled monopoles”, IEEE Transactions on Antennas and Propagation, vol. 58, no. 12 pp. 4063-4066, 2010.

[23] W.C. Liu, C. M. Wu, and N. C. Chu, “A compact CPW-fed slotted patch antenna for dual-band operation”, IEEE Antennas and Wireless Propagation Letters, vol. 9, pp. 110-113, 2010.

[24] X. L. Sun, L. Liu, S. W. Cheung, and T. I. Yuk, “Dual-band antenna with compact radiator for 2.4/5.2/5.8 GHz WLAN applications”, IEEE Transactions on Antennas and Propagation 60, no. 12, pp. 5924-5931, 2012.

[25] J. Kaur, and R. Khanna, “Development of dual band microstrip patch antenna for WLAN/MIMO/WIMAX/AMSAT/WAVE applications”, Microwave and Optical Technology Letters 56, no. 4, pp. 988-993, 2014.

[26] S. Bhardwaj, and Y. R. Samii, “A comparative study of c-shaped, e-shaped, and u-slotted patch antennas”, Microwave and Optical Technology Letters, vol. 54, no. 7, pp. 1746-1757, July 2012.

[27] Z. An, and M. He, “A simple planar antenna for sub-6 GHz applications in 5G mobile terminals”, Applied Computational Electromagnetics Society Journal, vol. 35, no. 1, pp. 10-15, Jan. 2020.

[28] R. Azim, AKM. M. H. Meaze, A. Affandi, Md. M. Alam, R. Aktar, Md. S. Mia, T. Alam, Md. Samsuzzaman, and Md. T. Islam, “A multi-slotted antenna for LTE/5G Sub-6 GHz wireless communication applications”, International Journal of Microwave and Wireless Technologies, vol. 13, no. 5, pp. 486-496, June 2021.

[29] W. An, Y. Li, H. Fu, J. Ma, W. Chen, and B. Feng, “Low-profile and wideband microstrip antenna with stable gain for 5G wireless applications”, IEEE Antennas and Wireless Propagation Letters, vol. 17, no. 4, pp. 621-624, April 2018.

[30] H. Zhai, K. Zhang, S. Yang, and D. Feng, “A low-profile dual-band dual-polarized antenna with an AMC surface for WLAN applications”, IEEE Antennas and Wireless Propagation Letters, vol. 16, pp. 2692-2695, Aug. 2017.

[31] E. W. Coetzee, J. W. Odendaal, and J. Joubert, “A Quad-Band Antenna with AMC Reflector for WLAN and WiMAX Applications”, Applied Computational Electromagnetics Society Journal, vol. 33, no. 10, pp. 1123-1128, Oct. 2018.

[32] Q. Liu, H. Liu, W. He, and S. He, “A low-profile dual-band dual-polarized antenna with an AMC reflector for 5G communications”, IEEE Access, vol. 8, pp. 24072-24080, Jan. 2020.

[33] G. Jin, C. Deng, J. Yang, Y. Xu, and S. Liao, “A new differentially fed frequency reconfigurable antenna for WLAN and Sub-6GHz 5G applications”, IEEE Access, vol. 7, pp. 56539-56546, Feb. 2019.

[34] Y. Liu, S. Wang, N. Li, J. Wang, and J. Zhao, “A compact dual-band dual-polarized antenna with filtering structures for sub-6 GHz base station applications”, IEEE Antennas and Wireless Propagation Letters, vol. 17, no. 10, pp. 1764-1768, Oct. 2018.

[35] J. Zhu, and G. V. Eleftheriades, “Dual-band metamaterial-inspired small monopole antenna for WiFi applications”, Electronics Letters, vol. 45, no. 22, pp. 1104–1106, 2009.

[36] A. Ghaffar, W. A. Awan, N. Hussain, S. Ahmad, and X. J. Li, “A compact dual-band flexible antenna for applications at 900 and 2450 MHz”, Progress in Electromagnetics Research Letters, vol. 99, pp. 83–92, 2021.

[37] F.J. H. Martinez, G. Zamora, F. Paredes, F. Martin, and J. Bonache, “Multiband printed monopole antennas loaded with OCSRRs for PANs and WLANs”, IEEE Antennas and Wireless Propagation Letters, vol. 10, pp. 1528–1531, 2011.

[38] W. A. Awan, A. Ghaffar, N. Hussain, and X. J. Li, “CPW-fed dual-band antenna for 2.45/5.8 GHz applications”, in 8th IEEE Asia-Pacific Conference on Antennas and Propagation (APCAP). Incheon (South Korea), pp. 246–247, 2019.

[39] A. Zaidi, W. A. Awan, N. Hussain, and A. Baghdad, “A wide and triband flexible antenna with independently controllable notch bands for Sub-6-GHz communication system”, Radio engineering, vol. 29, no. 1, pp. 44–51, 2020.

[40] H. Li, Q. Zheng, J. Ding, and C. Guo, “Dual-band planar antenna loaded with CRLH unit cell for WLAN/WiMAX application”, IET Microwaves, Antennas & Propagation, vol. 12, no. 1, pp. 132–136, 2018.

[41] A. Ghaffar, X. J. Li, W. A. Awan, S. I. Naqvi, N. Hussain, B. C. Seet, Md. Alibakshikenari, F. Falcone, and E. Limiti, “Design and realization of a frequency

reconfigurable multimode antenna for ISM, 5G-Sub-6-GHz, and S-band applications", Applied Sciences, vol. 11, no. 4, pp. 1–14, 2021.

[42] M. Borhani, P. Rezaei, and A. Valizade, "Design of a reconfigurable miniaturized microstrip antenna for switchable multiband systems", IEEE Antennas and Wireless Propagation Letters, vol. 15, pp. 822–825, 2015.

[43] A. Ghaffar, X. J. Li, W.A. Awan, and N. Hussain, "Capacitor loaded dual-band flexible antenna for ISM band applications", in 9th IEEE Asia-Pacific Conference on Antennas and Propagation (APCAP). Xiamen (China), pp. 1–2, 2020.

[44] H. Y. Chien, and C. H. Lee, "Dual-band meander monopole antenna for WLAN operation in laptop computer", IEEE Antennas and Wireless Propagation Letters, vol. 12, pp. 694–697, 2013.

[45] R. Sonak, M. Ameen, and R. K. Chaudhary, "CPW-fed electrically small open-ended zeroth order resonating metamaterial antenna with dual-band features for GPS/WiMAX/WLAN applications", AEU-International Journal of Electronics and Communications, vol. 104, pp. 99–107, 2019.

[46] F. B. Zarrabi, R. Ahmadian, M. Rahimi, and Z. Mansouri, "Dual band antenna designing with composite right/left-handed", Microwave and Optical Technology Letters, vol. 57, no. 4, pp. 774–779, 2015.

[47] M. Tamrakar, and U. K. Kommuri, "Dual band CRLH metal antenna for WLAN applications", Wireless Personal Communications, vol. 116, no. 4, pp. 3235–3246, 2021.

[48] M. Ameen, A. Mishra, and R. K. Chaudhary, "Dual-band CRLH-TL inspired antenna loaded with metasurface for airborne applications", Microwave and Optical Technology Letters, vol. 63, no. 4, pp. 1249–1256, 2021.

[49] B. Zong, G. Wang, C. Zho, and Y. Wang, "Compact low-profile dual band patch antenna using novel TL-MTM structures", IEEE Antennas and Wireless Propagation Letters, vol. 14, pp. 567–570, 2014.

[50] M. S. Majedi, and A. R. Attari, "Dual-band resonance antennas using epsilon negative transmission line", IET Microwaves, Antennas & Propagation, vol. 7, no. 4, pp. 259–267, 2013.

[51] L. M. Si, and W. Zhu, and H. J. Sun, "A compact, planar, and CPW-fed metamaterial-inspired dual-band antenna", IEEE Antennas and Wireless Propagation Letters, vol. 12, pp. 305–308, 2013.

[52] A. Pirooj, M. N. Moghadasi, and F. B. Zarrabi, “Design of compact slot antenna based on split ring resonator for 2.45/5 GHz WLAN applications with circular polarization”, Microwave and Optical Technology Letters, vol. 58, no. 1, pp. 12–16, 2016.

[53] C. Zhou, G. Wang, Y. Wang, B. Zong and J. Ma, “CPW-fed dual-band linearly and circularly polarized antenna employing novel composite right/left-handed transmission-line”, IEEE Antennas and Wireless Propagation Letters, vol. 12, pp. 1073–1076, 2013.

[54] N. Hussain, S. I. Naqvi, W, A. Awan, and T. T. Lee, “A metasurface-based wideband bidirectional same-sense circularly polarized antenna”, International Journal of RF and Microwave Computer-Aided Engineering, vol. 30, no. 8, pp. 1–10, 2020.

[55] N. Hussain, M. J. Jeong, J. Park, and N. A. M. Kim “A broadband circularly polarized Fabry-Perot resonant antenna using a single layered PRS for 5G MIMO applications”, IEEE Access, vol. 7, pp. 42897–42907, 2019.

[56] N. Hussain, and I. Park, “Design of a wide-gain-bandwidth metasurface antenna at terahertz frequency”, AIP Advances, vol. 7, no. 5, pp. 1–11, 2017.

[57] N. Amani, M. Kamyab, A. Jafargholi, A. Hosseinbeig, and J. S. Meiguni, “Compact tri-band metamaterial-inspired antenna based on CRLH resonant structures”, Electronics Letters, vol. 50, no. 12, pp. 847–848, 2014.

[58] K. Saurav, D. Sarkar, and K. V. Srivastava, “CRLH unit cell loaded multiband printed dipole antenna”, IEEE Antennas and Wireless Propagation Letters, vol. 13, pp. 852–855, 2014.

[59] H. Huang, Y. Liu, S. Zhang, and S.Gong, “Multiband metamaterial loaded monopole antenna for WLAN/WiMAX applications”, IEEE Antennas and Wireless Propagation Letters, vol. 14, pp. 662–665, 2014.

[60] M. A. Abdalla, Z. Hu, and C. Muvianto, “Analysis and design of a triple band metamaterial simplified CRLH cells loaded monopole antenna”, International Journal of Microwave and Wireless Technologies, vol. 9, no. 4, pp. 903–913, 2017.

[61] L. Li, X. Zhang, X. Yin, and L. Zhou, “A compact triple-band printed monopole antenna for WLAN/WiMAX applications”, IEEE antennas and wireless propagation letters 15, pp. 1853-1855, 2016.

[62] R. Hossein, V. A. Kooshki, and H. Oraizi, “Compact microstrip fractal Koch slot antenna with ELC coupling load for triple band application”, AEU-International Journal of Electronics and Communications 73, pp. 144-149, 2017.

[63] S. Dey, S. Mondal, and P. P. Sarkar, “Reactive Impedance Surface (RIS) based asymmetric slit patch antenna loaded with complementary split ring resonator (CSRR) for circular polarization”, Journal of Electromagnetic Waves and Applications, vol. 33, no. 8, pp.1003-1013, 2019.

[64] R. Samson Daniel, R. Pandeeswari, and S. Raghavan, “A compact metamaterial loaded monopole antenna with offset-fed microstrip line for wireless applications”, AEU-International Journal of Electronics and Communications, vol. 83, pp. 88-94, Jan. 2018.

[65] S. Ullah, S. Ahmad, B. A. Khan, U. Ali, F. A. Tahir, and S. Bashir. “Design and Analysis of a Hexa-Band Frequency Reconfigurable Monopole Antenna”, IETE Journal of Research, vol. 64, no. 1, pp. 59-66, 2018.

[66] Y. J. Zheng, J. Gao, X. Y. Cao, S. J. Li, and W. G. Li, “Wideband RCS reduction and gain enhancement microstrip antenna using chessboard configuration superstrate”, Microwave and Optical Technology Letters, vol. 57, no. 7, pp.1738-1741, 2015.

[67] J. Zhu, M. A. Antoniades, and G. V. Eleftheriades, “A compact tri-band monopole antenna with single-cell metamaterial loading”, IEEE Transactions on Antennas and Propagation, vol. 58, no. 4, pp. 1031-1038, 2010.

[68] D. R. Samson, R. Pandeeswari, and S. Raghavan, “A miniaturized printed monopole antenna loaded with hexagonal complementary split ring resonators for multiband operations”, International Journal of RF and Microwave Computer-Aided Engineering, vol. 28, no. 7, pp. e21401, 2018.

[69] H. Y. Chien, and C. H. Lee, “Dual-band meander monopole antenna for WLAN operation in laptop computer”, IEEE Antennas and Wireless Propagation Letters 12, pp. 694-697, 2013.

[70] R. Sonak, M. Ameen, and R. K. Chaudhary, “CPW-fed electrically small open-ended zeroth order resonating metamaterial antenna with dual-band features for GPS/WiMAX/WLAN applications”, AEU-International Journal of Electronics and Communications 104, pp. 99-107, 2019.

[71] M. Borhani, P. Rezaei, and P. Valizade, “Design of a reconfigurable miniaturized microstrip antenna for switchable multiband systems”, IEEE Antennas and Wireless Propagation Letters, vol. 15, pp. 822-825, 2016.

[72] M. S. Ali, S. K. Rahim, M. I. Sabran, M. Abedian, A. Eteng, and M. T. Islam, “Dual band miniaturized microstrip slot antenna for WLAN applications”, Microwave and Optical Technology Letters, vol. 58, no. 6, pp. 1358-1362, Mar. 2016.

[73] P. Garg, and P. Jain, “Design and analysis of a metamaterial inspired dual band antenna for WLAN application”, International Journal of Microwave and Wireless Technologies, vol. 11, no. 4, pp. 351-358, Feb. 2019.

[74] M. Singh, N. Kumar, P. Kala, and S. Dwari, “A compact short ended dual band metamaterial antenna loaded with hexagonal ring resonators”, AEU-International Journal of Electronics and Communications, vol. 135, pp. 153731, Jun. 2021.

[75] H. Huang, Y. Liu, S. Zhang, and S. Gong, “Multiband metamaterial-loaded monopole antenna for WLAN/WiMAX applications”, IEEE Antennas and wireless propagation letters, vol. 14, pp. 662-665, Jan. 2015.

[76] J. K. Ji, G. H. Kim, and W. M. Seong, “Bandwidth enhancement of metamaterial antennas based on composite right/left-handed transmission line”, IEEE antennas and wireless propagation letters, vol. 9, pp. 36-39, 2010.

[77] B. J. Niu, and Q. Y. Feng, “Bandwidth enhancement of asymmetric coplanar waveguide (ACPW)-fed antenna based on composite right/left-handed transmission line”, IEEE Antennas and Wireless Propagation Letters, vol. 12, pp. 563-566, Jan. 2013.

[78] S. K. Sharma, and R. K. Chaudhary, “A compact zeroth-order resonating wideband antenna with dual-band characteristics”, IEEE Antennas and Wireless Propagation Letters, vol. 14, pp. 1670-1672, 2015.

[79] A. Foroozesh, and L. Shafai, “Investigation into the application of artificial magnetic conductors to bandwidth broadening, gain enhancement and beam shaping of low profile and conventional monopole antennas”, IEEE Transactions on Antennas and Propagation, vol. 59, no. 1, pp. 4-20, Jan. 2011.

[80] H. Yi, and S. W. Qu, “A novel dual-band circularly polarized antenna based on electromagnetic band-gap structure”, IEEE Antennas and Wireless Propagation Letters, vol. 12, pp. 1149-1152, 2013.

[81] M. Rezvani, and P. Mohammadi. “Microstrip antenna with aperture reflector and C-shaped dipoles for LTE and wireless communications”, AEU-International Journal of Electronics and Communications, vol. 94, pp. 12-18, 2018.

[82] H. Zhai, K. Zhang, S. Yang, and D. Feng, “A low-profile dual-band dual-polarized antenna with an AMC surface for WLAN applications”, IEEE Antennas and Wireless Propagation Letters, vol. 16, pp. 2692-2695, 2017.

[83] S. X. Ta, and I. Park, “Dual-band low-profile crossed asymmetric dipole antenna on dual-band AMC surface”, IEEE Antennas and Wireless Propagation Letters, vol. 13, pp. 587-590, 2014.

[84] J. Chen, Y. Zhao, Y Ge, and L Xing, “Dual-band high-gain Fabry–Perot cavity antenna with a shared-aperture FSS layer”, IET Microwaves, Antennas & Propagation, vol. 12, no. 13, pp. 2007-2011, 2018.

[85] Y. H. Xie, C. Zhu, L. Li, and C. H. Liang, “A novel dual-band metamaterial antenna based on complementary split ring resonators”, Microwave and Optical Technology Letters, vol. 54, no. 4, pp. 1007-1009, 2012.

[86] J. J. Ma, X. Y. Cao, and T. Liu, “Design the size reduction patch antenna based on complementary split ring resonators”, in 2010 IEEE International Conference on Microwave and Millimeter Wave Technology, pp. 401-402, 2010.

[87] S. K. Sharma, and R. K. Chaudhary, “Metamaterial inspired dual-band antenna with modified CSRR and EBG loading”, in 2015 IEEE International Symposium on Antennas and Propagation & USNC/URSI National Radio Science Meeting, pp. 472-473, 2015.

[88] K. Saurav, D. Sarkar, and K. V. Srivastava, “Dual-polarized dual-band patch antenna loaded with modified mushroom unit cell”, IEEE Antennas and Wireless Propagation Letters, vol. 13, pp. 1357-1360, 2014.

[89] A. El Yousfi, A. E. Salhi, A. Lamkaddem, O. E. Mrabet, M. Aznabet, and M. A. Ennasar, “A dual band inverted L monopole antenna based on Complemenatry Split ring Resonator for RFID applications”, in 2019 IEEE International Conference on Wireless Technologies, Embedded and Intelligent Systems (WITS), pp. 1-3, 2019.

[90] A. El Yousfi, A. Lamkaddem, K. A. Abdalmalak, and D. Segovia-Vargas, “A Miniaturized Triple-Band and Dual-Polarized Monopole Antenna Based on a CSRR Perturbed Ground Plane”, IEEE Access, vol. 9, pp. 164292-164299, 2021.

[91] P. M. Paul, K. Kandasamy, and M. S. Sharawi, “A tri-band slot antenna loaded with split ring resonators”, Microwave and Optical Technology Letters 59, no. 10, pp. 2638-2643, 2017.

[92] S. C. Basaran, U. Olgun, and K. Sertel, “Multiband monopole antenna with complementary split-ring resonators for WLAN and WiMAX applications”, Electronics letters, vol. 49, no. 10, pp. 636-638, 2013.

[93] X. Q. Zhang, Y. C. Jiao, and W. H. Wang, “Compact wide tri-band slot antenna for WLAN/WiMAX applications”, Electronics Lett., vol. 48, no. 2, pp. 64-65, Jan. 2012.

[94] W. Hu, Y. Z. Yin, P. Fei, and X. Yang, “Compact triband square-slot antenna with symmetrical L-strips for WLAN/WiMAX applications”, IEEE Antennas and Wireless Propagation Letters., vol. 10, pp. 462-465, 2011.

[95] Y. F. Cao, S. W. Cheung, and T. I. Yuk, “A multiband slot antenna for GPS/WiMAX/WLAN systems”, IEEE Transactions on Antennas and Propagation. vol. 63, no. 3, pp.952-958, Mar. 2015.

[96] P. M. Paul, K. Kandasamy, and M. S. Sharawi, “A tri-band slot antenna loaded with split ring resonators”, Microwave and Optical Technology Letters, vol. 59, no. 10, pp. 2638-2643. 2017.

[97] S. C. Basaran, U. Olgun, and K. Sertel, “Multiband monopole antenna with complementary split-ring resonators for WLAN and WiMAX applications”, Electronics letters, vol. 49, no. 10, pp. 636-638, 2013.

[98] R. Xu, J. Li, Y.X. Qi, Y. Guangwei, and J.J. Yang, “A design of triple-wideband triple-sense circularly polarized square slot antenna”, IEEE Antennas and Wireless Propagation Letters, vol. 16, pp.1763-1766. 2017.

[99] J.G. Baek, and K.C. Hwang, “Triple-band unidirectional circularly polarized hexagonal slot antenna with multiple L-shaped slits”, IEEE Transactions on Antennas and Propagation, vol. 61, no. 9, pp.4831-4835. 2013.

[100] L. Wang, Y.X. Guo, and W.X. Sheng, “Tri-band circularly polarized annular slot antenna for GPS and CNSS applications”, Journal of Electromagnetic Waves and Applications, vol. 26, no. 14-15, pp.1820-1827. 2012.

[101] E. Ebrahimi, “Wideband and Reconfigurable Antennas for Emerging Wireless Networks”, A Thesis Submitted to the University of Birmingham School of Electronic, Electrical and Computer Engineering, College of Engineering and Physical Sciences, September 2011.

[102] Available online: http://www.peachwire.com/index.php/Faq_quare/che-differenza-ce-tra-lnfc-e-altretecnologie-come-il-bluetooth-e-il-wi-fi/.

[103] Available online: http://transition.fcc.gov/pshs/techtopics/techtopic8.html.

[104] Available online: http://cdn.arstechnica.net/Gadgets/uwb_tzero_chart.png.

[105] J. Pourahmadazar, C. Ghobadi, and J. Nourinia, "Novel Modified Pythagorean Tree Fractal Monopole Antennas for UWB Applications", IEEE Antennas and Wireless Propagation Letters, Vol. 10, pp. 484-487, 2011.

[106] S. Tripathi, A. Mohan, and S. Yadav, "Hexagonal Fractal Ultra-Wideband Antenna Using Koch Geometry with Bandwidth Enhancement", IET Microwaves, Antennas and Propagation, vol. 8, no. 15, pp. 1445-1450, 2014.

[107] G. K. Pandey, H. S. Singh, P. K. Bharti, and M. K. Meshram, "Metamaterial-based UWB Antenna", Electronics Letters, vol. 50, no. 18, pp. 1266–1268, 2014.

[108] M. M. Islam, M. T. Islam, M. Samsuzzaman and M. R. I. Faruque, "Compact Metamaterial Antenna for UWB Applications", Electronics Letters, vol. 51, no. 16, pp. 1222–1224, 2015.

[109] M. Djaiz, A. Habib, M. Nedil, and T. A. Denidni, "Design of UWB Filter-Antenna with Notched Band at 5.8 GHz", 3rd IEEE International Symposium on Microwave, Antenna, Propagation and EMC Technologies for Wireless Communications, pp. 1-4, June 2009.

[110] W. S. Lee, D. Z. Kim, K. J. Kim, and J. W. Yu, "Wideband Planar Monopole Antennas with Dual Band-Notched Characteristics", IEEE Transactions on Microwave Theory and Techniques, vol. 54, no. 6, pp. 2800–2806, June 2006.

[111] J. Y. Deng, Y. Z. Yin, S. G. Zhou, and Q. Z. Liu, "Compact Ultrawideband Antenna with Tri-Band Notched Characteristic", Electronics Letters, vol. 44, no. 21, pp. 1231–1233, Oct. 2008.

[112] Y. Zhang, W. Hong, C. Yu, Z. Q. Kuai, Y. D. Dong, and J. Y.Zhou, "Planar Ultra-Wideband Antennas with Multiple Notched Bands Based on Etched Slots on the Patch and/or Split Ring Resonators on the Feed Line", IEEE Transactions on antennas and propagation, vol. 56, no. 9, pp. 3063–3068, Sep.2008.

[113] M. Al-Husseini, Y. Tawk, A. El-Hajj, K. Y. Kabalan, "A Low-Cost Microstrip Antenna for 3G/WLAN/WiMAX and UWB Applications", in Proceedings of the IEEE International conference on Advances in Computational Tools for Engineering Applications (ACTEA'09), Zouk Mosbeh, Lebanon, pp. 68-70, July 2009.

[114] N. A. Kumar and A. S. Gandhi, "Small Size Planar Monopole Antenna for High Speed UWB Applications", in Proceedings of the Twenty-Second National Conference on Communications (NCC), Guwahati, Assam, India, pp. 1-5, March 2016.

[115] N. P. Agrawall, G. Kumar, and K. P. Ray, “Wide-Band Planar Monopole Antennas”, IEEE Transactions on Antennas and Propagation, vol. 46, no. 2, pp. 294-295, 1998.

[116] J. A. Evans and M. J. Ammann, “Planar Trapezoidal and Pentagonal Monopoles with Impedance Bandwidth in Excess of 10:1”, IEEE Antennas and Propagation International Symposium (Digest), Orlando, FL, vol. 3, pp. 1558-1561, 1999.

[117] S. Y. Suh, W. L. Stutaman and W. A. Davis, “A New Ultrawideband Printed Monopole Antenna: The Planar Inverted Cone Antenna (PICA)”, IEEE Transactions on Antennas and Propagation, vol. 52, no. 5, pp. 1361-1364, 2004.

[118] S. K. Sharma, A. Gupta, and R. K. Chaudhary, “UWB Ring-shaped Metamaterial Antenna with Modified Phi-shaped SRR”, in Proceedings of the IEEE International Symposium on Antennas and Propagation & USNC/URSI National Radio Science Meeting, British Columbia, Canada, pp. 1966 – 1967, July 2015.

[119] S. R. Zahran, O. H. El Sayed Ahmed, A. T. El-Shalakany, S. Saleh and M. A. Abdalla, “Ultra-Wide Band Antenna with Enhancement Efficiency for High Speed Communications”, in Proceedings of the IEEE 31st National Radio Science Conference (NRSC), Cairo, Egypt, pp. 65 - 72, April 2014.

[120] S. Weigand, G. H. Huff, K.H. Pan, and J.T. Bernhard, J. T, “Analysis and design of broad-band single-layer rectangular U-slot microstrip patch antennas”. IEEE transactions on antennas and propagation, vol. 51, no. 3, pp. 457-468, 2003.

[121] V. Natarajan and D. Chatterjee, “An Empirical Approach for Design of Wideband, Probe-Fed, U-Slot Microstrip Patch Antenna on Single-layer, Infinite, Grounded Substrates”. The Applied Computational Electromagnetics Society Journal (ACES), vol. 18, no. 3, pp. 191-201, 2003.

[122] G. M. Dandime, and V. G. Kasabegoudar, “A slotted circular monopole antenna for wireless applications”, International Journal of Wireless Communications and Mobile Computing, vol. 2, no. 2, pp. 30-34, 2014.

[123] R. Shi, X. Xu, J. Dong, and Q. Luo, “Design and Analysis of a Novel Dual Band-Notched UWB Antenna”, International Journal of Antennas and Propagation, vol. 2014, pp. 1-10, 2014.

[124] S. Jangid, and M. Kumar, “A Novel UWB Band Notched Rectangular Patch Antenna with Square slot”, in Proceedings of the IEEE Fourth International Conference on Computational Intelligence and Communication Networks (CICN), Uttar Pradesh, India, pp. 5 – 9, Nov. 2012.

[125] M. N. Srifi, S. K. Podilchak, M. Essaaidi, and Y. M. M. Antar, “Compact Disc Monopole Antennas for Current and Future Ultrawideband (UWB) Applications”, IEEE Transactions on Antennas and Propagation, vol. 59, no. 12, pp. 4470-4480, 2011.

[126] M. Tang, R. W. Ziolkowski, and S. Xiao, “Compact Hyper-Band Printed Slot Antenna with Stable Radiation Properties”, IEEE Transactions on Antennas and Propagation, vol. 62, no. 6, pp. 2962-2969, 2014.

[127] M. Al-Husseini, J. Costantine, C. G. Christodoulou, S. E. Barbin, A. El-Hajj, and K. Y. Kabalan, “A Reconfigurable Frequency-notched UWB Antenna with Split-ring Resonators”, in Proceedings of the IEEE Asia-Pacific Microwave Conference, Yokohama, Japan, pp. 618 - 621, Dec. 2010.

[128] Y. Wang, N. Wang, T. A. Denidni, Q. Zeng and G. Wei, “Integrated Ultrawideband/Narrowband Rectangular Dielectric Resonator Antenna for Cognitive Radio”, IEEE Antennas and Wireless Propagation Letters, vol. 13, pp. 694-697, 2014.

[129] E. Ebrahimi, J. R. Kelly, and P. S. Hall, “Integrated Wide-Narrowband Antenna for Multi-Standard Radio”, IEEE Transactions on Antennas and Propagation, vol. 59, no. 7, pp. 2628-2635, July 2011.

[130] M. G. Aly and Y. Wang, “An Integrated Narrowband-Wideband Antenna”, in Proceedings of the IEEE Loughborough Antennas & Propagation Conference (LAPC), UK, pp. 433 – 435, Nov. 2013.

[131] H. Boudaghi, M. Azarmanesh, and M. Mehranpour, “A Frequency-Reconfigurable Monopole Antenna Using Switchable Slotted Ground Structure”, IEEE Antennas and Wireless Propagation Letters, vol. 11, pp. 655-658, 2012.

[132] I. Messaoudene, T. A. Denidni, and A. Benghalia, “Ultra-Wideband CPW Antenna Integrated with Narrow Band Dielectric Resonator”, in Proceedings of the IEEE International Symposium on Antennas and Propagation (APSURSI), Florida, USA, pp. 1308 - 1309, July 2013.

[133] Y. Wang and G. Wei, T. A. Denidni, and Q. Zeng, “Ultra-Wideband Planar Monopole Integrated with Cylindrical Dielectric Resonator Antenna”, in Proceedings of the IEEE International Symposium on Antennas and Propagation (APSURSI), Florida, USA, pp. 1696 - 1697, July 2013.

[134] H. A. Majid, M. K. A. Rahim, M. R. Hamid, and M. F. Ismail, “A Compact Frequency-Reconfigurable Narrowband Microstrip Slot Antenna”, IEEE Antennas and Wireless Propagation Letters, vol. 11, pp. 616-619, 2012.

[135] Y. Tawk and C. G. Christodoulou, “A Cellular Automata Reconfigurable Microstrip Antenna Design”, in Proceedings of the IEEE Antennas and Propagation Society International Symposium, North Charleston, SC, USA, pp. 1-4, June 2009.

[136] X. Liu, X. Yang, and F. Kong, “A Frequency-Reconfigurable Monopole Antenna with Switchable Stubbed Ground Structure”, Radio Engineering, vol. 24, no. 2, 2015.

[137] M. Al-Husseini, A. Ramadan, A. El-Hajj and K. Y. Kabalan, “A Reconfigurable Antenna Based on an Ultra wide band to Narrowband Transformation”, PIERS Proceedings, Moscow, Russia, pp. 550-553, August 19-23, 2012.

[138] Y. Wang, T. A. Denidni, Q. Zeng and G. Wei, “A Design of Integrated Ultra-wideband/Narrow Band Rectangular Dielectric Resonator Antenna”, in Proceedings of the IEEE International Wireless Symposium (IWS), Xian, China, pp. 1-4, March 2014.

[139] K. Srivastava, A. Kumar, B. K. Kanaujia, S. Dwari, and S. Kumar, “A CPW-Fed UWB MIMO Antenna with Integrated GSM band and Dual Band Notches”, International Journal of RF and Microwave Computer-Aided Engineering, vol. 29, no. 1, 2018.

[140] R. Garg, I. Bahl, and M. Bozzi, “Microstrip lines and slotlines” (Microwave &RF, Artech House, 2013, 3rd edition).

[141] A. Kantemur, A. H. Abdelrahman, and H. Xin, “A Novel Compact Reconfigurable UWB Antenna for Cognitive Radio Applications”, IEEE International Symposium on Antennas and Propagation & USNC/URSI National Radio Science Meeting, pp. 1369-1370, 2017.

[142] Y. Tawk and C. G. Christodoulou, “A New Reconfigurable Antenna Design for Cognitive Radio”, IEEE Antennas and Wireless Propagation Letters, vol. 8, pp. 1378-1381, 2009.

[143] B. P. Chacko, G. Augustin and T. A. Denidni, "Electronically Reconfigurable Uniplanar Antenna with Polarization Diversity for Cognitive Radio Applications”, IEEE Antennas and Wireless Propagation Letters, vol. 14, pp. 213-216, 2015.

[144] R. Hussain, M. U. Khan and M. S. Sharawi, “An Integrated Dual MIMO Antenna System with Dual-Function GND-Plane Frequency-Agile Antenna”, IEEE Antennas and Wireless Propagation Letters, vol. 17, no. 1, pp. 142-145, 2018.

[145] R. Hussain and M. S. Sharawi, “A Cognitive Radio Reconfigurable MIMO and Sensing Antenna System”, IEEE Antennas and Wireless Propagation Letters, vol. 14, pp. 257-260, 2015.

[146] R. Hussain and M. S. Sharawi, "4-Element Planar MIMO Reconfigurable Antenna System for Cognitive Radio Applications", IEEE International Symposium on Antennas and Propagation & USNC/URSI National Radio Science Meeting, Vancouver, BC, Canada, pp. 717-718, 2015.

[147] R. Hussain, M. S. Sharawi and A. Shamim, "4-Element Concentric Pentagonal Slot-Line-Based Ultra-Wide Tuning Frequency Reconfigurable MIMO Antenna System", IEEE Transactions on Antennas and Propagation, vol. 66, no. 8, pp. 4282-4287, 2018.

[148] T. Alam, S. R. Thummaluru and R. K. Chaudhary, "Integration of MIMO and Cognitive Radio for Sub-6 GHz 5G Applications", IEEE Antennas and Wireless Propagation Letters, vol. 18, no. 10, pp. 2021-2025, 2019.

[149] R. Hussain, A. Raza, M. U. Khan, A. Shammim and M. S. Sharawi, "Miniaturized Frequency Reconfigurable Pentagonal MIMO Slot Antenna for Interweave CR Applications", International Journal of RF and Microwave Computer-Aided Engineering, vol. 29, no. 9, pp. 1-12, 2019.

[150] R. Hussain and M. S. Sharawi, "A Low Profile Compact Reconfigurable MIMO Antenna for Cognitive Radio Applications", 9th European Conference on Antennas and Propagation (EuCAP), Lisbon, Portugal, pp. 1-4, 2015.

[151] D. T. Le and Y. Karasawa, "A Simple Broadband Antenna for MIMO Applications in Cognitive Radio", IEEE International Symposium on Antennas and Propagation (APSURSI), Spokane, WA, USA, pp. 806-809, 2011.

[152] S. Keerthipriya and C. Saha, "Reconfigurable Multifunctional Vivaldi MIMO Antenna for Cognitive Radio Applications", IEEE Indian Conference on Antennas and Propogation (InCAP), Ahmedabad, India, pp. 1-4, 2019.

[153] Y. Tawk, F. Ayoub, C. G. Christodoulou and J. Costantine, "A MIMO Cognitive Radio Antenna System", IEEE Antennas and Propagation Society International Symposium (APSURSI), Orlando, FL, USA, pp. 572-573, 2013.

[154] R. K. Chaudhary and S. R. Thummaluru, "Reconfigurable MIMO Filtenna for Spectrum Underlay Cognitive Radio", Photonics & Electromagnetics Research Symposium - Spring (PIERS-Spring), Rome, Italy, pp. 582-586, 2019.

[155] S. Riaz and X. Zhao, "An Eight-Port Frequency Reconfigurable MIMO Slot Antenna with Multi-Band Tuning Characteristics", 12th International Symposium on Antennas, Propagation and EM Theory (ISAPE), Hangzhou, China, pp. 1-4, 2018.

[156] R. Hussain, M. U. Khan and M. S. Sharawi, “Meandered H-Shaped Slot-line Quad-Band Frequency Reconfigurable MIMO Antenna”, 13th European Conference on Antennas and Propagation (EuCAP), Krakow, Poland, pp. 1-3, 2019.

[157] R. Hussain and M. S. Sharawi, “An Integrated Slot-Based Frequency-Agile and UWB Multifunction MIMO Antenna System”, IEEE Antennas and Wireless Propagation Letters, vol. 18, no. 10, pp. 2150-2154, 2019.

[158] J. K. H. Gamage, B. Holter, I. A. Jensen, K. Husby and J. Kuhnle, “A Wideband Conformal Antenna Array for Cognitive Radio/MIMO Applications”, Proceedings of the 5th European Conference on Antennas and Propagation (EUCAP), Rome, Italy, pp. 725-729, 2011.

[159] R. Hussain, A. Ghalib and M. S. Sharawi, “Annular Slot-Based Miniaturized Frequency-Agile MIMO Antenna System”, IEEE Antennas and Wireless Propagation Letters, vol. 16, pp. 2489-2492, 2017.

[160] R. Hussain and M. S. Sharawi, “Two Element Wide-Band Frequency Reconfigurable MIMO Antenna System for 4G Applications”, IEEE 5th Asia-Pacific Conference on Antennas and Propagation (APCAP), pp. 11-12, 2016.

[161] M. Bouezzeddine and W. L. Schroeder, “Design of a Wideband, Tunable Four-Port MIMO Antenna System With High Isolation Based on the Theory of Characteristic Modes”, IEEE Transactions on Antennas and Propagation, vol. 64, no. 7, pp. 2679-2688, 2016.

[162] R. Hussain, M. U. Khan and M. S. Sharawi, “Design and Analysis of a Miniaturized Meandered Slot-Line-Based Quad-Band Frequency Agile MIMO Antenna”, IEEE Transactions on Antennas and Propagation, vol. 68, no. 3, pp. 2410-2415, March 2020.

[163] R. Hussain and M. S. Sharawi, “Reconfigurable Pentagonal Slot Based 4-Element MIMO Antennas”, IEEE International Symposium on Antennas and Propagation & USNC/URSI National Radio Science Meeting, San Diego, CA, pp. 1151-1152, 2017.

[164] R. Hussain and M. S. Sharawi, “Multi-Mode Ground Reconfigurable MIMO Antenna System”, IEEE 4th Asia-Pacific Conference on Antennas and Propagation (APCAP), Bali, Indonesia, pp. 144-145, 2015.

[165] R. Hussain and M. S. Sharawi, “Wide-Band Frequency Agile MIMO Antenna System with Wide Tunability Range”, Microwave and Optical technology Letters, vol. 58, no. 9, pp. 2276-2280, 2016.

[166] A. Raza, M. U. Khan, F. A. Tahir, R. Hussain and M. S. Sharawi, “A 2-Element Meandered-Line Slot-Based Frequency Reconfigurable MIMO Antenna System”, Microwave and Optical technology Letters, vol. 60, no. 11, pp. 1-8, 2018.

[167] S. C. Basaran and Y. E. Erdemli, “A Dual-Band Splitring Monopole Antenna for WLAN Applications”, Microwave and Optical Technology Letters, vol. 51 no. 11, pp. 2685-2688, 2009.

[168] V. Rajeshkumar and S. Raghavan, “A Compact Frequency Reconfigurable Split Ring Monopole Antenna for WLAN/WAVE Applications”, Applied Computational Electromagnetics Society Journal, vol. 30 no. 3, pp. 338-344, 2015.

[169] L. M. Si, W. Zhu, and H. J. Sun, “A Compact, Planar, and CPW-Fed Metamaterial-Inspired Dual-Band antenna”, IEEE Antennas and Wireless Propagation Letters, vol. 12, pp. 305-308, 2013.

[170] S. Nandi and A. Mohan, “CRLH Unit Cell Loaded Triband Compact MIMO Antenna for WLAN/WiMAX Applications”, IEEE Antennas Wireless Propagation Letters, vol. 16, pp. 1816-1819, 2017.

List of Publications

International Journals

1. Ashish, Junuthula, and Amara Prakasa Rao. "A Dual Band AMC Backed Antenna for WLAN, WiMAX and 5G Wireless Applications." The Applied Computational Electromagnetics Society Journal (ACES), pp. 1209-1214, 2021. **(SCIE)**
2. Ashish, Junuthula, and Amara Prakasa Rao. "A Dual Band CRLH Metamaterial-Inspired Planar Antenna for Wireless Applications." Radioengineering, Vol. 31, no. 1, pp. 15, 2022. **(SCIE)**
3. Ashish, Junuthula, and Amara Prakasa Rao. " A dual-band meandered line antenna loaded with metasurface for wireless applications ". Journal of Electromagnetic Waves and Applications. **(SCIE-UNDER REVIEW)**

International Conferences

1. Ashish, Junuthula, and A. Prakasa Rao. "Design and Implementation of Compact Dual band U-slot Microstrip Antenna for 2.4 GHz WLAN and 3.5 GHz WiMAX Applications." In 2019 International Conference on Smart Systems and Inventive Technology (ICSSIT), pp. 1084-1086, 2019.
2. Junuthula Ashish and Amara Prakasa Rao “A CSRR based dual band antenna for WLAN/WiMAX/sub-6 GHz 5G applications” in ATMS 2022 Conference.
3. Junuthula Ashish and Amara Prakasa Rao “A Triband Dual SRR Loaded Antenna for Wireless Applications”. (To be communicated)